General Disclaimer

One or more of the Following Statements may affect this Document

- This document has been reproduced from the best copy furnished by the organizational source. It is being released in the interest of making available as much information as possible.

- This document may contain data, which exceeds the sheet parameters. It was furnished in this condition by the organizational source and is the best copy available.

- This document may contain tone-on-tone or color graphs, charts and/or pictures, which have been reproduced in black and white.

- This document is paginated as submitted by the original source.

- Portions of this document are not fully legible due to the historical nature of some of the material. However, it is the best reproduction available from the original submission.

Produced by the NASA Center for Aerospace Information (CASI)

Final Report
Contract NAS 9-7029

DEVELOPMENT OF COMPUTER TECHNOLOGY

FOR

MEDICAL DATA ANALYSIS

TO BE APPLIED TO

APOLLO AND FOLLOW-ON SPACE MISSIONS

N69-10567 (ACCESSION NUMBER) (THRU)
915 (PAGES) 1 (CODE)
CR-92377 (NASA CR OR TMX OR AD NUMBER) 04 (CATEGORY)
FACILITY FORM 602

August, 1968

The University of Texas
Graduate School of Biomedical Sciences at Houston

NOV 1968
RECEIVED
NASA STI FACILITY
INPUT BRANCH

NASA CR 92377

PREFACE

The work performed under this contract is a continuation of efforts initiated under previous National Aeronautics and Space Administration contracts NAS 9-1461, NAS 9-5821, and NSR 44-024-006. There is represented an attempt to integrate experimental and ground-based medical data collection and analysis schemes into the medical data processing needs and capabilities of Project Apollo and follow on space missions at the Manned Spacecraft Center.

This contract to The University of Texas Graduate School of Biomedical Sciences was sponsored by the National Aeronautics and Space Administration, Manned Spacecraft Center, with Dr. Edward Moseley as Technical Monitor.

The computer work performed under this contract utilized the Common Research Computer Facility sponsored by National Institutes of Health Grant F R 00254; The University of Texas M.D. Anderson Hospital and Tumor Institute computer facility sponsored by National Institutes of Health Grants FR 00258 and CA 06939 and National Aeronautics and Space Administration Contracts NSR 44-012-039, NAS 9-7029, and NAS 9-7153; and computational facilities at the Manned Spacecraft Center.

FINAL REPORT - CONTRACT NAS 9-7029

The collection, processing, analysis, and evaluation of biomedical data collected from astronauts in association with spaceflights requires the collaborative efforts of many groups of people to provide meaningful information on the status and well-being of the astronaut. To achieve an effective system for processing and evaluation of such biomedical data requires interfacing the efforts of numerous activities of different groups including medical specialists, engineers, and computer scientists. It was the overall goal of the work performed under this contract to help define the methodology to assist in the development of computer technology for medical data analysis to be applied to medical data collection and monitoring for Apollo and follow-on space missions. Delay in the manned Apollo missions resulted in some changes in the timing of original goals. However, the general technology developed and partially implemented should find usefulness during future space flights.

The following is a brief summary of the work accomplished to achieve the Purposes and Goals defined in the Unsolicited Proposal and Statement of Work of the resulting contract. The appendix of this report contains descriptive material on selected phases of the work.

2.0 Purposes and Goals:

2.1 The primary purpose and goal of this contract is to develop and assist in implementing of medical computer technology into the NASA flight medical data system. This implementation will be achieved by considering the many components of data collection, transmission, storage, display and interpretation.

Effort: Numerous meetings of the contractor were held with personnel from the Manned Spacecraft Center to plan future system development at the Manned Spacecraft Center or to implement technology developed by the contractor by providing programming and statistical assistance. Medical, engineering, computer and statistical scientists of the contractor met individually and in groups to effect optimum communication for exchange of ideas and technology. Computer programs and techniques developed by the contractor were made available to NASA personnel and other contractors.

2.1.1 Electrocardiogram (ECG) data collected using the NASA lead system will be evaluated in terms of signal degradation due to analog filtering for noise suppression, effect of reduced sampling of the signal for transmission of data, and the effect of reduced digitizing rates on distortion of meaningful components of analog data. Particular emphasis will be placed on those records demonstrating cardiac abnormalities.

Effort: An extensive demonstration and several discussion meetings were held jointly between the contractor, The University of Texas M.D. Anderson Hospital personnel, and NASA personnel to demonstrate the above. The hybrid computer system of The University of Texas M.D. Anderson Hospital was utilized to provide computer processing and output which demonstrated considerations of importance in processing electrocardiogram data.

2.1.2 Preprocessing circuitry and hybrid computer techniques will be evaluated for meaningful implementation into the updated NASA monitoring system, considering the measurements made in association with the flights.

Effort: The results of these efforts are reflected in techniques described in Appendices A and C of this report for processing of blood pressure, electroencephalogram, electrocardiogram, and impedance pneumogram data. A hybrid computer capability was developed jointly through this contract and contract NAS 9-7153 for development and evaluation of further techniques.

2.1.3 Because of the proximity to the Manned Spacecraft Center, daily consultation and assistance can be provided to the NASA medical data group in order to facilitate updating of a practical monitoring system for Apollo flights.

Effort: This consultation and assistance was provided by exchange visits of personnel to NASA facilities and facilities of the contractor.

2.1.4 Statistical techniques and computer technology reports will be prepared to document available software for data processing by large scale digital computers. This will provide a very concrete transfer of information on the application of certain computer and statistical technology which can be applied to medical problems, such as cardiac deconditioning, noise reduction, etc.

Effort: Data were processed from previous studies conducted by NASA or its contractors. Computer programs were provided to NASA for implementation on computers located at the Manned Spacecraft Center. The contractors provided statisticians, computer programmers, and system analysts to interface with NASA personnel to implement technology useful to the NASA computer centers.

2.1.5 A determination of operational definitions of heart rate and respiration rate limits will be tabulated for different activity schedules for space flight by evaluation of data from space flights. Such tabulating is predisposed by the need for adequate identification and logging of data to assure accurate retrieval of information.

Effort: No data were available from Apollow missions because of the delay in the flight schedule. Data from previous Gemini flights were evaluated, but were found to be inadequately identified to provide meaningful data for different activity schedules. Assistance was provided to the Technical Monitor for planning an appropriate identification system for future biomedical data collected by NASA.

2.1.6 Using heart rate and respiratory rate information, an attempt will be made to define the sleep-wake schedules of the astronaut data. An evaluation will be made of selected ground-based data to define the appropriateness of the measurement by relating it to EEG criteria.

Effort: An extensive report on this effort is described in Appendix C. Part of the effort represented a Master's Thesis project for a graduate student who was employed part-time on this contract.

2.1.7 An evaluation will be made of the feasibility of incorporating analog computer techniques for computing statistical quantities, such as cross products, to allow near real-time processing of telemetered medical data.

Effort: These efforts were performed in conjunction with The University of Texas M.D. Anderson Hospital and are reported under contract NAS 9-7153.

2.1.8 Techniques will be established to allow consideration of selected PCM telemetry environmental parameters, such as temperature or oxygen tension, into an interpretation of biomedical measurements.

Effort: Environmental parameters collected from ground based chambers were introduced into NASA monitoring system planning to gain experience with the usefulness of these measures.

2.1.9 Electronic circuitry will be developed for automatic recognition and display of systolic and diastolic blood pressure using the cuff-microphone technique, and thus allow its automatic incorporation into techniques for evaluation of cardiovascular data. Such a system would also find usefulness in evaluation of blood pressure data from tilt table studies, centrifuge runs, chamber studies, etc.

Effort: A detailed report on this effort is described in Appendix A. Part of this effort represented a Master's Thesis project for a graduate student who was employed part-time on this contract.

2.1.10 Using existing computer and statistical techniques, an analysis can be made of data collected pre and post-flight, for example, tilt table and blood volume data, to correlate it with changes observed during flight.

Computer programs for statistical analysis and display of such data were provided to the Manned Spacecraft Center. Data were evaluated from past Gemini flights to demonstrate the effectiveness of the techniques as they may be applied to future Apollo flights.

2.1.11 Consultative assistance will be provided in the design, development and implementation of ground-based monitoring and research such as in conjunction with altitude chambers, centrifuge, and simulator training. This would involve consideration of the needs or requirements of instrumentation to answer questions proposed in hypotheses of changes expected in medical data.

Effort: Meetings were held at the contractor's facilities and at NASA; special emphasis was placed on techniques for implementation of a system for use with the NASA altitude chambers.

2.1.12 The Contractor will carry out studies to routinely re-examine data from each Apollow flight in order to provide updated biomedical data baselines. These baseline data will serve as criteria for ground-based studies as well as for input to the real-time mission monitoring system, where the updated baselines will be incorporated into the flight summaries for real-time comparisons. This task will ensure comprehensive sampling of all aspects of the data in order to empirically establish a broad base of data concerning significant relationships existing among biomedical measurements. This task will also serve to establish optimum data handling schemes.

Effort: Since no manned Apollo flights were made, this goal could not be achieved.

2.1.13 The Contractor shall carry out a study to determine the adequacy of appropriate nonparametric statistics in analyzing data acquired from the Gemini Cardiovascular Reflex Conditioning Experiment, operational tilt table studies, and other operational experiments analyxed under Contract NSR 44-024-006. This task will include a comparison between prior analyses and the nonparametric methods in order to demonstrate associated advantages and/or disadvantages. Also included will be brief discussions pertaining to limitations of each technique.

Effort: A detailed report on this effort using tilt table data is presented in Appendix B of this report.

A SYSTEM FOR THE AUTOMATIC MEASUREMENT AND DIGITAL DISPLAY OF SYSTOLIC AND DIASTOLIC BLOOD PRESSURES

by

Arthur Edward Schulze, B.S.E.E., M.S.E.E.

THESIS

Presented to the Faculty of The University of Texas
Graduate School of Biomedical Sciences at Houston
in Partial Fulfillment

of the Requirements

For the Degree of

Master of Science

THE UNIVERSITY OF TEXAS

Houston, Texas

January, 1969

PRECEDING PAGE BLANK NOT FILMED

PREFACE

The work reported in this thesis was supported, in part, by Contract Number NAS 9-7029 from the National Aeronautics and Space Administration, Manned Spacecraft Center, Houston, Texas. The project was housed in the facilities of The University of Texas Graduate School of Biomedical Sciences at Houston and was under the direction of Dr. Fred B. Vogt, principle investigator, whose assistance and advice have made the project and this report possible.

I sincerely appreciate the efforts of Dr. F. B. Vogt, Dr. L. S. Meharg, Dr. D. C. Kroeger, and Dr. S. O. Zimmerman in guiding the preparation of this thesis. Also, I thank Mr. Michael A. Craig for his assistance in the preparation of the illustrations, typing of preliminary drafts, and for his untiring service as a subject; Mr. Tommy Record for his assistance in assembling the circuitry and in the packaging of the apparatus; Mr. Thor O. Hallen and Dr. Fred B. Vogt for their preliminary design of the circuitry; Dr. Louis S. Meharg for advice on technical aspects of the system design; and the many other associates of the Graduate School of Biomedical Sciences for their direct and indirect contributions to the project. The assistance of Dr. J. K. Alexander, Mr. Larry Kvols, and Miss Bobelai Malick of Baylor University College of Medicine in the recording of the direct (intra-arterial) blood pressure data is sincerely appreciated. Finally, it is a pleasure to thank my wife and sons for the encouragement, support, and cooperation which have facilitated the completion of this project.

Arthur E. Schulze
Houston, Texas
August, 1968

TABLE OF CONTENTS

		Page No.
	PREFACE	iii
	LIST OF FIGURES	v
	LIST OF TABLES	viii
I.	INTRODUCTION	1
II.	THE TECHNIQUES AND PHYSIOLOGY OF THE AUSCULTATORY METHOD FOR THE MEASUREMENT OF BLOOD PRESSURE	5
III.	PURPOSE	11
IV.	SYSTOLIC AND DIASTOLIC DETECTION CRITERIA	12
V.	DESCRIPTION OF THE SYSTEM	32
VI.	DATA ON SYSTEM PERFORMANCE	43
VII.	ANALYSIS OF DATA AND DISCUSSION OF SYSTEM OPERATION	47
VIII.	CONCLUSIONS	54
	BIBLIOGRAPHY AND REFERENCES	55
	APPENDICES	
	A. Circuit Diagrams	
	B. Bilateral Direct Blood Pressure Data	
	C. Cuff Microphone Characteristics	
	D. Bandpass Characteristics of Variable Bandpass Filters	
	E. Bandpass Characteristics of Pre-Processing Filters	
	VITA	

LIST OF FIGURES

Figure No.	Title	Page No.
1	Data required for the indirect measurement of blood pressure by the auscultatory method	13
2	Arm surface pulsations and observer's decision marks for 3 subjects	15
3	Arm surface pulsations filtered by various high-pass filters	19
4	Arm surface pulsations filtered by various band-pass filters	20
5	Arm surface pulsations filtered by various wide band-pass filters	21
6	Arm surface pulsations filtered by 10-30 Hz and 80-110 Hz band-pass filters (24 db/octave)	23
7	Selective filtering as a method for obtaining systolic and diastolic criteria	24
8	Simultaneous direct and indirect blood pressure measurements on an obese 49-year-old female	26
9	Simultaneous direct and indirect blood pressure measurements during irregular heart activity	27
10	Block diagram of system for automatic measurement and digital display of systolic and diastolic blood pressures	33
11	The Vital Signs Indicator, cuff pump/deflator, pressure transducer, occluding cuff with mounted microphone, and electrodes	39
12	The automatic sphygmomanometer connected to a subject	40
13	The Vital Signs Indicator with the top panel removed to show the internal layout	41

LIST OF FIGURES (Cont.)

Figure No.	Title	Page No.
14	The circuit boards used for the sphygmomanometer portion of the Vital Signs Indicator	42
15	Calibration curve	44
16	Automated systolic blood pressure readings versus clinical systolic blood pressure readings	48
17	Automated diastolic blood pressure readings versus clinical diastolic blood pressure readings	49
18	Histogram of systolic blood pressure readings	50
19	Histogram of diastolic blood pressure readings	51
A1	Electrocardiograph preamplifier (Board BP-7)	A-2
A2	Sounds and pressure preamplifiers (Board BP-6)	A-3
A3	Sounds filter pre-processor and pressure inverter (Board BP-1)	A-5
A4	ECG filter pre-processor and pulse generator (Board BP-100)	A-6
A5	Sounds and pressure recognition pre-processor (Board BP-2)	A-8
A6	Analog-to-digital converter, ECG SEARCH generator, and systolic/diastolic recognition logic (Board BP-3)	A-10
A7	Decade counter, storage register, and decoder/driver circuitry (Boards BP-4 and BP-5, two required)	A-12
A8	Calibrator unit (Board S-100)	A-14
A9	Systems wiring diagram	A-15

LIST OF FIGURES (Cont.)

Figure No.	Title	Page No.
B1	Bilateral intra-arterial blood pressure during a slow cuff inflation	B-2
B2	Bilateral intra-arterial blood pressure during a cuff deflation	B-3
B3	Bilateral intra-arterial blood pressure during cuff inflation and sustained cuff pressure	B-5
B4	Bilateral intra-arterial blood pressure during sustained cuff pressures and rapid deflation	B-6
B5	Bilateral intra-arterial blood pressure with cuff on forearm (distal to $1A_1$)	B-7
B6	Bilateral intra-arterial blood pressure during cuff inflation and deflation with cuff on forearm (distal to $1A_1$)	B-8
C1	Detailed drawings of cuff microphone and coaxial cable	C-2
D1	Measured bandpass characteristics of Krohn-Hite filter for dial settings of 10 and 30 Hz	D-2
D2	Measured bandpass characteristics of Krohn-Hite filter for dial setting of 80 and 110 Hz	D-3
E1	Bandpass characteristics of low-frequency filter circuit shown in Figure A3	E-2
E2	Bandpass characteristics of high-frequency filter circuit shown in Figure A3	E-3

LIST OF TABLES

Table No.	Title	Page No.
I.	Summary of filter frequencies used for pre-procession sound signals	17
II.	Data for diastolic decision thresholds	29
III.	Measured time relationships between R-wave of ECG and the sounds recognized as Korotkoff sounds	37
IV.	Blood pressure measurements	45

I. INTRODUCTION

The auscultatory method for the indirect measurement of blood pressure was proposed by N. S. Korotkov (Korotkoff) in 1905 (21). Since that time, the method has gained acceptance as a clinical technique for measuring arterial blood pressure. The origin and significance of the auscultatory blood pressure sounds (called Korotkoff sounds) were the subject of controversy when Korotkoff first presented his work. The exact mechanisms of origin are still unresolved (10), but the significance of the sounds in blood pressure measurement has gained wide acceptance. The best index of identifying the diastolic end point is still being debated (27).

Theories on the genesis of the Korotkoff sounds have included water hammer effects, preanacrotic effects, heart sounds transmission through the blood stream, fluttering vessel walls, blood turbulence, and blood cavitation mechanisms (10,27,28). The first sound obtained during deflation after occlusion of the artery by a cuff has been universally accepted as the index of systolic pressure. The index for identifying diastolic pressure has been studied by many investigators. Some investigators have proposed that the point of muffling of sounds be used as the diastolic index as opposed to the last audible sound which Korotkoff used (33,38,43,47). In 1951, a committee of the American Heart Association recommended that the cessation of sounds be accepted as the diastolic index (6). Research which recently was reported (27) has supported this recommendation (6). Thus, the method for the indirect measurement of blood pressure proposed by Korotkoff is used today in essentially the same manner as it was used over sixty years ago, even though no universally accepted explanations exist for the genesis of the Korotkoff sounds.

Under ideal measuring circumstances, with well-trained observers, indirect auscultatory blood pressure measurements on normal subjects have been shown to correlate well with intra-arterial pressures in the brachial artery (3,17,18,26,34,36,38, 47). The following factors are among those which contribute to variances in the measurement of blood pressure by the auscultatory method:

A. Instrument errors

1. Inaccuracies of sphygmomanometer (calibration errors, hysteresis, etc.)
2. Cuff width
3. Cuff length
4. Stethoscope response characteristics

B. Observer errors

1. Mental concentration
2. Reaction time
3. Auditory acuity
4. Confusion of auditory and visual cues
5. Interpretation of sounds (training and experience)
6. Rate of inflation
7. Rate of deflation
8. Prejudice (anticipation of reading in the region about 120/80 mm Hg)
9. Terminal digit preference
10. Excessive or inadequate pressure applied to stethoscope

11. Cuff placement and circumference adjustment

12. Stethoscope placement

C. Background noise

D. Artifacts in arterial pressure due to compression of the brachial artery

E. Patient condition (obesity, shock, various heart valvular conditions, etc.)

The magnitude of these variances still permits the use of the auscultatory blood pressure readings to make clinical decisions regarding diagnosis and treatment of hypertension and hypotension. However, in epidemiological studies of blood pressure, the variations in measurements that can be found between observers on a given individual impedes the comparison of data (25,41). Thus, the problem of obtaining uniform data lies more with the erratic utilization of the auscultatory technique than it does with the technique itself.

Automatic instrumentation designed for monitoring blood pressure has the potential of performing in a uniform manner, over extended periods of time, without fatigue or inter-observer variations. The advantages of such an instrument would benefit the epidemiologist, surgeon, anesthesiologist, nursing staff of intensive care units, as well as the clinician. The extensive use of the auscultatory technique makes it a natural choice as the technique to be instrumented for the automatic indirect measurement and monitoring of blood pressure. The data obtained from such a system are then more comparable to the usual clinical measurements than would data gathered

by other blood pressure measurement techniques. In addition to eliminating inter-observer variations, it is possible that the automatic electronic blood pressure monitor can provide the additional selectivity, reproducibility, and sensitivity which might be required to realize the full potential of the auscultatory technique for the measurement of arterial blood pressure. For example, perhaps more information is contained in the sounds from a compressed artery than can be heard and properly interpreted by a clinician using a stethoscope. The clinician hears the sounds within a very limited bandwidth (determined by his ear and stethoscope) located in a particular portion of the spectrum; whereas, the bandwidth of an electronic system can be controlled and placed in a more optimum portion of the spectrum for the purpose of making the systolic and diastolic decisions. These considerations comprise the impetus for the development of a system for the automatic measurement and digital display of systolic and diastolic blood pressures and for the selection of the auscultatory technique.

II. THE TECHNIQUES AND PHYSIOLOGY OF THE AUSCULTATORY METHOD FOR THE MEASUREMENT OF BLOOD PRESSURE

The auscultatory method of measuring systolic and diastolic blood pressures involves the use of an inflatable cuff to temporarily occlude an artery in an extremity. After rapidly inflating the cuff, a stethoscope is placed gently over the artery distal to the cuff and the cuff is deflated slowly. Usually, the cuff is placed around the arm and the stethoscope is placed over the artery in the antecubital space. The air pressure in the cuff is read when the first sound is heard through the stethoscope; this pressure is called the systolic pressure. As the cuff is deflated further, the character of the sounds due to each heart beat (called Korotkoff sounds) changes; and in most patients, the sounds quite suddenly disappear. The pressure measured at the time that the sounds disappear (or suddenly muffle, if they do not disappear) is called the diastolic pressure. A complete description of the recommended standard procedure for human blood pressure determinations by sphygmomanometers is given by Bordley, et al. (6).

The Korotkoff sounds are postulated by some investigators to be produced by changes in the rate of blood flow through a partially occluded artery. If the externally applied pressure from an inflatable cuff is transmitted, without amplification or attenuation, through the tissues to the brachial artery, and if the arterial wall offers little resistance to the compressive force, then the artery will collapse totally when the pressure in the cuff equals or exceeds the intraluminal systolic arterial pressure. When this total collapse and cessation of flow occurs, no sound is heard through a stethoscope placed over the brachial artery, distal to the cuff, at the antecubital space. As the external pressure is reduced, four sound phases are identified as the blood flow progresses

from no blood flow to full or unrestricted blood flow (11). It is postulated that, when the occluding pressure falls slightly below the systolic pressure, a small quantity of blood is ejected past the constrictive point and a "light tap" or "thud" occurs which is identified as the first phase of the Korotkoff sounds. The first such pulse to occur during deflation, after occlusion, is recognized as the index of systolic pressure. In a normal person, phase I sounds are heard over a range of approximately 10 millimeters of mercury. As the cuff pressure is further reduced, blood flows through longer portions of the cardiac cycle and changes occur in both the quality and intensity of the Korotkoff sounds. The phase 2 sounds are "soft, inconstant murmurs" which occur over a range of approximately 10 millimeters of mercury in the normal person. "Loud," "long," and "clear" sounds distinguish the phase 3 sounds which are heard over a range of approximately 15 to 20 millimeters in the normal person. At the end of the third phase, the sounds become "dull and muffled" and these fourth phase sounds are normally heard over a range of approximately 10 millimeters of mercury. The sounds disappear as the cuff pressure is reduced further. The diastolic index of pressure is the disappearance of the fourth phase sounds.

One commonly occurring anomaly is the phenomenon known as the "auscultatory gap" (11, 36, 43). This term is used to refer to the disappearance of the Korotkoff sounds during cuff deflation over a fairly large range of pressures between the first sounds and a cuff pressure level above that of the diastolic pressure. Although the cause of the auscultatory gap is not known, the disappearance and reappearance of the sounds are related to the venous pressure in the arm (36). The auscultatory gap has been reported to occur more often when the cuff is inflated slowly (36).

The Korotkoff sounds appear to be generated as the leading edge (rising portion) of the interluminal arterial blood pressure pulse exceeds the externally applied pressure. The temporal relationships of the Korotkoff sounds and the electrical activity of the heart have been examined in detail by London and London (26) and by Rodbard, et al. (39). It was observed that the Korotkoff sounds occurred progressively earlier in the cardiac cycle as the cuff pressure was reduced from the systolic pressure toward the diastolic pressure. The time interval between the R wave and the first Korotkoff sound is reported in one study (26) to average 160 milliseconds with a range of 140 to 220 milliseconds. Rodbard (39) succeeded in constructing a calibrated upstroke of an arterial blood pressure curve by using the cuff pressure and the temporal relationships between the arterial sounds and the electrocardiogram.

The quality and intensity of the Korotkoff sounds appear to be related to the anacrotic gradient of the pressure pulse; i.e., the rate of change of the arterial pressure during systole (53). This would explain, in part, the difficulties involved in distinguishing and recognizing the Korotkoff sounds on patients in shock and the clinical experience where radial pulsations are detected before Korotkoff sounds are heard. Experiments have shown that, after an injection of norepinephrine, only those pressure waves which possess a steep anacrotic gradient generate audible Korotkoff sounds (53).

The sound[1] waveforms recorded from over the brachial artery during an indirect

---

[1]The word "sound" is used to denote the arm surface pulsation recorded from a microphone which may be associated with a Korotkoff sound heard through a stethoscope. The term "Korotkoff sounds" is reserved for those audible sounds identified by an investigator employing a stethoscope. The term "arm surface pulsations" refers to the pulsations measured at the surface of the arm regardless of their spectral content; i.e., the frequency components might all be below the audible range.

blood pressure measurement are complex waveforms which vary in amplitude, period, and spectral content from pulse-to-pulse during a single measurement, from measurement-to-measurement on the same person, and from individual-to-individual. The frequency content of the blood pressure sounds has been measured by several researchers using a variety of techniques (8,15,35,37,49,50). The reports on this research have revealed a large divergence of opinions on the spectral content of the sounds. Significant data are given by Ware and Anderson (50) and Rauterkus, et al. (37). These data are the measured frequency spectrum for each of the four phases of the sounds.

Rauterkus, et al. (37) conclude that:

> Most of the sound energy is generally located below 50 cps with the most prominent peaks occurring below 20 cps. For phases 1 and 4 sounds the sound energy is often heavily localized below 20 cps, whereas for phase 2, and especially, phase 3 sounds the energy tends to be more broadly distributed in the 0 to 50 cps range.

Ware and Anderson (50) sum up their findings as follows:

> ...the following sequence of events [occurs] during a cuff deflation cycle: 1) appearance of sounds with low-frequency energy predominating (systolic pressure endpoint), 2) appearance of greater high-frequency energy content (phases 2 and 3), 3) disappearance of high-frequency components (diastolic pressure endpoint).

It is interesting to note that the impetus for studies of the spectral content of the blood pressure sounds has been the acquisition of data for the design of indirect blood pressure monitoring equipment. However, the researchers have omitted the sound spectra which exist prior to the systolic index (phase 0) and those which exist after the diastolic index (phase 5). A knowledge of these spectra is essential to the

development of criteria for the systolic and diastolic decisions. The following statement by Rauterkus, et al. (37) points up the need for missing data:

> Any device designed to recognize Korotkov sounds must do so on an individual, real time basis; the device cannot respond to the average components of a sequence of sounds.

McCutcheon and Rushmer (31) have reported the spectral changes in the sounds that occur at muffling. The spectrum of the sound preceding muffling was compared with that of the muffled sound and with that of the sound following muffling. They observed that an attenuation of the frequencies above approximately 60 Hz corresponds with muffling. In an earlier report, McCutcheon, et al. (32) concluded that the muffling of the Korotkoff sounds resulted from the attenuation of sound frequencies between 50 and 90 Hz.

There are several dynamic reactions which are produced by compression of the brachial artery, but they are seldom discussed in connection with the indirect measurement of blood pressure because it is thought that they usually neutralize each other (53). London and London (26) observed that as the cuff pressure rises above the distal diastolic pressure the distal intra-arterial systolic peaks also rise. The systolic pressure distal to the cuff remains elevated until the artery is completely occluded and through the decompression phase until the cuff pressure falls below the diastolic pressure. They report that "[i]n 135 recordings, the average rise in distal systolic pressure during compression was 11 millimeters of mercury above resting levels." During decompression, they report an average rise in distal systolic pressure of 12 millimeters of mercury. No significant change in the systemic arterial pressure was observed. They speculate that the rise in the distal systolic pressure might be attributed to venous occlusion or

to some form of local vascular reaction such as a change in arterial tone. In a second paper (27), they state that "[t]his response of the distal brachial artery to compression and decreased blood flow suggests local vasoconstriction." Whenever the flow of blood in an artery is stopped by occlusion, the kinetic energy associated with the blood flow is converted into the potential energy associated with blood pressure. Studies have shown that such energy conversion elevates the systolic pressure (53). The summation of reflected waves in an occluded artery could also influence the pressures in the artery. The arterial pressure pulse loses energy to the tissues of the arm, cuff, and sphygmomanometer. Thus, there are disturbance mechanisms associated with the blood pressure measurement which may tend to cancel each other. It would not be expected that these dynamic reactions exactly cancel each other; however, the clinical accuracy of the technique for the measurement of the undisturbed arterial blood pressure appears adequate.

III. PURPOSE

The purpose of this project was to design, construct, and preliminarily evaluate a system for the automatic measurement and real-time digital display of systolic and diastolic blood pressures (a) by the utilization of the auscultatory indirect method, and (b) by the utilization of the relative advantages of analog and digital techniques in data processing and decision making. Design criteria for the system were to include provisions for a high degree of noise and motion artifact rejection by the use of (a) selective filtering, and (b) digital logic circuitry for inhibition of systolic and diastolic detection during cuff inflation and time periods of the cardiac cycle when auscultatory sounds cannot exist at the position of the microphone. The design was also to take advantage of current technology. The systolic and diastolic decision criteria were to be derived from simultaneous direct and indirect measurements. The system was to be preliminarily evaluated by obtaining readings of systolic and diastolic simultaneously by experienced observers and by the electronic system.

IV. SYSTOLIC AND DIASTOLIC DETECTION CRITERIA

In the measurement of blood pressure by the auscultatory technique, two channels of data are utilized--the cuff pressure and the Korotkoff sounds. Figure 1 is a diagrammatic representation of the data utilized by a clinician for the indirect measurement of blood pressure by the auscultatory method. The sounds shown on this chart were those sounds transduced by a piezoelectric microphone placed over the brachial artery at the antecubital fossa and filtered at 45 Hz (3-db point) by a high-pass filter with a 12-db per octave slope. Thus, the sounds shown here may be considered to be a representation of the Korotkoff sounds which the clinician might hear through his stethoscope during the measurement.

The design of an electronic system to automatically make auscultatory blood pressure measurements requires that an analysis be made of the characteristics of sounds recognized in the auscultatory method such that the bases of systolic and diastolic decisions can be expressed in terms of parameters which can be measured. An encapsulated piezoelectric microphone manufactured by Air Shields, Inc. for use in the measurement of blood pressure was chosen. Appendix C describes the characteristics of the microphone. This microphone is placed in a pocket at the distal edge of a standard blood pressure cuff (a "Tycos" snap-fastened cuff manufactured by Taylor Instrument Co., possessing an inflatable bladder which is 13 cm. wide) such that the face of the microphone contacts the surface of the arm during the inflation and deflation of the cuff. When the microphone was driven mechanically by a displacement source (another similar microphone), the output

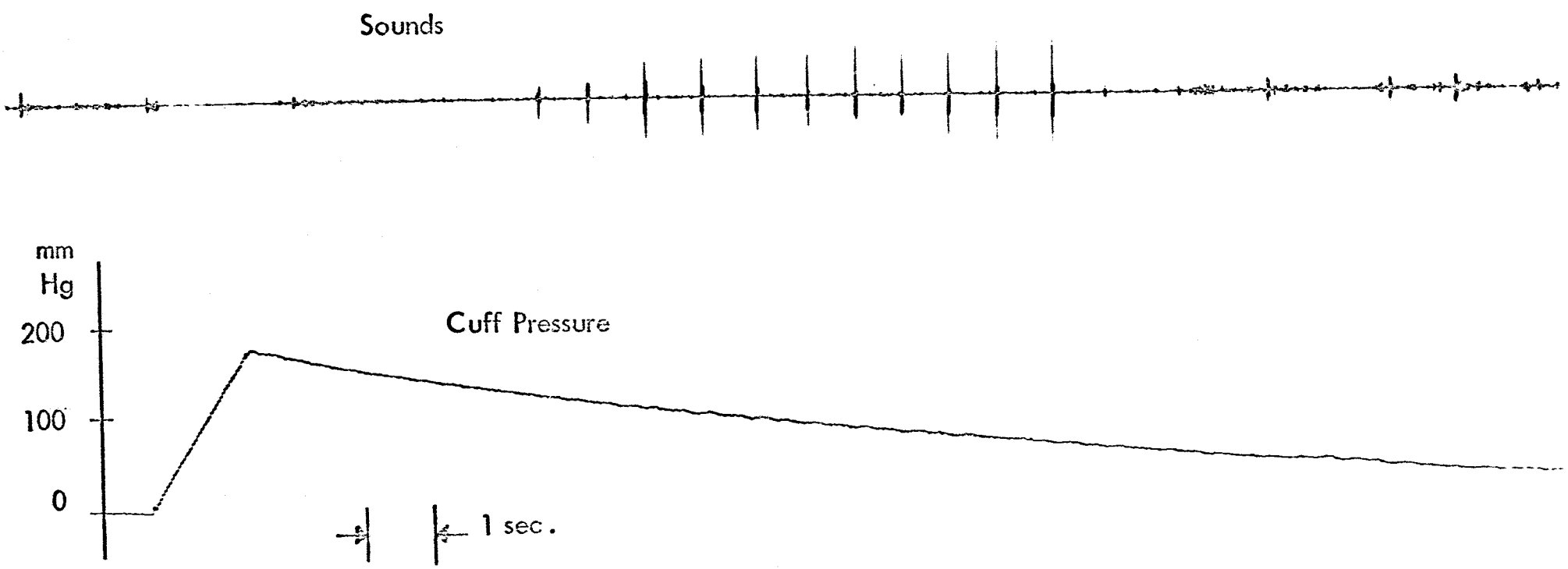
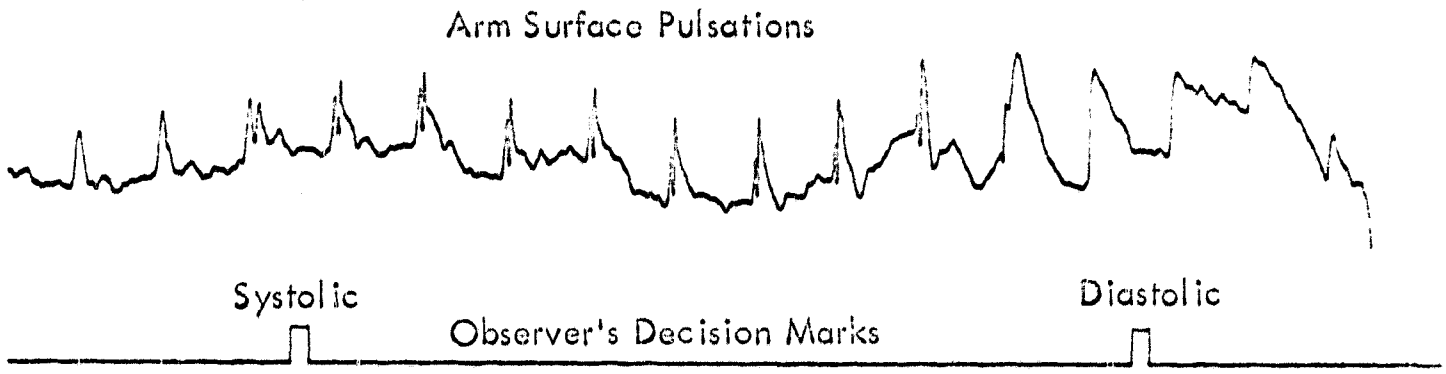


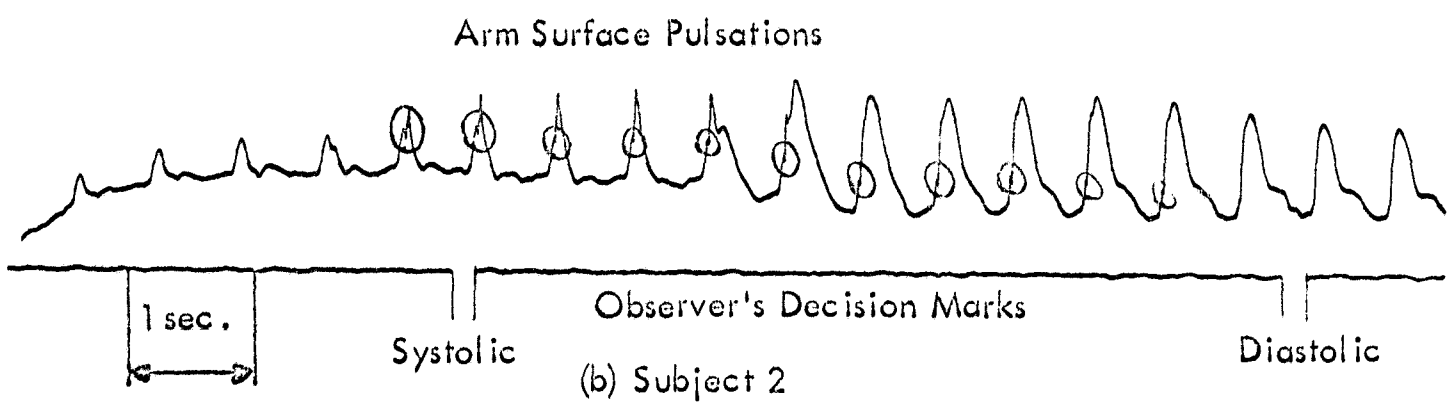
Figure 1 - Data required for the indirect measurement of blood pressure by the auscultatory method

impedance of the microphone and cable were found to vary from approximately 500,000 ohms at 10 Hz to approximately 60,000 ohms at 100 Hz in a manner defining a series capacitance model for the microphone and cable with a capacitance of approximately 0.027 microfarads. The usual equivalent circuit for a piezoelectric element is a voltage source in series with a capacitor. Such a microphone is responsive to displacement and the low-frequency cutoff is determined by the input impedance of the preamplifier. It is obvious that, in order to preserve the very low frequency components of the transduced signal, the use of a preamplifier with an input impedance of 10 megohms or greater is essential. A field-effect transistor was used in the design of the preamplifier which had a 3-db bandwidth extending from 3.5 Hz to 450 kHz. Since the output of the microphone is on the order of one volt (peak-to-peak) for normal sound input levels, a voltage gain of 2 was sufficient for satisfactory recording of sounds.

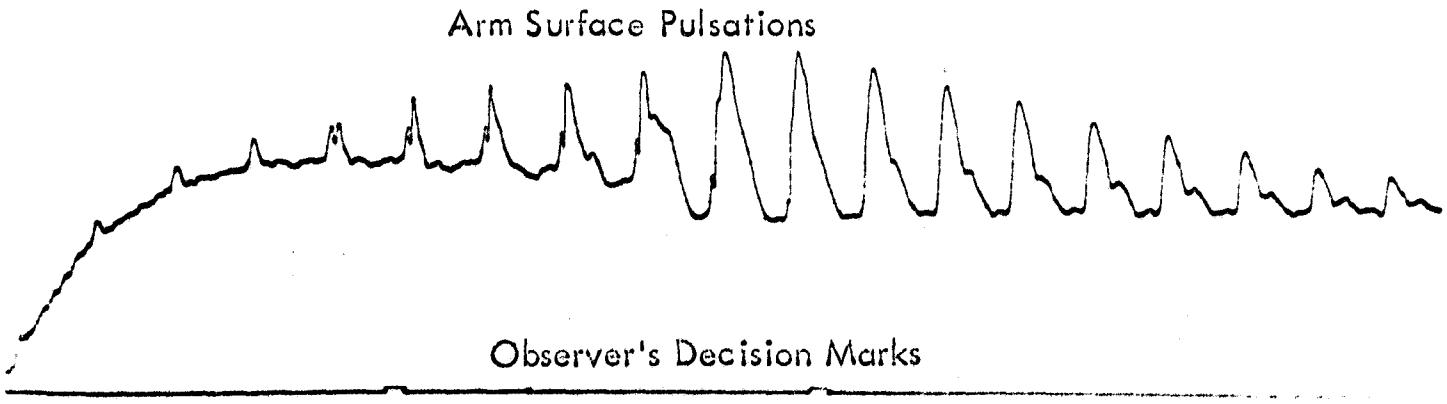
The microphone and preamplifier were used to record the data shown in Figure 2. In Figure 2 is shown the chart tracings from one measurement on each of three subjects. In each of the three measurements, the upper tracing is the arm surface pulsations as transduced by the microphone and amplified by the preamplifier described above. The 3.5-Hz low-frequency cutoff of the preamplifier is suffiently low to permit the recording of the pressure wave at the surface of the arm. The waveforms recorded in this manner are similar in shape to intra-arterial waveforms. The lower tracings are decision marks which were made by an experienced clinician based upon the auditory indices of systolic and diastolic blood pressure as he heard them through his stethoscope. The reaction time of the observer was approximately 0.3 second.



(a) Subject 1



(b) Subject 2



(c) Subject 3

Figure 2 - Arm surface pulsations and observer's decision marks for 3 subjects

The diastolic decision mark was made when the observer failed to hear a sound at the approximate expected time interval from the previous recognized sound. Hence, the diastolic decision mark should lag the pressure pulse immediately following the last recognized sound by approximately the reaction time of the observer. Examination of numerous recordings of this type revealed that certain changes in the character of the recorded arm surface pulsation signals are related to the occurrence of the various Korotkoff sounds as heard by an observer through a stethoscope. These characteristics are of the form of high-frequency notches and can be seen in Figure 2 (they are circled on the data for the second subject). The notches were found to occur initally with the onset of the Korotkoff sounds and to disappear with the cessation of Korotkoff sounds. Thus, empirically, it appears that the notches could be a manifestation of the Korotkoff sounds. Examination of these data suggests that a basis for the systolic and diastolic pressure decisions might be developed if the changes in the characteristics of the arm surface pulsations at the systolic and diastolic cuff pressures which are evident in Figure 2 could be accentuated by proper processing of the microphone signal.

Pre-processing of the sounds signal through filters of various bandpasses is reported in the literature. Table I is a summary of filters which have previously been used in the development of automatic indirect blood pressure measuring devices. It is obvious from Table I that there is no universally accepted filter developed for this purpose--the variance in filter frequencies is large. Each filter which is reported as a part of a system is, to a large extent, designed around the microphone and pre-amplifier which were used.

TABLE I

SUMMARY OF FILTER FREQUENCIES USED FOR PRE-PROCESSING SOUND SIGNALS

Reported by	Filter Pass-Band Frequencies	Comments
Bolie et al. (5)	2 to 100 Hz	
London and London (27)	120 to 500 Hz	Set to correspond with their clinical acuity. Very gradual roll-off. The only lower frequency tried was 40 Hz.
Ono (35)	28 and 45 and 150 Hz (three filters)	"narrow bandpass filters"
Follett et al. (14)	1,000 to 2,000 Hz	"falling rapidly above or below this range"
Allred and Johnson (1)	40 Hz (essentially low pass)	48 db/octave roll-off above 40 Hz 7 db/ octave roll-off below 40 Hz
Rogge et al. (40)	12 to 34 Hz	Probably 12 db/octave roll-off
Smith and Bickley (46)	32 to 40 Hz	
Canzoneri et al. (9)	0 to 50 Hz	
Ware and Kahn (51)	40 and 90 and 150 Hz (three filters)	"sharply tuned filters"
Geddes (15)	15 to 50 Hz	"effective frequency band width"

In this project, the sounds recorded from numerous subjects were passed through variable band-pass filters in an attempt to determine the pre-processing filter which would allow reliable detection of both the systolic and diastolic indices for the microphone and preamplifier described above. The outputs of a Krohn-Hite Corp. Model 330M variable filter (typical bandpass characteristics shown in Appendix D) for a typical recording of sounds is shown in Figure 3. For these recordings, the upper cut-off frequency of the filter was set at 5 kHz on the dial. The frequency response of the Brush Mark 280 recorder which was used is flat within 2% to 100 Hz for a 10-division peak-to-peak signal. The lower cut-off frequency is marked on each tracing. Narrow band-pass filter studies were also made. The arm surface pulsations filtered by various bandpass filters are shown in Figures 4 and 5. The upper and lower cut-off frequencies from the dials of the variable filter are marked above each of the tracings.

When the piezoelectric microphone and preamplifier above were used on 13 adult subjects (4 females and 9 males) ranging in age from 26 to 53, it was found that filtering of the preamplifier output with a 10 to 30 Hz[2] bandpass filter possessing slopes of 24 db/octave (Appendix D) provided excellent detection of the changes in the characteristics of the arm surface pulsations that occur at cuff pressures coincident with the systolic index. The detection of the first occurrence of the notch on the

---

[2]These values are the nominal values marked on the dials of the Krohn-Hite Corp. Model 330M variable filter. The measured bandpass characteristics are shown in Appendix D. Thus, the bandpasses stated in this chapter; marked on Figures 6,7,8, and 9; and used in gathering the data of Table II, refer to the dial markings on the variable filter and the actual bandpasses resemble those shown in Appendix D.

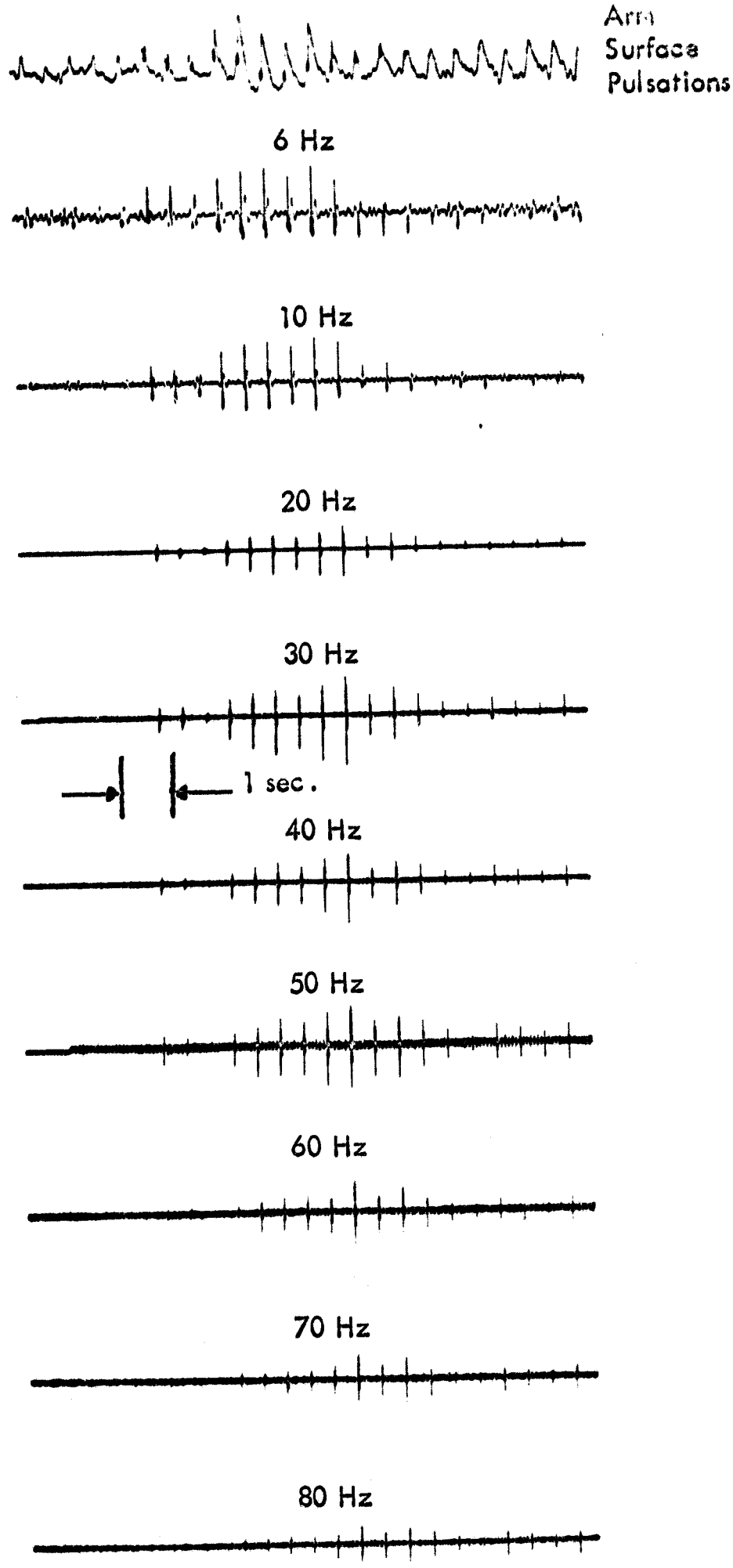


Figure 3 - Arm surface pulsations filtered by various high-pass filters

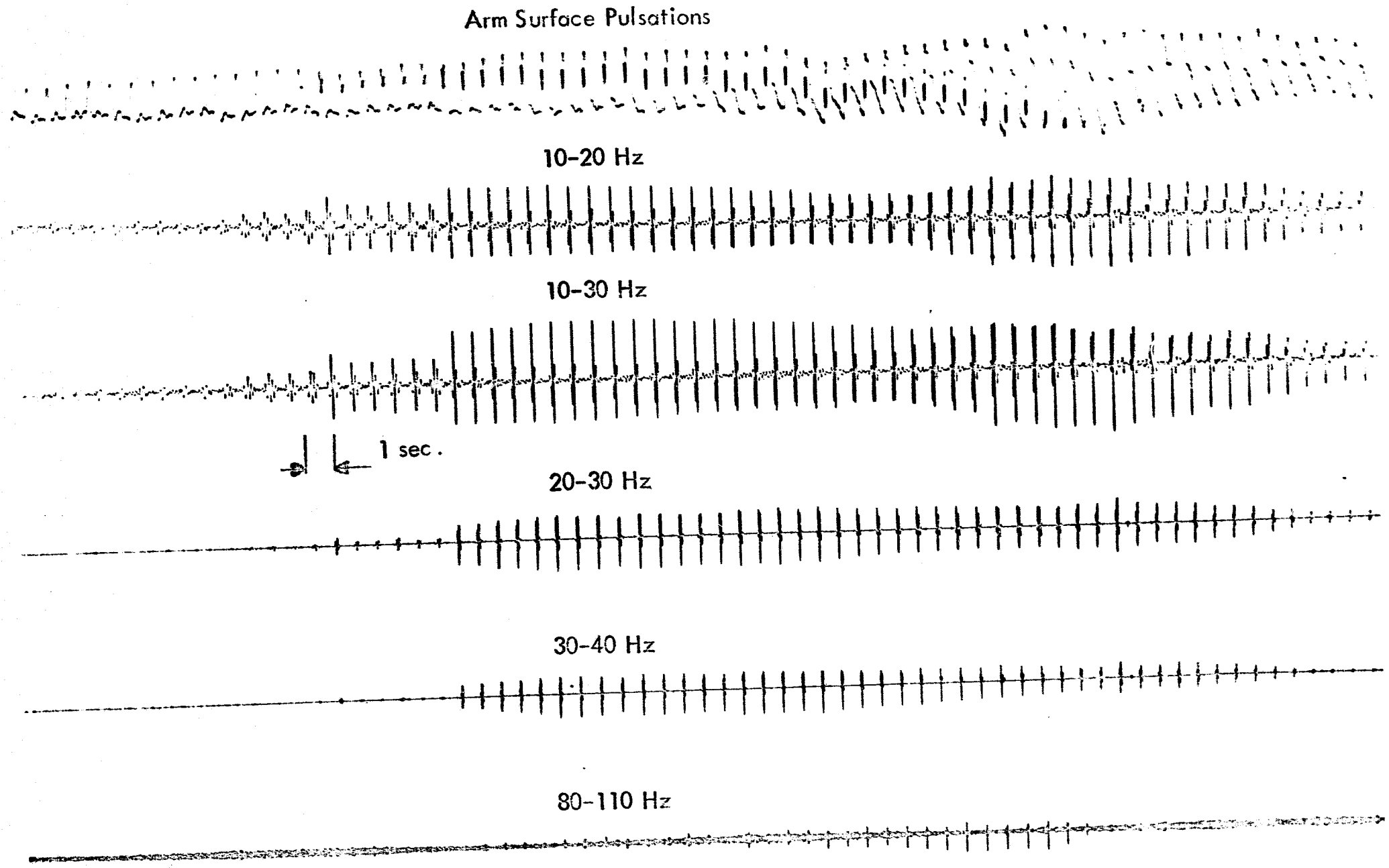


Figure 4 - Arm surface pulsations filtered by various band-pass filters

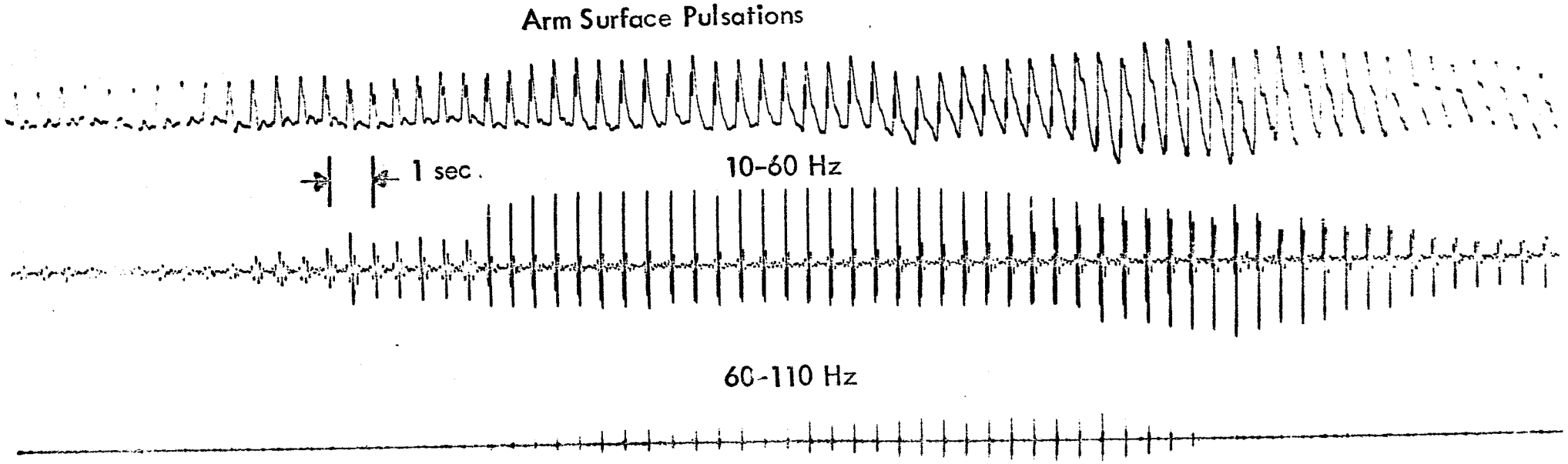
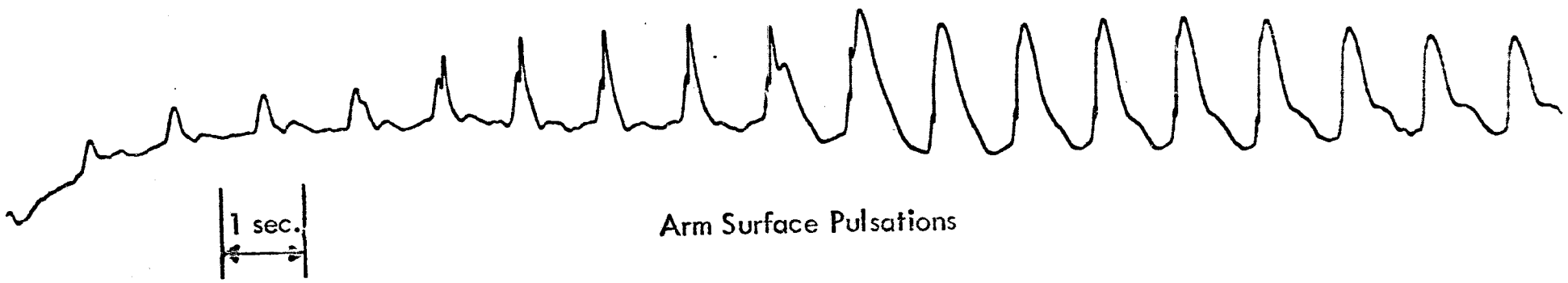


Figure 5 – Arm surface pulsations filtered by various wide band-pass filters

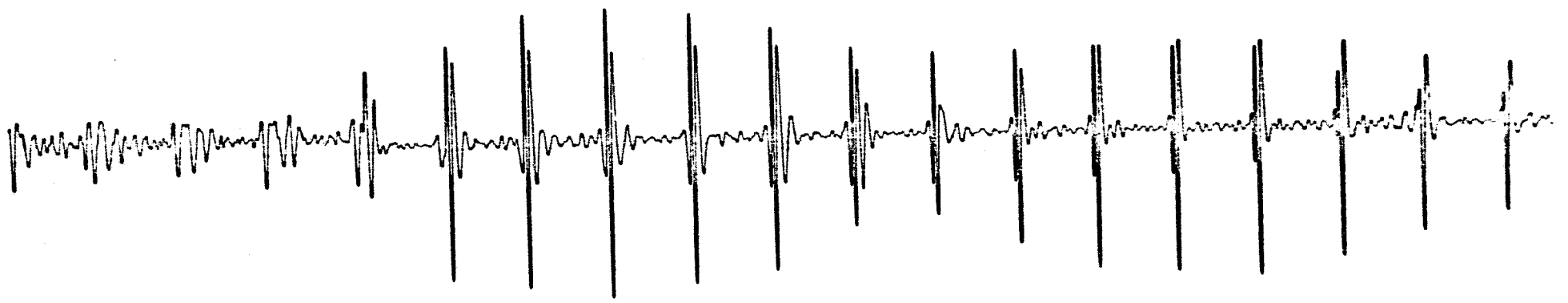
output of the arm surface pulsations by the 10 to 30 Hz bandpass filter is evident in Figures 6 and 7. When the arm surface pulsations were applied to an 80 to 110 Hz bandpass filter (24 db/octave) (Appendix D), the output was found to provide a demarcation between the last sound possessing the higher frequency notch and the arm surface pulsation following that sound (as shown in Figures 6 and 7 where the amplitude of the output of the 80 to 110 Hz bandpass filter suddenly drops). A single filter was not found which would adequately filter the arm surface pulsations such that both the systolic and diastolic decisions could be made precisely. Thus, selective filtering by the use of two filters of different bandpasses appears to be a usable method for obtaining the respective systolic and diastolic criteria required for electronic decision making.

The selection of the filter frequencies was confirmed by simultaneous direct and indirect measurements on four patients using the procedure of London and London (26). Under a local anesthetic, a #16 Cournand needle was placed into the brachial artery distal to the occluding cuff and connected to a Statham Model P23Db pressure transducer. The needle was flushed periodically with a heparinized saline solution. The cuff pressure was connected to another P23Db pressure transducer. The carrier amplifiers contained in an Electronics for Medicine recording oscilloscope system were used as pressure preamplifiers to drive a magnetic tape recorder. The sounds were recorded through the same microphone and preamplifier that were previously described. Results which are typical of these measurements are shown in Figures 8 and 9. The subject was a 49-year-old female Negro who had entered the hospital with congestive heart failure two weeks prior to the measurement.



Arm Surface Pulsations

10-30 Hz



80-110 Hz

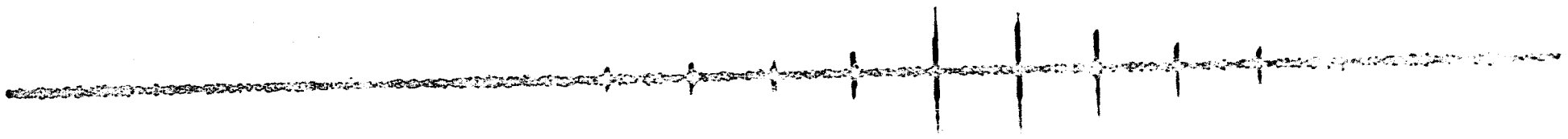


Figure 6 - Arm surface pulsations filtered by 10-30 Hz and 80-110 Hz band-pass filters (24 db/octave)

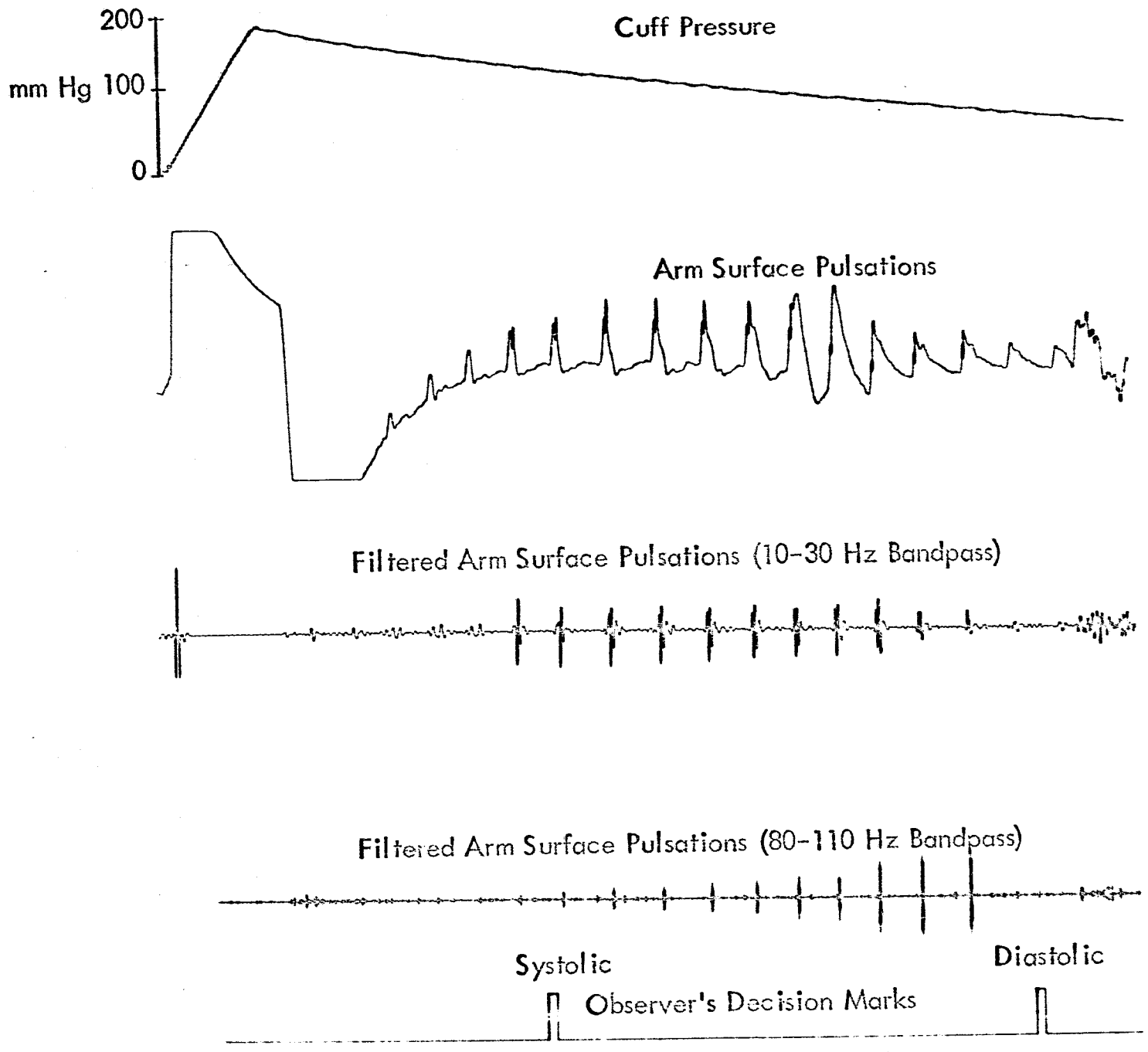


Figure 7 - Selective filtering as a method for obtaining systolic and diastolic criteria

She weighed 296 pounds at the time of the measurement and had lost over 40 pounds since entering the hospital. Inspection of Figure 8 shows that the observer did not hear a Korotkoff sound as the first pulse of blood flowed past the occluding cuff; however, a low frequency notch did appear in the corresponding arm surface pulsation. The following pulse did not penetrate the occluding cuff. A pronounced notch appeared on the arm surface pulsation corresponding to the pulse for which the first Korotkoff sound was recognized by the observer. This technique with a single direct connection to an artery does not allow an accurate determination of the last pulse for which the flow is partially occluded by the cuff. The data shown in Figure 8 would tend to suggest that the small oscillations on the intra-arterial pressure curves may be associated with partial occlusion of the artery; however, this has not been proven. Pulse-to-pulse variations in the systolic and diastolic pressures (especially in the patient from whom the data of Figures 8 and 9 were gathered) render the comparisons of direct and indirect blood pressures based on resting levels of direct blood pressure as practically useless where accuracies of a few millimeters of mercury are desired.

The problem of inadequate pressure and sound transmission in the arm of the obese patient can contribute to indirect blood pressure measuring variances (2). From the data of Figure 9, it is obvious that the observer did not recognize the first Korotkoff sound until the third pulse had flowed beneath the cuff. However, the first notch on the arm surface pulsations occurred with the first pressure pulse received by the pressure transducer from the artery distal to the cuff. The output of the 10 to 30 Hz filter on the arm surface pulsations also detected the event. On this same

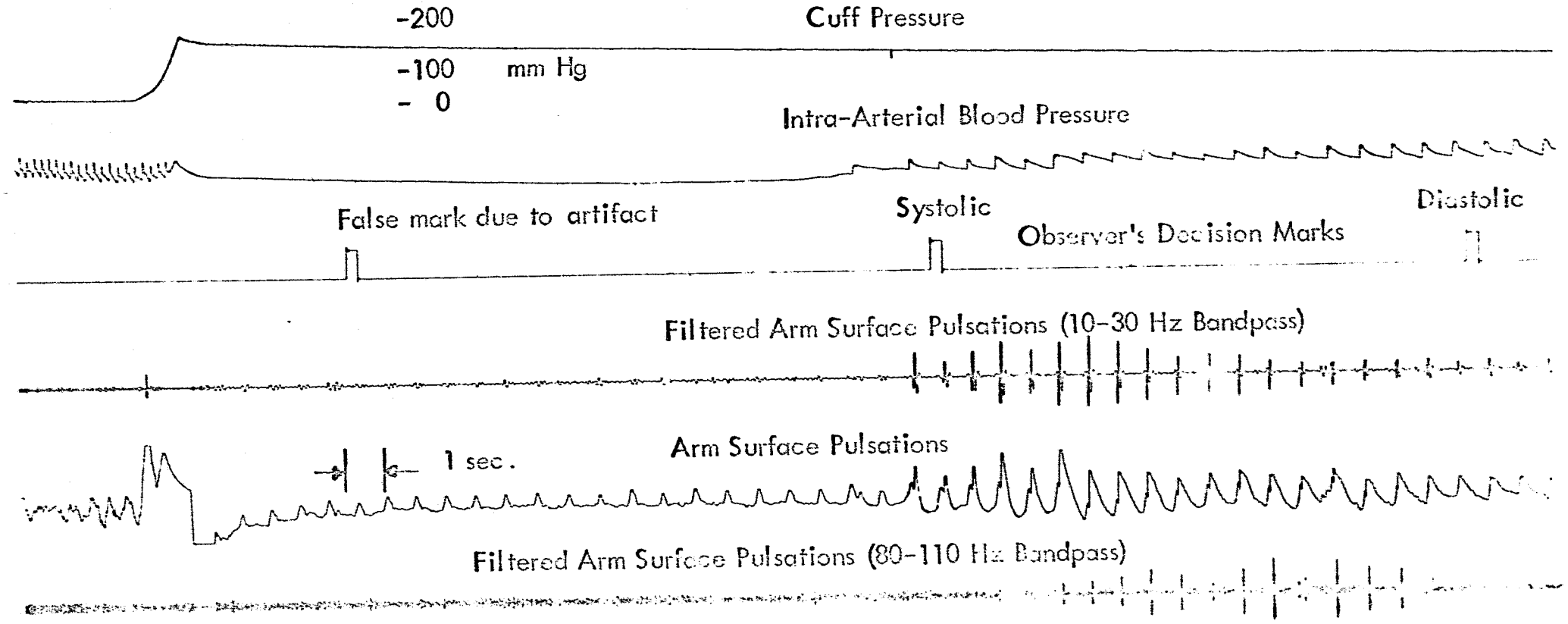


Figure 8 - Simultaneous direct and indirect blood pressure measurements on an obese 49-year-old female

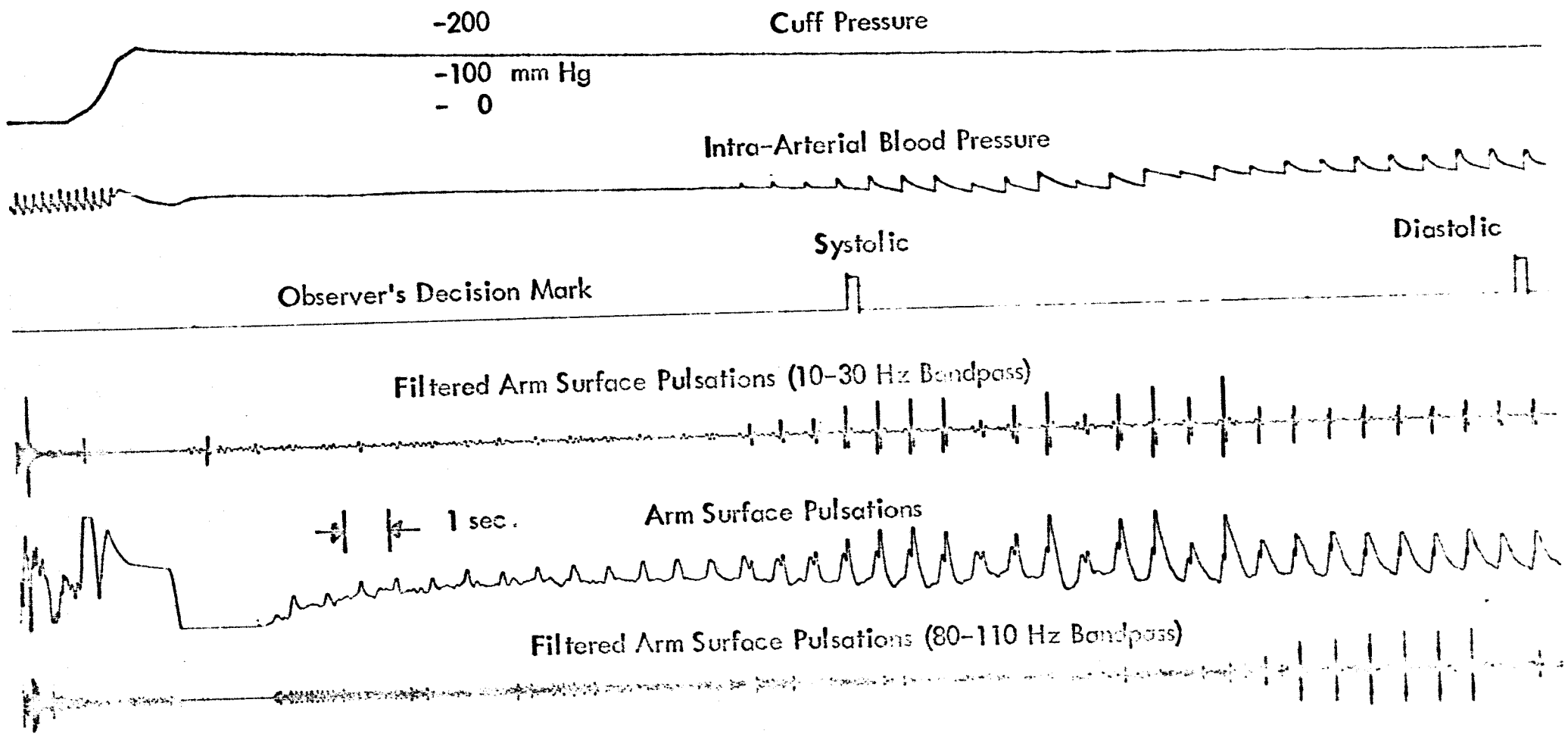


Figure 9 - Simultaneous direct and indirect blood pressure measurements during irregular heart activity

measurement, the observer marked the pulse for which he heard no sound in accordance with the diastolic pressure end-point criteria. However, on the pulse following the pulse for which a Korotkoff sound was not heard, the arterial diastolic pressure suddenly became lower and a Korotkoff sound was generated. The notch reappeared on the arm surface pulsations and the event is recognizable in the output of the 80 to 110 Hz filter. These data represent an example of a severe test of the performance of systolic and diastolic detection criteria.

It was determined that the systolic decision could be simply made by detecting the first output of the filters which exceeded a preset threshold. The threshold was set to a level slightly above the noise level and for the gain characteristics reported, a threshold of 0.3 volt was adequate.

A preliminary study to determine the proper utilization of the outputs of the 10 to 30 Hz and 80 to 110 Hz filters for the diastolic decision was conducted on 5 young male subjects. A summary of these data is given in Table II. The peak magnitude of the output of each filter at the last sound was determined (E_{HD} and E_{LD} for the 80 to 110 Hz and 10 to 30 Hz outputs respectively). Then, the peak amplitude of the output of each filter for the entire deflation cycle was determined (E_H peak and E_L peak for the high and low frequency filters respectively). The ratios of the peak magnitude of the outputs at the last recognized Korotkoff sound to the peak outputs for the entire deflation cycle were tabulated (E_{HD} / E_H peak and E_{LD} / E_L peak). Similar ratios were formed by dividing the peak amplitude of the output of each of the filters for the arm surface pulsation following the last recognized Korotkoff sound (E_{HPD} and E_{LPD} for the high and low frequencies respectively) by the same peak

TABLE II - DATA FOR DIASTOLIC DECISION THRESHOLDS

SUBJECT	$\frac{E_{HD}}{E_H \text{ PEAK}}$	$\frac{E_{HPD}}{E_H \text{ PEAK}}$	$\frac{E_{LD}}{E_L \text{ PEAK}}$	$\frac{E_{LPD}}{E_L \text{ PEAK}}$
RES	0.208	0.200	0.385	0.077
RES	0.330	0.170	0.272	0.100
RES	0.910	0.294	0.440	0.086
RES	0.555	0.220	0.278	0.178
RES	0.728	0.200	0.500	0.172
RES	1.000	0.175	0.490	0.302
RES	0.286	0.139	0.431	0.270
RES	0.670	0.258	0.410	0.393
TJR	0.768	0.238	1.000	0.780
TJR	1.000	0.150	0.441	0.231
TJR	1.000	0.100	0.500	0.187
TJR	0.300	0.100	0.364	0.216
TJR	0.460	0.150	0.500	0.248
TJR	0.342	0.276	0.470	0.355
TJR	1.200	0.180	0.772	0.303
SMS	0.333	0.145	1.000	0.680
SMS	0.402	0.400	1.040	1.115
SMS	0.260	0.200	0.568	0.512
SMS	0.500	0.222	0.684	0.724
SMS	0.284	0.133	1.000	0.772
SMS	0.134	0.134	0.920	0.840
SMS	0.350	0.143	1.090	1.190
SMS	0.400	0.050	0.422	0.367
SMS	0.702	0.198	0.388	0.456
SMS	0.613	0.148	0.428	0.328
SMS	0.621	0.200	0.412	0.412
FBV	0.166	0.083	0.612	0.408
FBV	0.100	0.100	0.681	0.407
FBV	0.212	0.169	0.610	0.411
FBV	0.139	0.092	0.757	0.445
FBV	0.156	0.085	0.865	0.369

continued on next page

TABLE II - (continued)

SUBJECT	$\frac{E_{HD}}{E_H \text{ PEAK}}$	$\frac{E_{HPD}}{E_H \text{ PEAK}}$	$\frac{E_{LD}}{E_L \text{ PEAK}}$	$\frac{E_{LPD}}{E_L \text{ PEAK}}$
MAC	1.440	0.087	1.285	0.500
MAC	0.850	0.160	0.755	0.755
MAC	1.000	0.144	1.020	0.850
MAC	1.000	0.125	0.893	0.853
MAC	0.870	0.111	1.040	0.670
MAC	0.318	0.146	1.040	0.692
MAC	0.308	0.185	1.000	0.893
MAC	1.285	0.074	0.798	0.760
MAC	0.615	0.192	1.045	0.900

E_{HD} = Peak output of 80-100 Hz filter at last sound.

E_{HPD} = Peak output of 80-110 Hz at pulse immediately following last sound.

E_{LD} = Peak output of 10-30 Hz filter at last sound.

E_{LPD} = Peak output of 10-30 Hz filter at pulse immediately following last sound.

E_H PEAK = Peak output of 80-110 Hz filter for entire deflation cycle.

E_L PEAK = Peak output of 10-30 Hz filter for entire deflation cycle.

amplitude of the output of each filter for the entire deflation cycle. These ratios (E_{HPD} / E_H peak and E_{LPD} / E_L peak) were also tabulated such that a comparison of ratios could be made. These data formed the basis for the design of the sounds detection logic of the pre-processor of the automatic system. A sound is detected whenever the output of either filter exceeds an initial threshold or a set fraction of its maximum peak value during a deflation cycle. The diastolic decision requires the outputs of both filters to drop below their respective set fractions of their maximum peak value. The utilization of two filters in this manner appears to be unique, although at least two investigators have used multiple filters (35, 51) in different detection schemes.

V. DESCRIPTION OF THE SYSTEM

A system was constructed utilizing the previously-stated detection criteria for the automatic measurement of blood pressure. Figure 10 is a block diagram of the system. The waveforms shown in this figure represent, in principle, system operation but are not actual waveform samples. The entire system may be divided by function into eight major units; (1) transducers, (2) cuff pump/deflator, (3) preamplifier, (4) preprocessor, (5) systolic/diastolic converter, (6) output unit, and (7) calibrator. The preamplifier unit consists of the electrocardiogram (ECG), arm surface pulsations (sounds), and pressure preamplifiers which are used to provide the proper input impedance characteristics. The preamplifier unit may be used simultaneously with, or independently of, the rest of the system to provide signals for tape recording or it may be bypassed for processing tape recorded signals.

The preprocessor unit is used to convert the raw signals from the preamplifier unit into usable form for making the systolic and diastolic decisions. The ECG band-pass filter has essentially the same characteristics that previously have been used in a cardiotachometer preprocessor (48). After the ECG signal is filtered, the absolute value of the ECG signal is compared against a fixed level which is set such that an output occurs for each R-wave from the ECG. The comparator output triggers a pulse with a 100-millisecond delay time and a 200-millisecond pulse width. This pulse is used to provide a time period of searching (or "listening") for the arm pulse sounds. The arm surface pulsations from the preamplifier unit (or tape recorder) pass

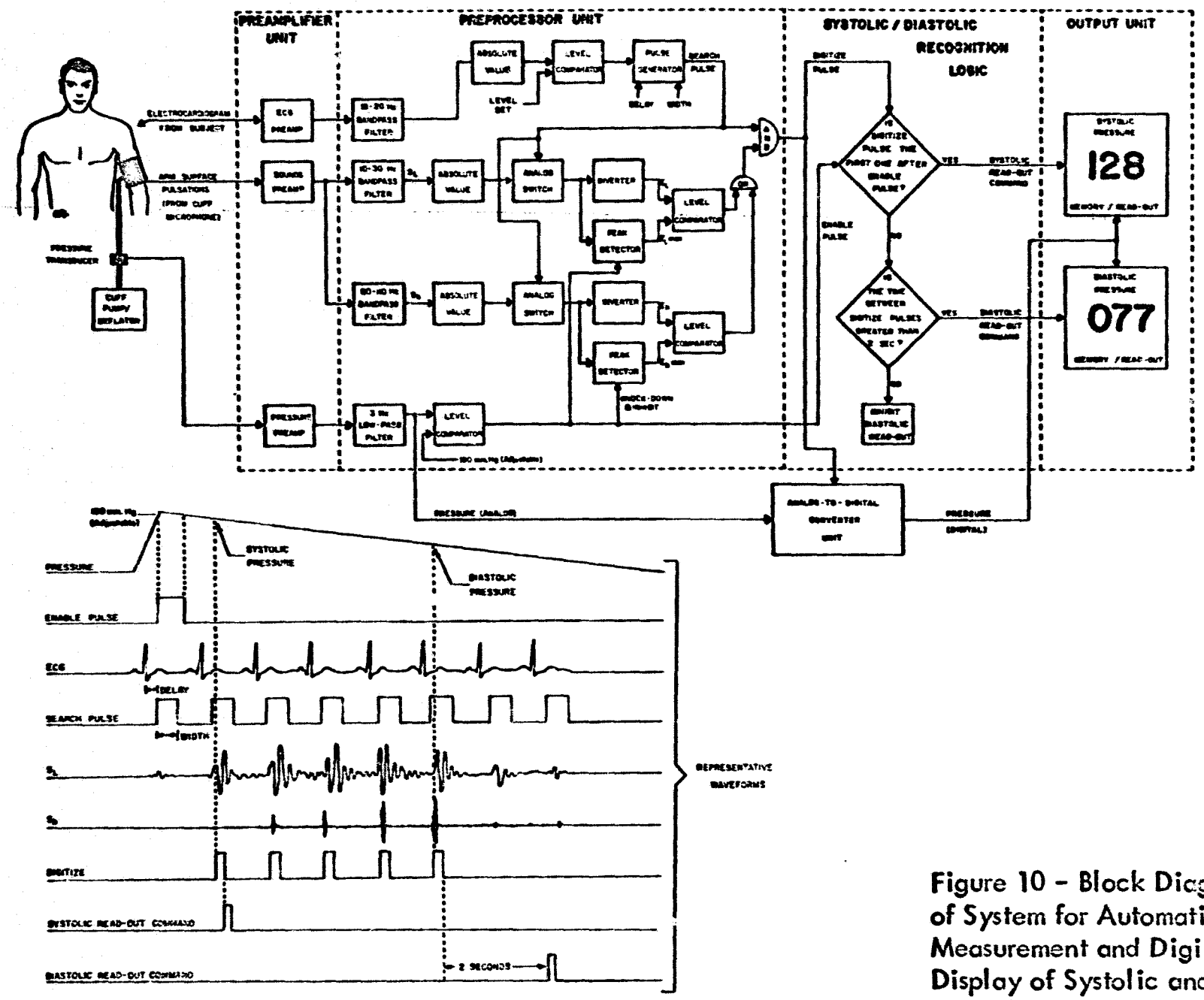


Figure 10 - Block Diagram of System for Automatic Measurement and Digital Display of Systolic and Diastolic Blood Pressures

simultaneously through 10 to 30 Hz[3] and 80 to 110 Hz[3] bandpass filters. These filters are active filters which provide an attenuation of 24 db/octave for signals outside of the bandpass (Appendix E). The absolute values of the outputs of these filters are fed into analog switches controlled by the SEARCH pulse. Thus, the only signals which pass through the analog switch are those which occur within the time period of the SEARCH pulse. The absolute value of the filtered arm pulse sounds within each bandpass then is compared with a set fraction (or ratio) of the peak amplitude of the absolute value of all previous filtered sounds within a single cuff deflation cycle. The peak amplitudes of the absolute value of the filtered sounds are stored in the peak detectors which are set to fixed threshold values (or knocked-down) and inhibited during each cuff inflation. Initally, the systolic decision threshold is set by the KNOCK-DOWN and INHIBIT pulse. The comparator produces an output whenever the absolute value of the filtered sound signal exceeds a set fraction (selectable) of the value stored in the peak detector. The comparator output of both high and low frequency channels is fed into an OR gate. This circuitry also serves as a form of automatic gain control and is essential to a valid diastolic pressure decision by this system (see discussion of diastolic detection criteria, Chapter IV and Table II). The pressure input to the preprocessor unit may be a pressure analog signal alone or it may consist of an analog signal of pressure plus sounds. The 3 Hz low-pass filter is used to eliminate noise as

---

[3]The 10 to 30 Hz and 80 to 110 Hz bandpass filters are those filters shown in Figure A3. The bandpass characteristics of these filters are shown in Appendix E. The values of the actual cutoff frequencies of the filters vary from the approximate values of 10 to 30 Hz and 80 to 110 Hz.

well as unnecessary sounds from the pressure analog signal. A comparator is used in order to provide a logic signal each time that the cuff inflates and the pressure exceeds a preset value. The output of this comparator is the ENABLE pulse which is used to inhibit and "knock-down" the peak detector and to reset the systolic/diastolic recognition logic.

The analog-to-digital converter unit (which is essentially a digital voltmeter) converts the pressure analog into digital form by the use of the dual-slope integration technique. This technique minimizes digitizing errors due to errors in clock frequency. The pressure analog signal is sampled, digitized, and stored each time that a preprocessed sound of sufficient amplitude is detected within the SEARCH pulse.

The systolic/diastolic recognition logic completes the systolic and diastolic decisions which were begun in the preprocessor. The SYSTOLIC READ-OUT COMMAND signal and DIASTOLIC READ-OUT COMMAND signal strobe the systolic read-out and diastolic read-out respectively in the time sequence in which they occur during cuff deflation.

A two-second timer is used to assure that the outputs of both the high and the low frequency sound channels are below their respective set ratios for at least one heartbeat before the DIASTOLIC READ-OUT COMMAND occurs. The pressure value read as the diastolic pressure is the value which was stored in the diastolic memory by the last recognized sound. This technique reduces the probability of reading a false diastolic pressure due to a weak sound or due to beat-to-beat variations in diastolic blood pressure.

The decoder/driver units and indicator tubes provide the final output and display of systolic and diastolic pressures. A calibrator unit simulates the required input signals and permits calibration of the system from known pressures generated at the pressure transducer or on tape.

Integrated circuits are used for both the analog and the digital portions of the system, and the entire system with the exception of the power supplies, indicator tubes, sensor hardware, and calibrator is mounted on seven 4" by 6" printed circuit boards. Appendix A contains the detailed schematics for the system.

The leading edge of the ECG SEARCH pulse occurs 100 milliseconds after the R-wave and the trailing edge occurs 300 milliseconds after the R-wave. These values were selected to minimize the width of the SEARCH pulse and to encompass the range of time of occurrence of a sound in relation to the ECG. The width is minimized in order to reduce the susceptibility of the system to extraneous noise. Table III is a tabulation of the time intervals from the peak of the R-wave of the ECG to the first sound (RGS), to a sound intermediate in the deflation cycle (RGM), and to the last sound (RGD). These values were determined in experiments on adult subjects and agree with other published data (9,26,39).

The level comparators shown in Figure 10 are set based on the data tabulated in Table II. The portion of the pre-processor concerned with the processing of the output of the 80 to 110 Hz filter (S_H) is important to the diastolic decision. The level comparator is set such that an output is obtained whenever the ratio of E_H to $E_{H\ max}$ is greater than 0.2. The other level comparator is set to provide an output whenever the ratio of E_L to $E_{L\ max}$ is greater than 0.9. Thus, the design, by the utilization of

TABLE III

MEASURED TIME RELATIONSHIPS BETWEEN
R WAVE OF ECG AND THE SOUNDS RECOGNIZED AS KOROTKOFF SOUNDS

SUBJECT	RGS (in milliseconds)	RGM (in milliseconds)	RGD (in milliseconds)
MH	150	130	110
LK	270	237	210
LK	263	237	190
BM	248	225	210
BM	255	222	200
BM	260	230	210
AS	225	208	188
AS	237	207	185
AS	210	195	178
AS	220	190	170
HS	270	255	220
HS	270	260	220
HS	250	235	190
HS	280	245	215
HS	300	265	200
HS	255	230	200
HS	280	220	195
HS	280	240	195
HS	255	230	210

RGS = Time interval from peak of R-Wave to onset of first sound.

RGM = Time interval from peak of R-Wave to onset of an intermediate sound in the deflation cycle.

RGD = Time interval from peak of R-Wave to onset of last sound.

an OR gate, incorporates some degree of compensation for gross variations in sound characteristics at the diastolic end-point.

The system for the automatic measurement of blood pressure has been physically incorporated into a larger system which also measures heart rate (cardiotachometer) and respiration rate (pneumotachometer). This system is called a Vital Signs Indicator, and is shown in Figure II along with the cuff pump/deflator, pressure transducer, occluding cuff, microphone, and electrodes. The systolic pressure is displayed on the upper center digital display and the diastolic pressure is displayed on the lower center digital display. The controls for the automatic sphygmomanometer include a course GAIN switch for the sounds (3-db steps), a fine gain control (TRIGGER) for the sounds, and ZERO and AMPLITUDE controls for calibration of the pressure signal. In Figure 12 is shown the sphygmomanometer connected to a subject. A view of the Vital Signs Indicator with the top panel removed to show the layout of the circuit boards and power supplies is shown in Figure 13. Test points are located on the lower part of the front panel adjacent to the handles on either side. The seven circuit boards of the sphygmomanometer portion of the Vital Signs Indicator are shown in Figure 14. The two boards on the left of Figure 14 contain the sounds, pressure, and ECG preamplifier circuitry. The upper center card contains the sounds and pressure filters and a switch which provides for the processing of data with an inverted pressure ramp. The center card contains the preprocessor unit with the exception of the filters which are on the top card. The bottom center card contains the analog-to-digital converter and the systolic/diastolic recognition logic. The two boards on the right contain the decade counters, storage registers, and decoder/driver circuitry for the systolic and diastolic displays.

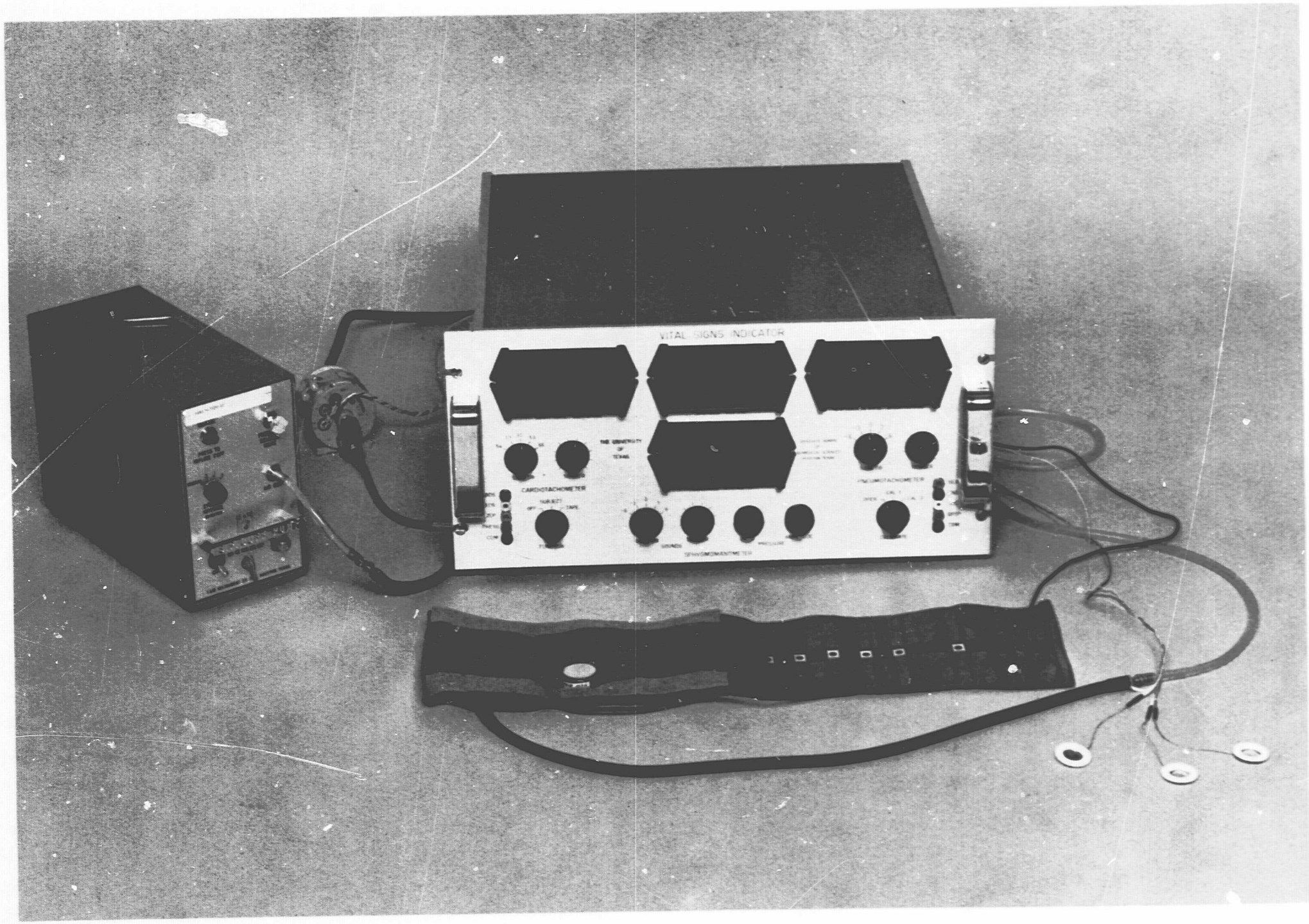


Figure 11 - The Vital Signs Indicator, cuff pump/deflator, pressure transducer, occluding cuff with mounted cuff microphone, and electrodes

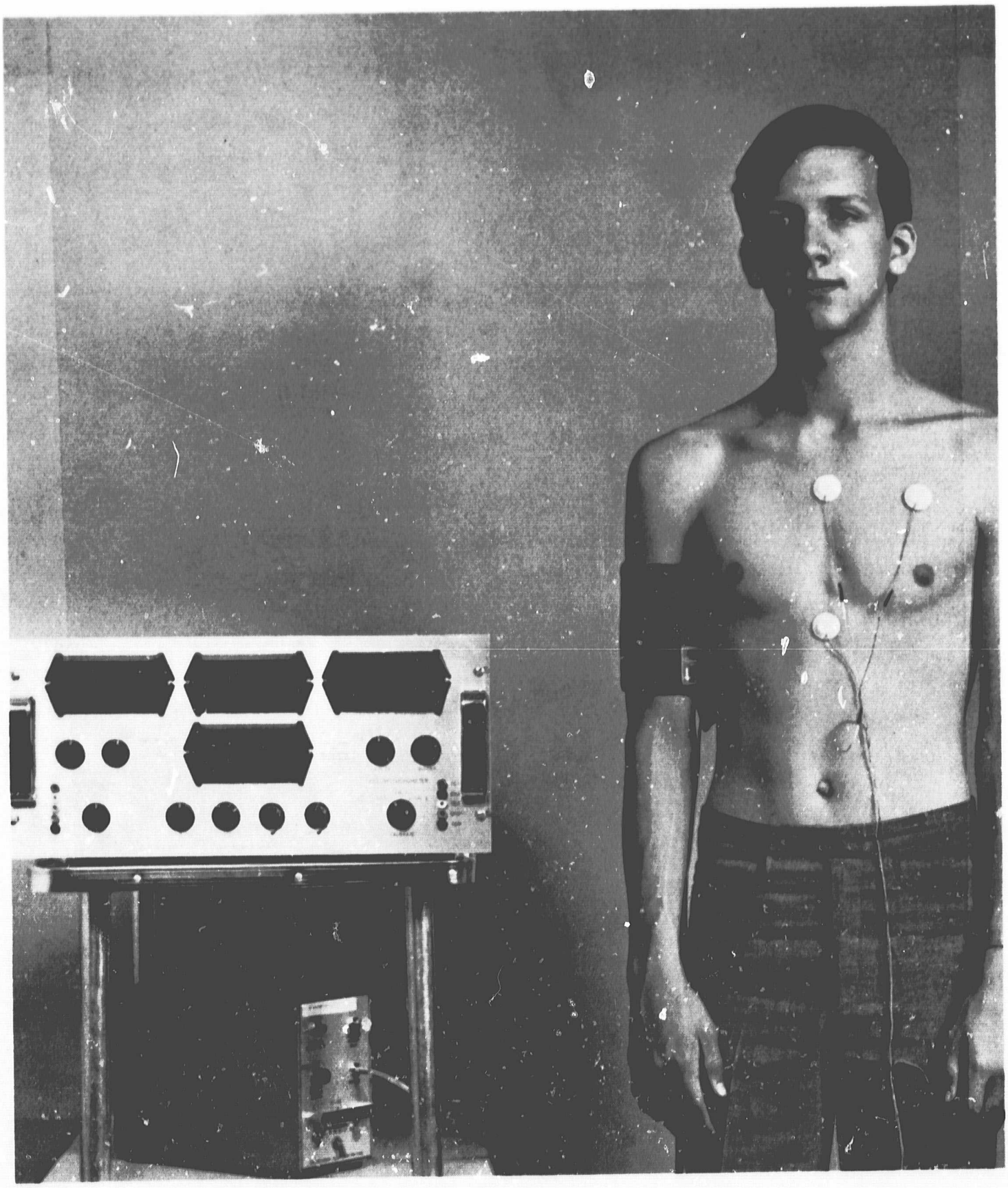


Figure 12 - The automatic sphygmomanometer connected to a subject

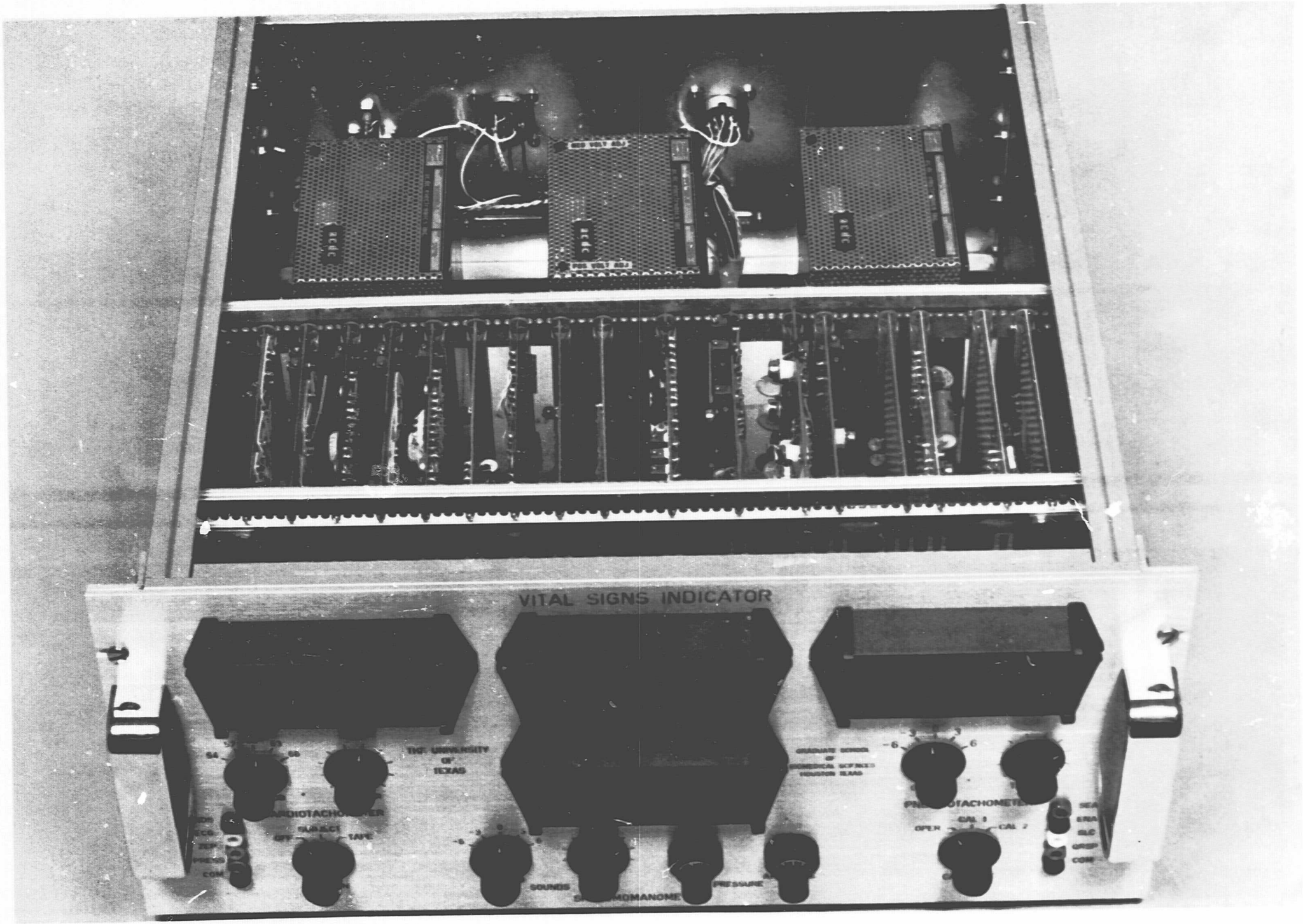


Figure 13 – The Vital Signs Indicator with the top panel removed to show the internal layout

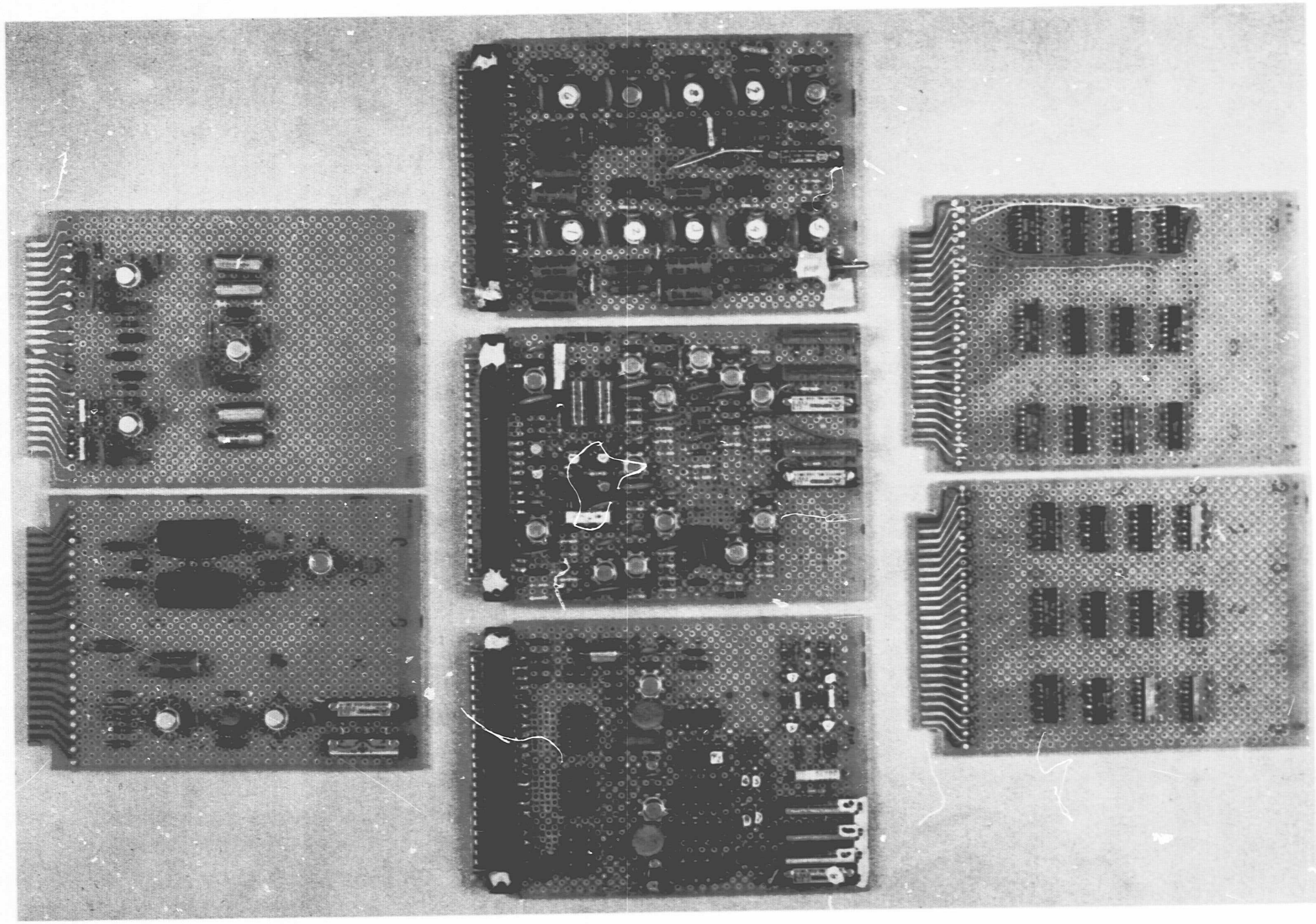
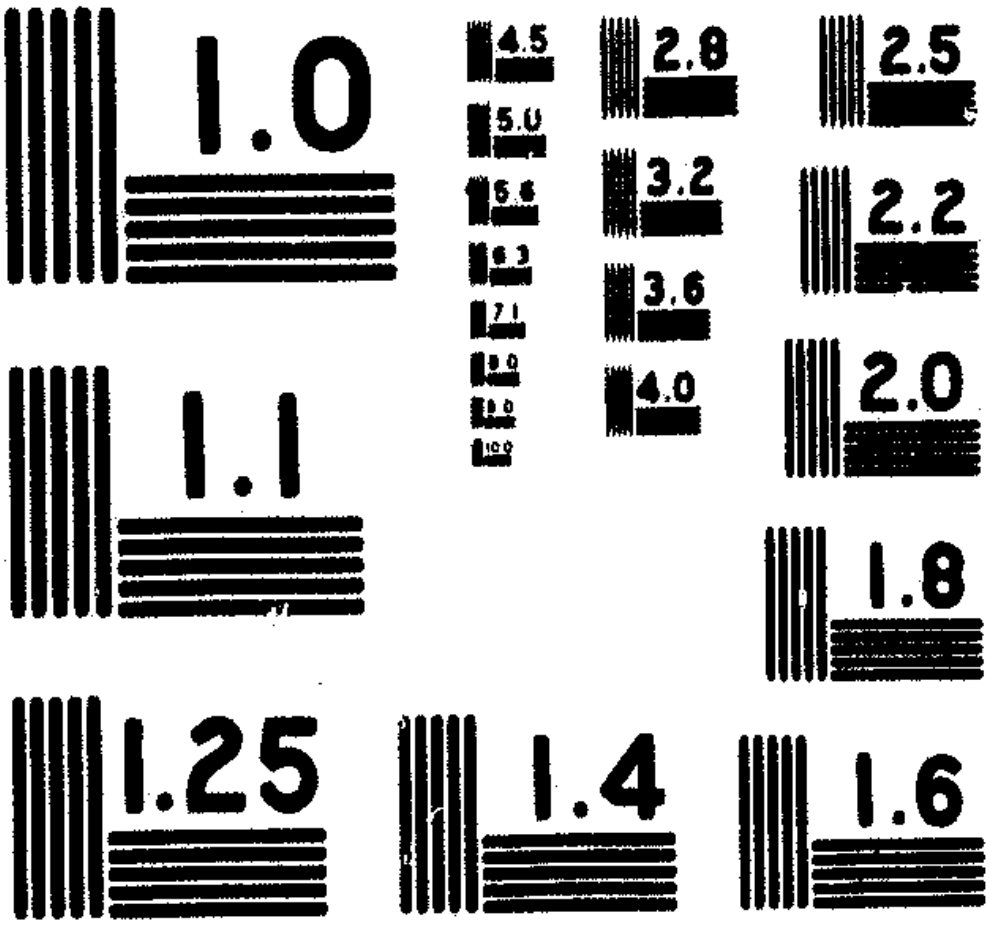


Figure 14 – The circuit boards used for the sphygmomanometer portion of the Vital Signs Indicator

VI. DATA ON SYSTEM PERFORMANCE

The pressure signal of the system was calibrated by applying air pressure simultaneously to both the pressure transducer and a manometer filled with mercury. The manometer pressure was set at intervals of 10 millimeters of mercury from 0 to 200 mm Hg. The microphone was physically struck at each pressure and the systolic and diastolic displays were read and recorded. In this manner, the calibration curve of Figure 15 was obtained.

The data of Table IV are the simultaneous and independent readings of systolic and diastolic blood pressures by experienced observers and by the electronic system. The "double-blind" technique of London and London (25) was used whereby a simultaneous, independent, clinical measurement is performed by an experienced clinician whose readings cannot be influenced by the readout of the electronic system. Three readings were taken on each of ten subjects by each of the two observers. The same mercury sphygmomanometer was used for the clinical measurements that was used for the calibration of the system. The ten subjects ranged in age from 8 to 46 years old and three were females. Excellent auscultatory conditions were established by the use of a high-precision stethoscope and a separate room with minimum background noise. Each observer was allowed two practice measurements on each of the subjects before the data were recorded. This was done in order for the observer to become acquainted with the magnitude and tonal characteristics of the Korotkoff sounds peculiar to the subject. The electrocardiogram signal was not used; hence, the SEARCH pulse portion of the circuitry was disabled in a manner such that operation of the rest of the system was not altered.



MICROCOPY RESOLUTION TEST CHART

NATIONAL BUREAU OF STANDARDS - 1963

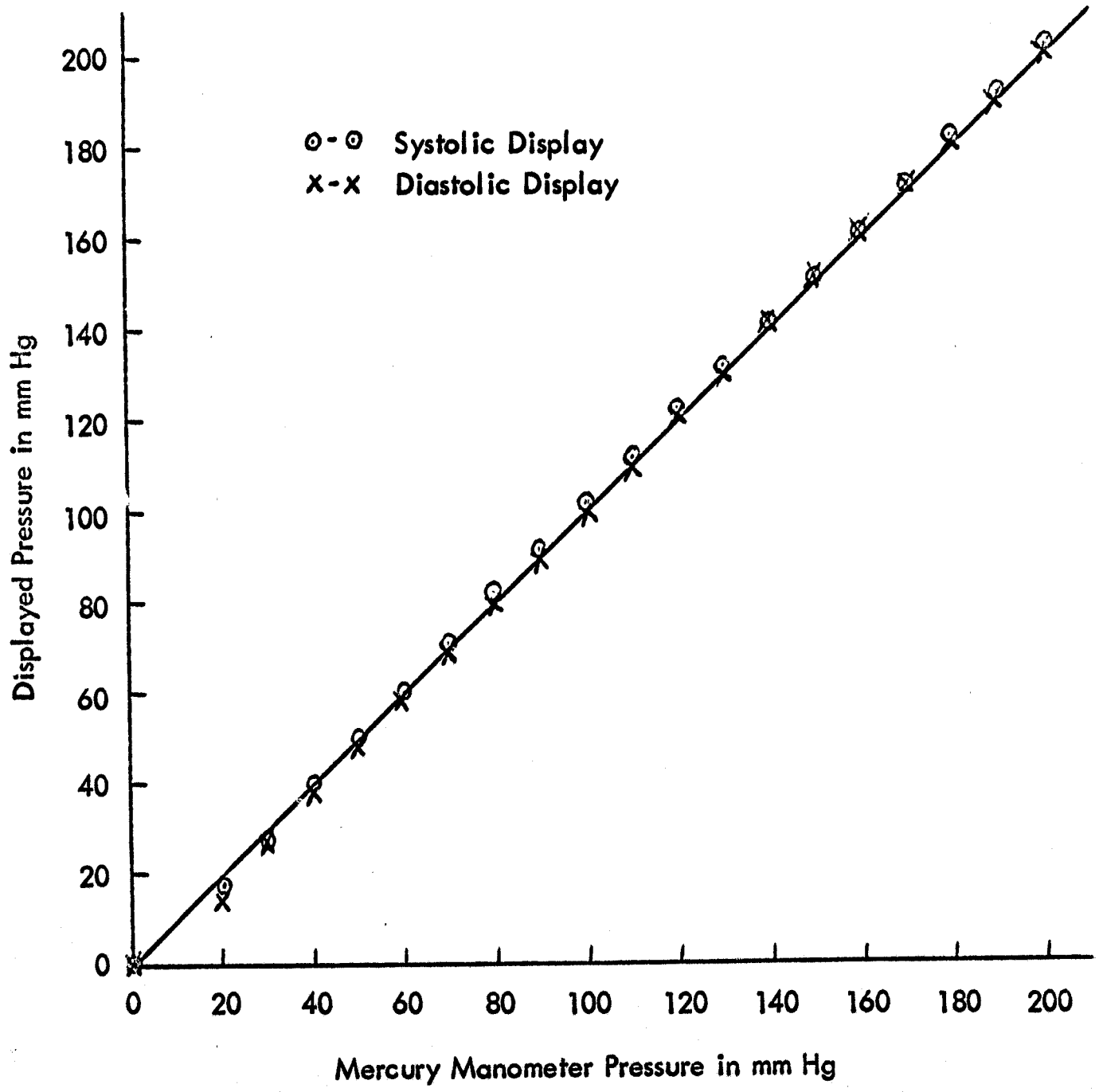


Figure 15 - Calibration curve

TABLE IV

BLOOD PRESSURE MEASUREMENTS

SUBJECT	OBSERVER	CLINICAL Blood Pressure	AUTOMATED Blood Pressure
SMS	FBV	126/78	124/75
SMS	FBV	127/72	124/75
SMS	FBV	124/78	122/78
SMS	AES	127/73	128/75
SMS	AES	125/78	126/79
SMS	AES	126/73	125/74
BPY	AES	118/73	120/70
BPY	AES	114/70	115/70
BPY	AES	111/70	110/70
BPY	FBV	132/81	134/84
BPY	FBV	126/80	131/74
BPY	FBV	126/74	125/74
MAC	AES	118/80	122/79
MAC	AES	117/80	117/81
MAC	AES	121/83	119/81
MAC	FBV	110/60	111/60
MAC	FBV	108/65	107/60
MAC	FBV	112/70	114/70
FBV	AES	138/103	140/100
FBV	AES	135/105	136/104
FBV	AES	136/105	137/101
FBV	FBV	140/100	140/108
FBV	FBV	136/107	138/108
FBV	FBV	144/109	143/108
MEA	AES	121/74	122/75
MEA	AES	119/73	111/71
MEA	AES	111/73	109/71
MEA	FBV	108/70	104/68
MEA	FBV	106/74	107/71
MEA	FBV	104/78	107/70
FBV Jr.	AES	97/66	102/71
FBV Jr.	AES	96/69	96/65
FBV Jr.	AES	98/66	101/69
FBV Jr.	FBV	98/66	96/55
FBV Jr.	FBV	97/67	95/61
FBV Jr.	FBV	100/69	101/55

(continued on next page)

TABLE IV - (continued)

BLOOD PRESSURE MEASUREMENTS

SUBJECT	OBSERVER	CLINICAL Blood Pressure	AUTOMATED Blood Pressure
MLV	AES	98/57	99/60
MLV	AES	98/61	98/61
MLV	AES	104/63	104/60
MLV	FBV	102/56	104/54
MLV	FBV	96/58	93/55
MLV	FBV	94/60	94/59
APM	AES	108/68	109/65
APM	AES	110/67	111/68
APM	AES	103/72	102/64
APM	FBV	106/73	106/61
APM	FBV	102/62	101/60
APM	FBV	102/63	100/60
LSM	FBV	122/77	118/79
LSM	FBV	116/82	119/81
LSM	AES	126/72	132/70
LSM	AES	122/80	126/78
LSM	AES	125/82	125/74
AES	FBV	162/102	163/101
AES	FBV	156/101	162/94
AES	FBV	146/101	143/101
AES	AES	153/95	154/94
AES	AES	153/90	153/85
AES	AES	156/89	156/90

VII. ANALYSIS OF DATA AND DISCUSSION OF SYSTEM OPERATION

Figure 16 is a plot of the automated systolic blood pressure readings versus the simultaneous clinical systolic blood pressure readings. The linear regression equation for these data is $y = 1.019x - 2.0$. Figure 17 is a plot of the automated diastolic blood pressure readings versus the simultaneous clinical diastolic blood pressure readings. The linear regression equation for these data is $y = 1.020x - 3.3$. The mean error[4] (clinical minus automated) is -0.3 mm Hg for systolic pressures and +1.5 mm Hg for the diastolic pressures. The larger error in the diastolic pressure may, in part, be explained by the consistently lower readings of the diastolic display as compared with the readings of the systolic display during calibration over the range of the measured diastolic pressures. The diastolic display was consistently 1 to 2 mm Hg below the systolic display over this range of pressures. Thus, the mean error of +1.5 mm Hg for the diastolic pressures is not a large error. From the histograms of Figures 18 and 19, the errors in the systolic and diastolic measurements appear to be distributed about zero without an appreciable bias although the diastolic distribution is more skewed. Using the same method for the evaluation of a semi-automatic electronic sphygmomanometer, McCaughan (30) found that in 72 readings the mean errors were -2.5 mm Hg for systolic pressures and -0.9 mm Hg for diastolic pressures.

---

[4]The word "error" is used to mean the difference between the clinical and automated blood pressure readings.

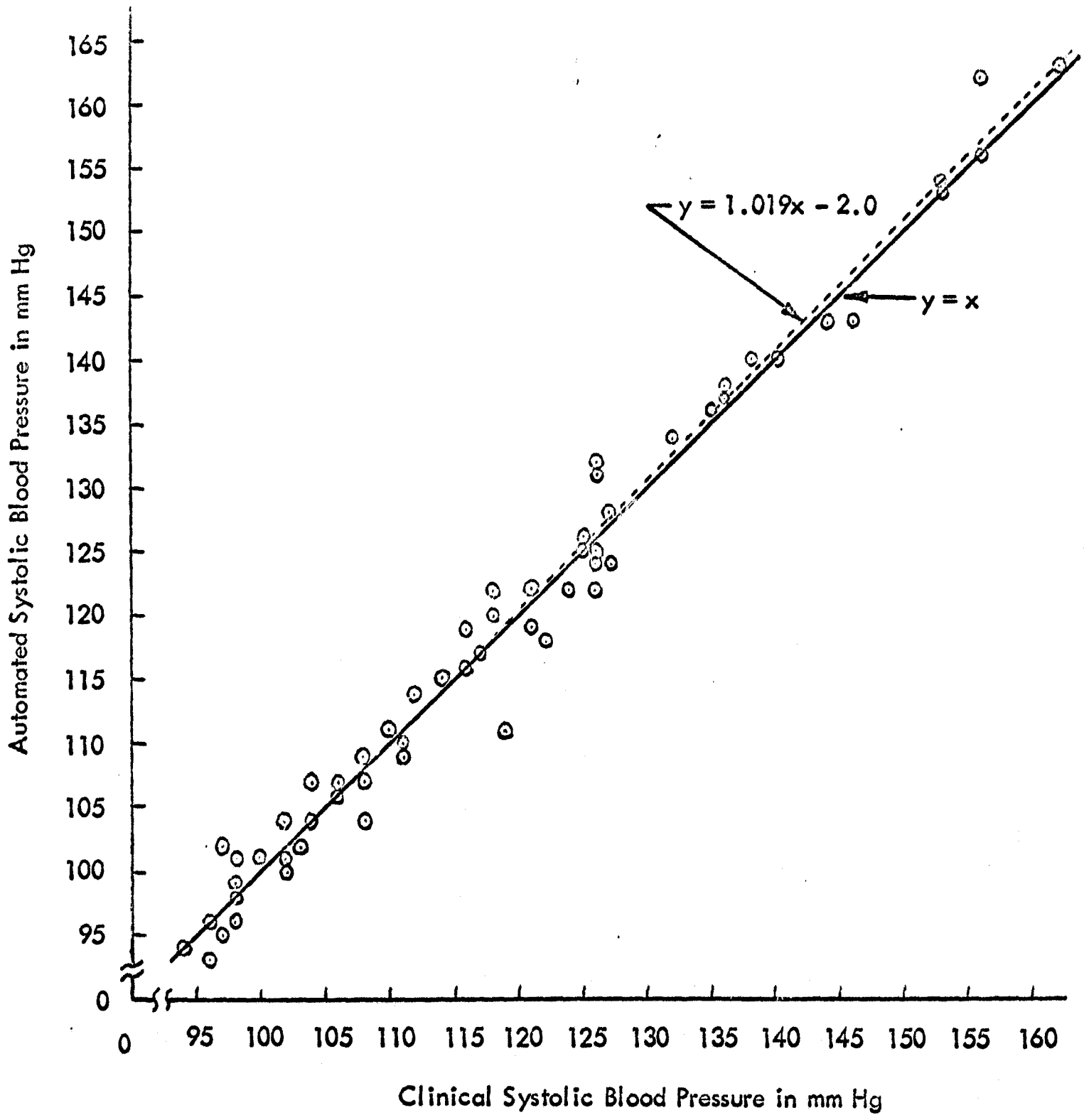


Figure 16 - Automated systolic blood pressure readings versus clinical systolic blood pressure readings

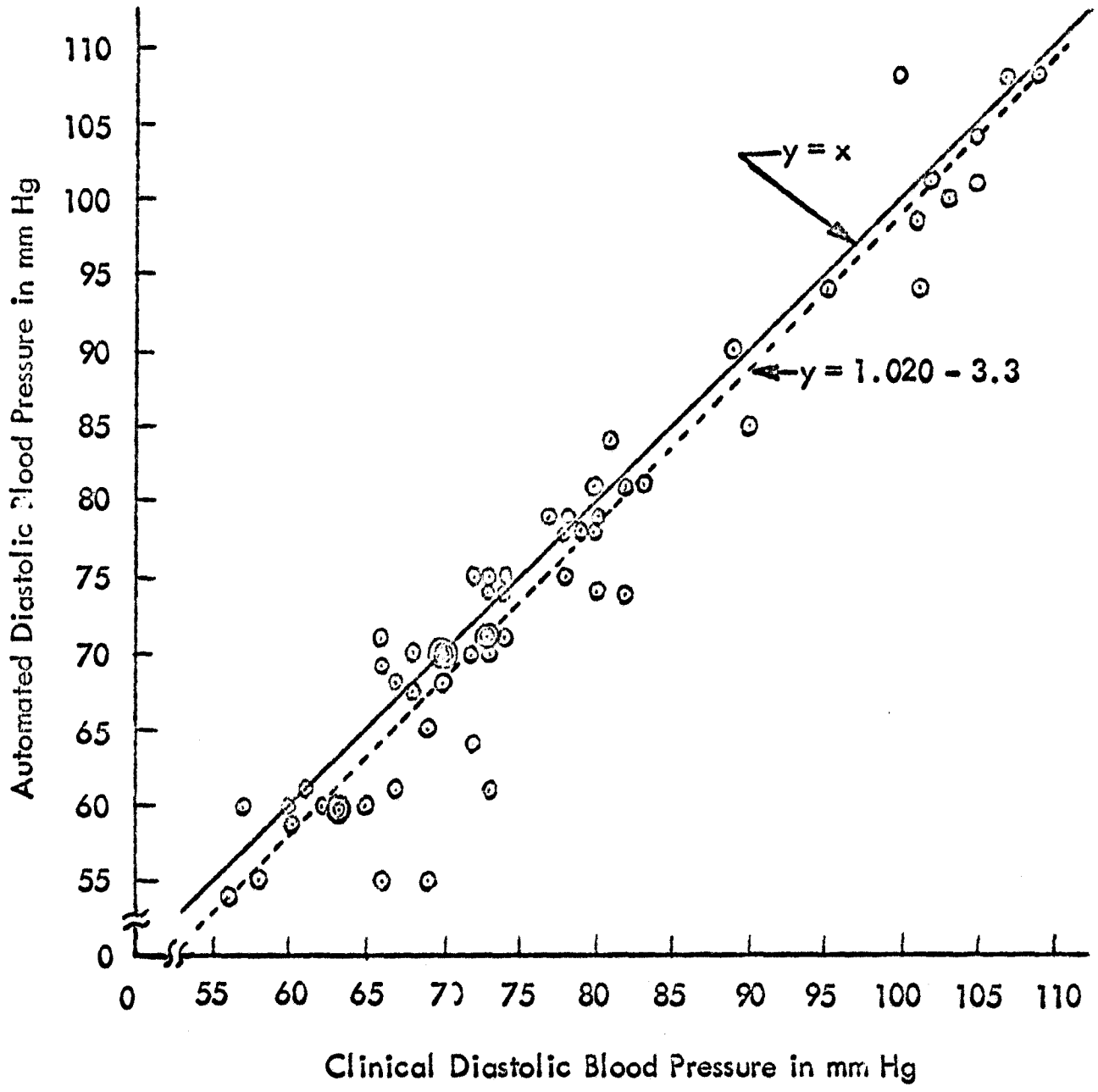


Figure 17 - Automated diastolic blood pressure readings versus clinical diastolic blood pressure readings

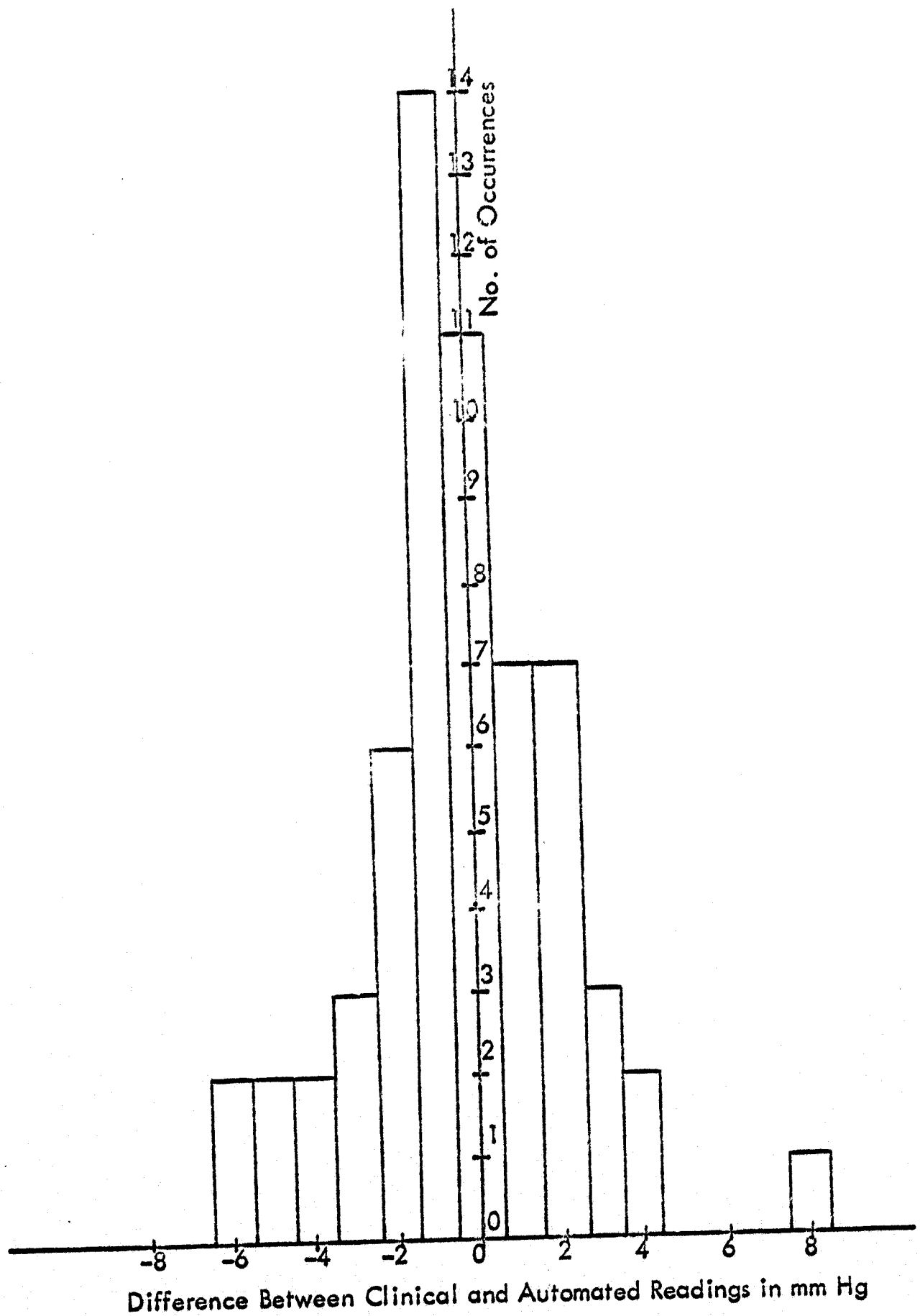


Figure 18 – Histogram of systolic blood pressure readings

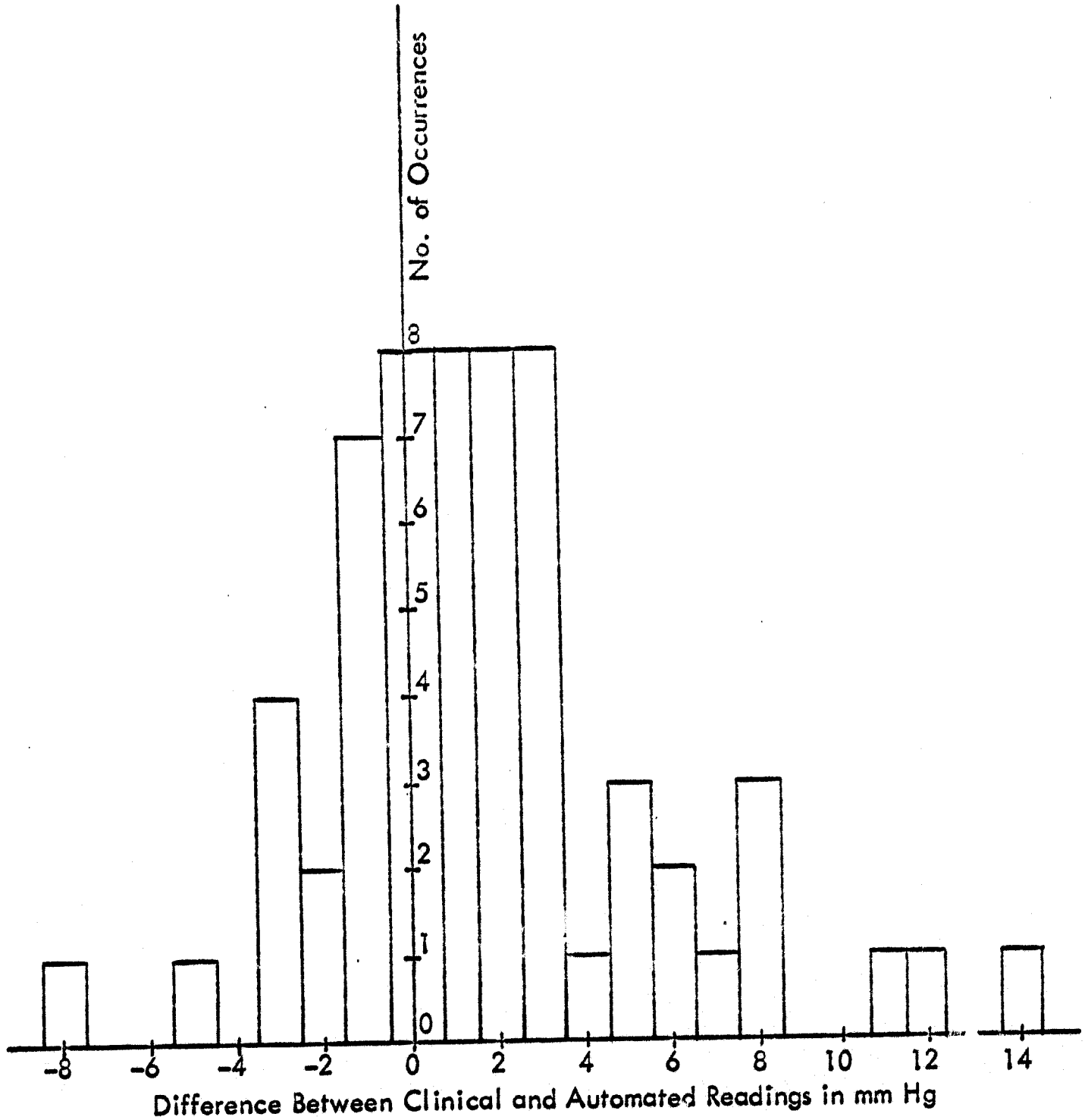


Figure 19 – Histogram of diastolic blood pressure readings

The means of the absolute values of the errors were 1.3 mm Hg for the systolic pressure and 2.9 mm Hg for the diastolic pressure. The standard deviation of the errors is 2.5 mm Hg for the systolic pressures and 3.9 mm Hg for the diastolic pressures. Wilcox (52) found that the standard deviations of readings made by 349 graduate nurses from a motion picture film of a falling mercury column with sound varied from subject-to-subject and ranged from 4 to 16 mm Hg for systolic pressures and from 2 to 45 mm Hg for diastolic pressures. These observer errors are probably major components of the differences between clinical and automated readings in spite of the use of excellent auscultatory conditions.

In general, the automated systolic pressures were greater than the clinical systolic pressures and the automated diastolic pressures were less than the clinical diastolic pressures. This is an indication that the automatic system may possess the additional sensitivity required to make auscultatory measurements compare more favorably with direct blood pressure measurements. Comparison measurements have repeatedly shown that the indirect auscultatory measurements of blood pressures tend to underestimate the direct systolic blood pressure and overestimate the direct diastolic blood pressure (3,26,38). Intra-arterial measurements (of which Figure 9 is typical) indicate that the systolic decision based on the output of the 10 to 30 Hz filter detects the true systolic index which an observer listening through a stethoscope often misses by two or three heartbeats, especially in obese subjects.

In a few instances, ususally during a very slow deflation cycle, an auscultatory gap occurred wich lasted for greater than two seconds. The automatic system very precisely recognized as the diastolic pressure the last sound before the extended

auscultatory gap occurred. These data were not recorded in Table IV since the error was one of an inadequate deflation rate by the observer and it is obvious that this error could be eliminated simply by adjusting the length of the two-second diastolic timer to three or four seconds. This timer should prove to be very useful in preventing false readings of diastolic pressures, especially on patients with heart problems where large variations in pressure occur on a beat-to-beat basis (the patient of Figure 9, for example).

The following improvements are suggested for future modifications of the system:

1. Incorporation of a cuff pump/deflator that inflates approximately 30 mm Hg above the systolic pressure and enables the system at that point.

2. Elimination of the DIGITIZE pulse AND gate since it is a redundant logic element.

3. Correction of the discrepancy between the systolic and diastolic display for the same input pressure.

4. Investigation of different methods of mounting the cuff microphone to prevent amplification of cuff pressure locally under the microphone.

In addition, the system should be more thoroughly tested with a well-planned experiment involving subjects representative of the clinical utilization of the instrument and using both trained and untrained observers. Automatic measurements on exercising subjects should be made simultaneously with direct intra-arterial measurements in order to determine the degree of motion artifact rejection which is provided within the system. The characteristics of various microphone and microphone mounting configurations should be studied for possible improvement of motion artifact rejection.

VIII. CONCLUSIONS

A system for the automatic measurement and digital display of systolic and diastolic blood pressures has been built utilizing the relative advantages of analog and digital techniques in data processing and decision making. The criteria for recognition of systolic and diastolic pressures which are programmed into the system are unique and are based upon experimental data. Noise and motion artifact rejection capabilities were provided in the design by the use of selective filtering and digital logic circuitry for the inhibition of systolic and diastolic detection during cuff inflation and time periods of the cardiac cycle when sounds cannot exist at the position of the microphone. The measurements of the automatic system compare well with the readings of a trained clinician under good auscultatory conditions.

BIBLIOGRAPHY AND REFERENCES

1. Allred, James E., and Johnson, Jack B.: "Design and Development of an Automatic Indirect Blood Pressure Monitoring Device," USAF School of Aerospace Medicine, Brooks Air Forch Base, Texas, Project No. 6320, Task No. 632001, Sept., 1966.

2. Berliner, K.; Fujiy, D. Ho Lee; Yildiz, M., and Garnier, B.: "Blood Pressure Measurements in Obese Persons: Comparison of Intra-Arterial and Auscultatory Measurement," The American Journal of Cardiology, July, 1961, pp. 10-17.

3. Berliner, K.; Fujiy, D. Ho Lee; Yildiz, M., and Garnier, B.: "The Accuracy of Blood Pressure Determinations: A Comparison of Direct and Indirect Measurements," Cardiologia, Vol. 37, No. 2, 1960, pp. 118-128.

4. Best, Charles H., and Taylor, Norman B.: The Physiological Basis of Medical Practice, The Williams and Wilkins Co., Baltimore, Md., 1966, pp. 722-730.

5. Bolie, Victor W.; Goven, Richard J.; Tennant, Jerry R., and Sander, Duane E.: "Electronic Blood Pressure Sampler and Printer," Aerospace Medicine, Oct., 1964, pp. 954-957.

6. Bordley, James, III; Connor, Charles A. R.; Hamilton, W. F.; Kerr, William J., and Wiggers, Carl J.: "Recommendations for Human Blood Pressure Determinations by Sphygmomanometers," Circulation, Vol. 4, Oct., 1951, pp. 503-509.

7. Boyd, William A.: "Blood Pressure Monitoring," Electronics in Anesthesiology, Vol. 3, No. 3, May, 1965, pp. 417-433.

8. Bramwell, J. Crighton, and Hickson, Sylvia K.: "The Relation of Pulse Form to Sound Production in Arteries," Heart, Vol. 13, 1926, pp. 109-151.

9. Canzoneri, Joseph, III; Geddes, Leslie A.; Valbona, Carlos, and Viscusi, Richard L.: "A New Electronic Indirect Systolic and Diastolic Blood Pressure Measuring System," SWIEEECO Record, April, 1967, pp. 10-6-1 to 10-6-8.

10. Chungcharoen, D.: "Genesis of Korotkoff Sounds," American Journal of Physiology, Vol. 207, 1964, pp. 190-194.

11. Collins, Vincent J., and Magora, Florella: "Sphygmomanometry: The Indirect Measurement of Blood Pressure," Anesthesia and Analgesia...Current Researches, Vol. 42, No. 4, July-August, 1963, pp. 443-452.

12. de Dobbeleer, G. D. P.: "Determination of the Clinical Value of the Systolic and Diastolic Blood Pressure," Godart Bulletin, Vol. 2, No. 1, Sept., 1962, pp. 2-10.

13. Edinger, Leslie, and Spring, Maxwell: "Automatic Electronic Blood Pressure Apparatus," The American Journal of Medical Electronics, Vol. 2, April-June, 1963, pp. 138-142.

14. Follett, D. H.; Freundlich, H. F.; Shaw, D. B., and Davies, D. H.: "An Apparatus for the Automatic Recording of Systolic and Diastolic Blood-Pressure," The Lancet, April 13, 1963, pp. 808-809.

15. Geddes, L. A.; Spencer, W. A., and Hoff, H. E.: "Graphic Recording of the Korotkoff Sounds," American Heart Journal, Vol. 57, March, 1959, pp. 361-370.

16. Guyton, Arthur C.: Textbook of Medical Physiology, W. B. Saunders Co., Philadelphia, Pa., 1966, pp. 249-278.

17. Harrison, Edgar G., Jr.; Roth, Grace M., and Hines, Edgar A., Jr.: "Bilateral Indirect and Direct Arterial Pressures," Circulation, Vol. 22, Septl, 1960, pp. 419-436.

18. Henschell, Austin; De La Vega, Frederick, and Taylor, Henry Longstreet: "Simultaneous Direct and Indirect Blood Pressure Measurements in Man at Rest and Work," Journal of Applied Physiology, Vol. 6, Feb., 1954, pp. 506-508;

19. Hinman, Allen T.; Engel, Bernard T., and Bickford, Arthur F.: "Portable Blood Pressure Recorder Accuracy and Preliminary Use in Evaluating Intradaily Variations in Pressure," American Heart Journal, Vol. 63, No. 5, May, 1962, pp. 663-668.

20. Kahn, Alan; Ware, Ray W., and Siahaya, Odo: "A Digital Readout Technic for Aerospace Biomedical Monitoring," The American Journal of Medical Electronics, April-June, 1963, pp. 152-157.

21. Korotkoff, N. S.: "A Contribution to the Problem of Methods for the Determination of the Blood Pressure," Translated in Ruskin, A.: Classics in Arterial Hypertension, Charles C. Thomas, Springfield, Illinois, 1956, pp. 126-133.

22. Kroeker, Edwin J., and Wood, Earl H.: "Comparison of Simultaneously Recorded Central and Peripheral Arterial Pressure Pulses During Rest, Exercise, and Tilted Position in Man," Circulation Research, Vol. 3, 1955, pp. 623-632.

23. Lange, R. L., and Hecht, H. H.: "Genesis of Pistol-Shot and Korotkoff Sounds," Circulation, Vol. 18, No. 5, Nov., 1958, pp. 975-982.

24. Lategola, Michael T.; Harrison, Hiley, and Barnard, Charles: "A Virtually Continuous Measurement of Human Systolic and Diastolic Blood Pressure Transients without Direct Arterial Puncture," Aerospace Medicine, March, 1966, pp. 228-233.

25. London, Rose E., and London, Seymour B.: "Blood Pressure Survey of Physicians: Use of Automated Measurements," Journal of the American Medical Association, Vol. 198, No. 9, Nov. 28, 1966, pp. 981-984.

26. London, Seymour B., and London, Rose E.: "Comparison of Indirect Pressure Measurements (Korotkoff) with Simultaneous Direct Brachial Artery Pressure Distal to the Cuff," Advances in Internal Medicine, Vol. 13, 1967, pp. 127-142.

27. London, Seymour B., and London, Rose E.: "Critique of Indirect Diastolic End Point: 'Muffling' v. 'Last' Sound," Archives of Internal Medicine, Vol. 119 Jan., 1967, pp. 39-49.

28. Malcolm, John E.: Blood Pressure Sounds and Their Meanings, Part I, Charles C. Thomas, Springfield, Illinois, 1957, pp. 10-69 and pp. 82-83.

29. Maltby, Alice B, and Wiggers, Carl J.: "Studies on Human Blood Pressure Criteria and Methods," American Journal of Physiology, Vol. 100, 1932, pp. 604-613.

30. McCaughan, Donald: "Comparison of an Electronic Blood Pressure Apparatus with a Mercury Manometer," 1966 Annual Symposium of the Association for the Advancement of Medical Instrumentation, Boston, Mass., July 29, 1966.

31. McCutcheon, Ernest P., and Rushmer, Robert F.: "Korotkoff Sounds: An Experimental Critique," Circulation Research, Vol. 20, No. 2, Feb., 1967, pp. 149-161.

32. McCutcheon, Ernest P.; Wiederhielm, Curt A., and Baker, Donald W.: "Frequency Spectrum Changes of Korotkov Sounds with Muffling," The Physiologist, Vol. 7, No. 3, 1964, pp. 203.

33. Moss, Arthur J., and Adams, Forrest H.: "Index of Indirect Estimation of Diastolic Blood Pressure," American Journal of Diseases of Children, Vol. 106, Oct., 1963, pp. 74-77.

34. Nagle, Francis J.; Naughton, John, and Balke, Bruno: "Comparisons of Direct and Indirect Blood Pressure with Pressure-Flow Dynamics During Exercise," Journal of Applied Physiology, Vol. 21, No. 1, Jan., 1966, pp. 317-320.

35. Ono, K.: "A New Principle for Spectral Detection of Korotkoff Sound," 7th International Conference on Medical and Biological Engineering, Stockholm, Sweden, August, 1967.

36. Ragan, Charles, and Bordley, James, III: "The Accuracy of the Clinical Measurements of Arterial Blood Pressure with a Note on the Auscultatory Gap," Bulletin John Hopkins Hospital, Vol. 69, 1941, pp. 504-508.

37. Rauterkus, Thomas; Feltz, John F., and Fickes, Joy W.: "Frequency Analysis of Korotkov Blood Pressure Sounds Using the Fourier Transform," Final Report, USAF Contract AF41 (609)-2753, Feb., 1966.

38. Roberts, L. N.; Smiley, J. R., and Manning, G. W.: "A Comparison of Direct and Indirect Blood Pressure Determinations," Circulation, Vol. 8, Aug., 1953, pp. 232-242.

39. Rodbard, Simon; Rubinstein, Herbert M., and Rosenblum, Sol: "Arrival Time and Calibrated Contour of the Pulse Wave, Determined Indirectly from Recordings of Arterial Compression Sounds," American Heart Journal, Vol. 53, 1957, pp. 205-212.

40. Rogge, James D.; Brown, William K., and Brown, Clay A.: "An Automatic System for the Indirect Determination and Recording of Human Arterial Blood Pressure," SAM-TR-68-25, USAF School of Aerospace Medicine, Brooks Air Force Base, Texas, March, 1968.

41. Rose, G. A.; Holland, W. W., and Crowley, E. S.: "A Sphygmomanometer for Epidemiologists," The Lancet, Vol. 1, Feb. 8, 1964, pp. 296-300.

42. Rueger, Milton J.: "Blood Pressure Variations in the Two Arms," Annals of Internal Medicine, Vol. 35, 1951, pp. 1023-1027.

43. Rushmer, Robert F.: Cardiovascular Dynamics, Second Edition, W. B. Saunders Co., Philadelphia, Pa., 1961, pp. 134-141.

44. Schneider, Robert A.: "A Fully Automatic Portable Blood Pressure Recorder," Journal of Applied Physiology, Vol. 24, No. 1, Jan., 1968, pp. 115-118.

45. Siahoya, Odo; Kahn, Alan R., and Ware, Ray W.: A Digital Readout Technic Applicable to Laboratory and Aerospace Medical Monitoring of Physiologic Data, Technical Documentary Report No. SAM-TDR-62-139, USAF School of Aerospace Medicine, Brooks Air Force Base, Texas, Feb., 1963.

46. Smith, C. R., and Bickley, W. H.: The Measurement of Blood Pressure in the Human Body, NASA Technology Survey, NASA SP-5006, April, 1964.

47. Van Bergen, F. H.; Weatherhead, D. S.; Treloar, A. E.; Dobkin, A. B., and Buckley, J. J.: "Comparison of Indirect and Direct Methods of Measuring Arterial Blood Pressure," Circulation, Vol. 10, No. 4, Oct., 1954, pp. 481-490.

48. Vogt, Fred B., and Hallen, Thor O.: "Electrocardiogram Preprocessing Unit," Aerospace Medicine, Vol. 38, No. 2, Feb., 1967, pp. 123-126.

49. Wallace, John D.; Lewis, David H., and Khalil, Sami Abow: "Korotkoff Sounds in Humans," The Journal of the Acoustical Society of America, Vol. 33, No. 9, Sept., 1961, pp. 1178-1182.

50. Ware, Ray W., and Anderson, Wallace.: "Spectral Analysis of Korotkov Sounds," IEEE Transactions on Biomedical Engineering, Vol. BME-13, No. 4, Oct., 1966, pp. 170-174.

51. Ware, Ray W., and Kahn, Alan R.: "Automatic Indirect Blood Pressure Determination in Flight," Journal of Applied Physiology, Vol. 18, No. 1, Jan., 1963, pp. 210-214.

52. Wilcox, Jane: "Observer Factors in the Measurement of Blood Pressure," Nursing Research, Vol. 10, No. 1, 1961, pp. 4-17.

53. Wiggers, Carl J.: "Dynamic Reactions Induced by Compression of an Artery," Circulation Research, Vol. 4, Jan., 1956, pp. 4-7.

54. Zuidema, George D.; Edelberg, Robert, and Salzman, Edwin W.: "A Device for the Indirect Recording of Blood Pressure," USAF, Wright-Patterson Air Force Base, Ohio, WADC Technical Note 55-427, Project 7216, Task 71712, Sept., 1955.

APPENDIX A

CIRCUIT DIAGRAMS

The circuit diagrams for the system for indirect measurement and digital display of systolic and diastolic blood pressures are shown in Figures A1 through A9. In all diagrams, the capacitance values are in microfarads unless otherwise indicated. Also, all resistors are ± 5% except where indicated. The integrated circuit operational amplifiers labeled UA 709C are manfactured by Fairchild and are numbered U5B770939-714.

Input transducers which have been used with the system are the cuff microphone described in Appendix C, silver-silver chloride ECG electrodes, and a Giannini 5,000-ohm potentiometer-type pressure transducer Model No. CA-D-, 5-50. This transducer has a range of 0-5 p.s.i.d. and one of the differential inputs is open to atmospheric pressure. A cuff pump/deflator manufactured by E & M Instrument Co. has been used for automatic inflation and deflation of the cuff.

In Figure A1 is shown the ECG preamplifier. The differential input is applied to amplifiers A1 and A2. Amplifier A3 converts the differential signal to a single-ended signal. The gain of amplifier A3 is controlled by switching the feedback resistance with the ECG GAIN switch on the front panel (see Figure A9). The bandwidth of the preamplifier extends from approximately 0.1 Hz to 100 Hz.

The sounds and pressure preamplifiers are shown in Figure A2. The pressure transducer is supplied with + 15 VDC and - 15 VDC in such a manner that the pressure analog signal becomes more negative with increasing pressure. The pressure analog signal enters at BP-6 P and amplifier A2 is used to adjust the gain and bias

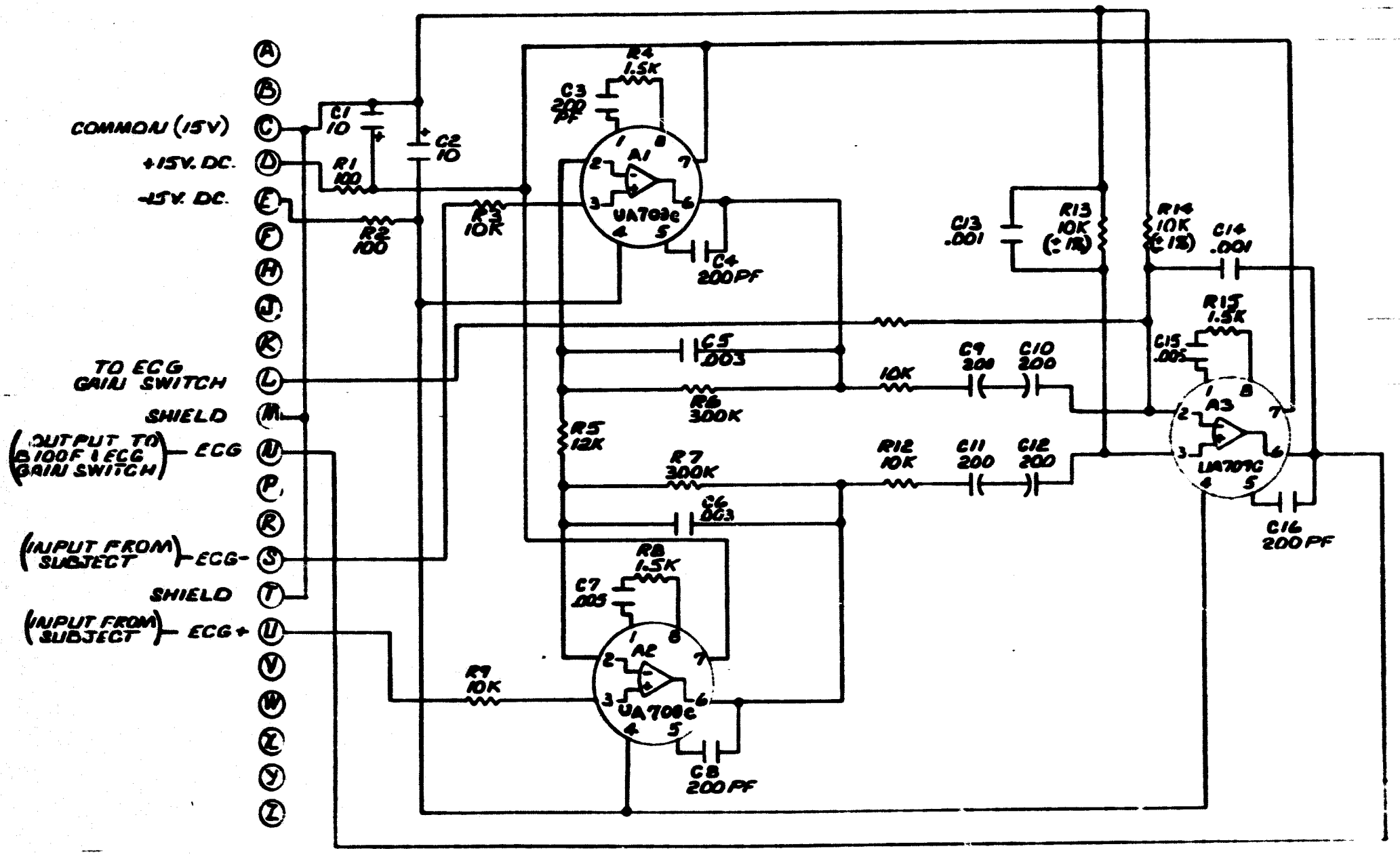


Figure A1 – Electrocardiograph preamplifier (Board BP-7)

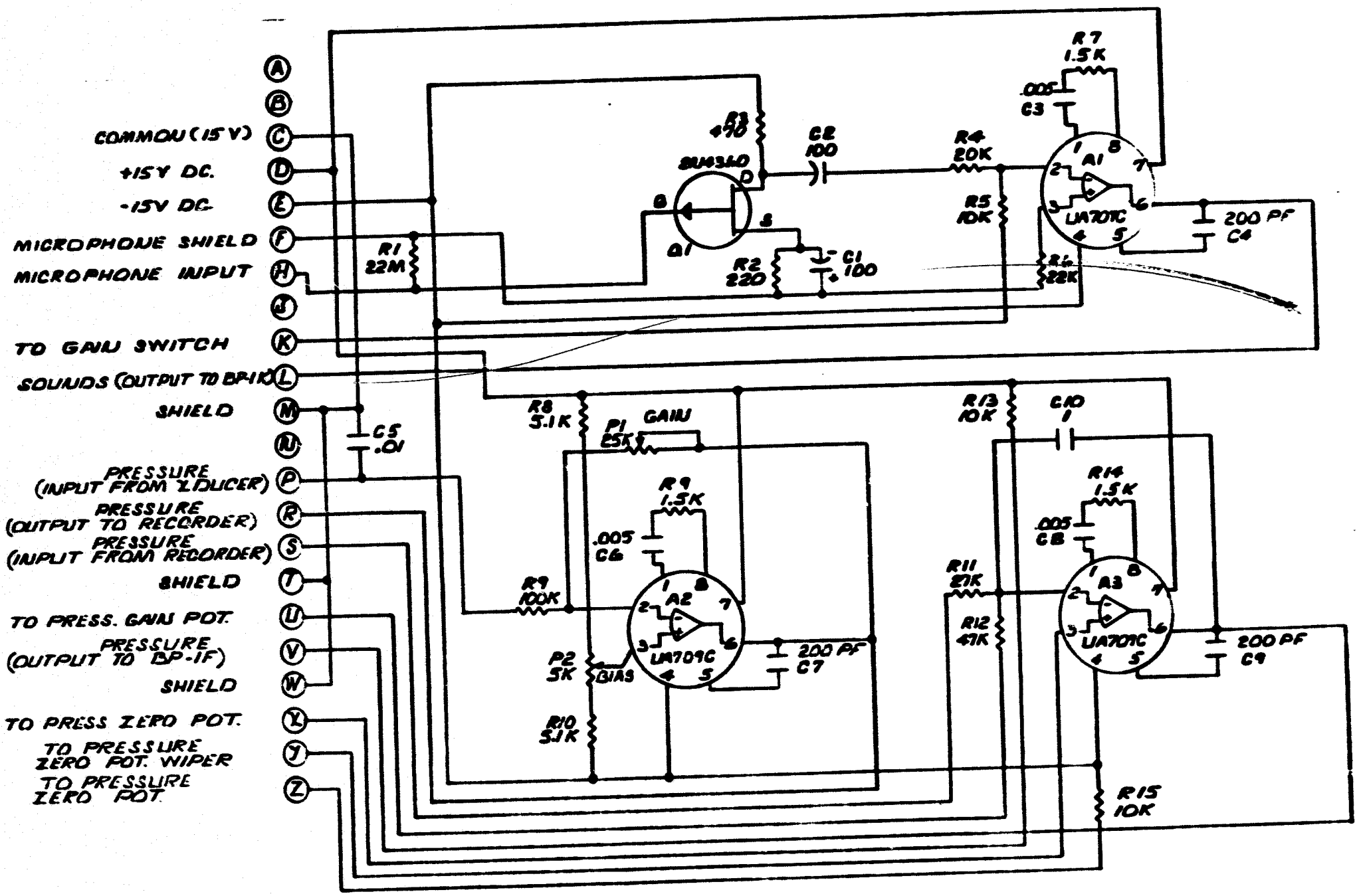


Figure A2 – Sounds and pressure preamplifiers (Board BP-6)

of the signal for compatibility with magnetic tape recorders. Amplifier A3 provides filtering and gain and bias adjustments on the front panel (see Figure A9) for calibration of the unit both for self-contained operation and for processing of recorded signals with different pressure gradients. The signal from the cuff microphone enters through BP-6F and is amplified and inverted by Q1. Amplifier A1, combined with the front panel gain switch, provides a gain adjustment for the incoming sounds.

The sounds filter pre-processor and pressure inverter board is shown in Figure A3. Amplifiers A1 and A3 and associated circuitry serve as high-pass filters with a low-frequency cutoff of approximately 10 Hz while amplifiers A2 and A4 are configured as low-pass filters with a high-frequency cutoff of approximately 30 Hz. The overall response of this combined filter configuration is given in Appendix E. Similarly, amplifiers A6 and A8 and associated circuitry are 80-Hz (approximately) high-pass filters while A7 and A9 are 110 Hz (approximately) low-pass filters. The measured characteristics of this combined filter configuration are also given in Appendix E. Amplifier A5 and switch S1 provide the capability of processing an inverted pressure analog signal. Amplifier A10 is a summing amplifier which adds the filtered sounds output of the 10 to 30 Hz filter with the pressure signal. This combined signal is available on pin BP-1T, but is not used in the system.

Figure A4 is a circuit diagram of a circuit board located physically in the cardiotachometer section of the Vital Signs Indicator. This circuit is a filter and monostable multivibrator of the type described by Vogt and Hallen (48). The filter has a center frequency of approximately 17 Hz and the 3-db bandwidth extends from approximately 13 to 20 Hz. Transistors Q1, Q2, Q3, and Q4 and their associated components

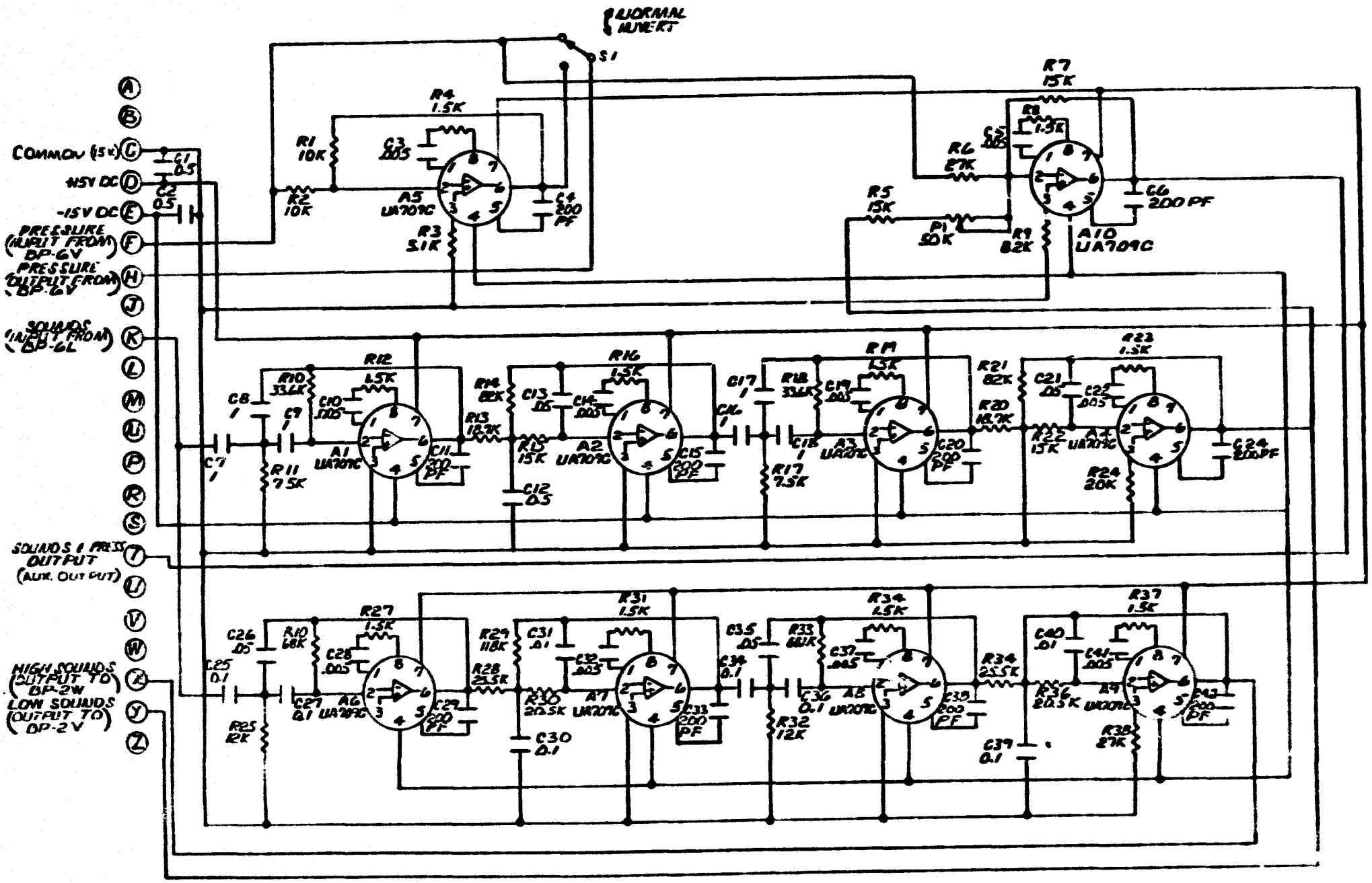


Figure A3 – Sounds filter pre-processor and pressure inverter (Board BP-1)

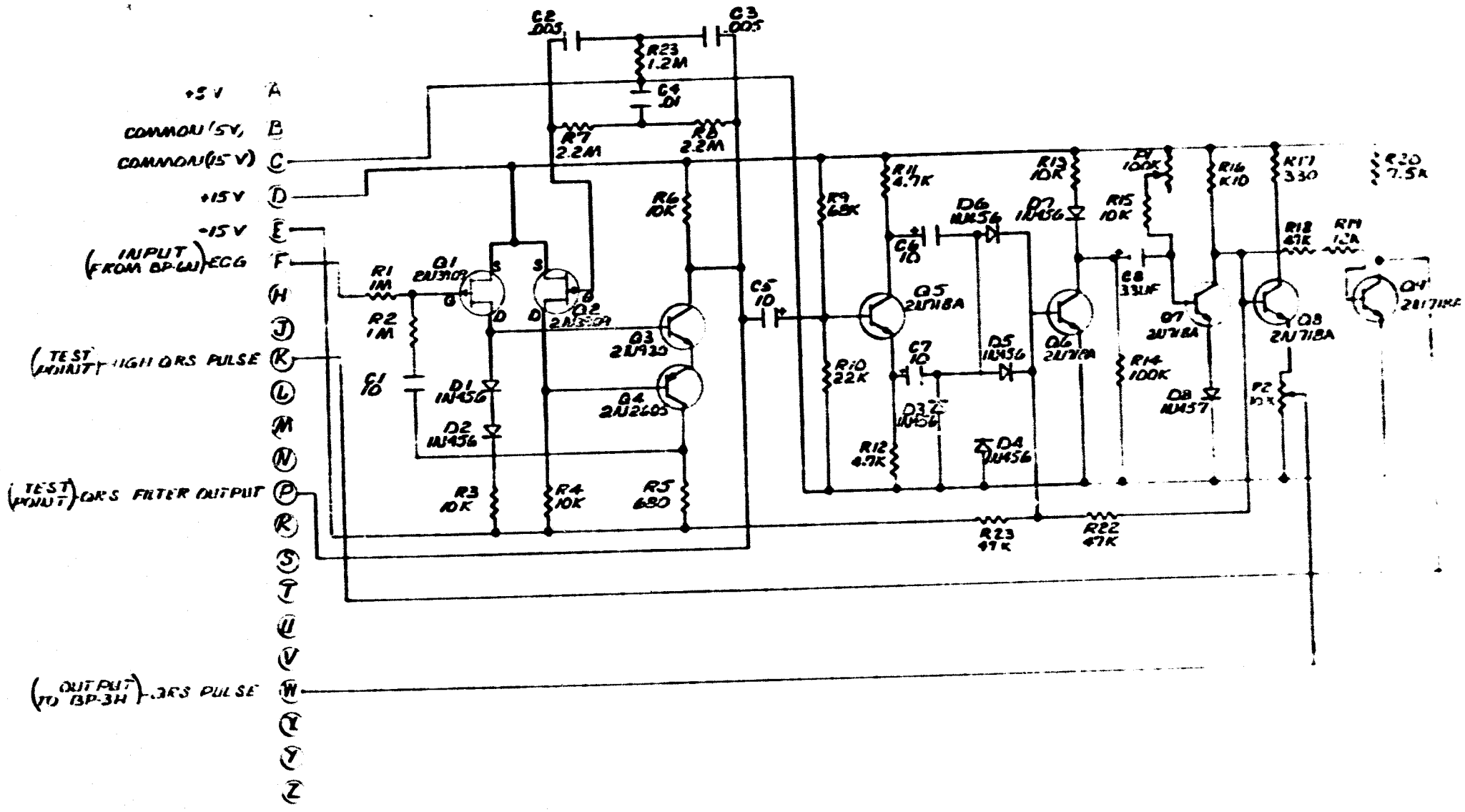


Figure A4 – ECG filter pre-processor and pulse generator (Board B-100)

comprise the filter. Transistor Q5 drives the diode bridge composed of D3, D4, D5, and D6. Thus, the absolute value of the filtered ECG drives the monostable multivibrator composed of Q6 and Q7 and associated components. Output pulses are available of opposite polarities from emitter follower Q8 (from P2) and from the collector of Q9. The QRS output pulse used in this system is on pin B-100W.

The sounds and pressure recognition pre-processor is shown in Figure A5. Whenever the pressure analog voltage exceeds a set value (set by P5), comparator A13 changes states and the output of the comparator is inverted by Q1 such that Q3 and Q5 are turned "ON". This action depletes or "knocks down" the charge on capacitors C9 and C25. Transistors Q2 and Q4 serve to establish an initial charge on C25 and C9, respectively, such that a threshold is established after the system is enabled by the decay of the pressure signal and the corresponding change of state of the comparator A13. The initial voltage on C25 and C9 is adjustable by P4 and P3, respectively. The output of the 10 to 30 Hz sounds filter enters on pin BP-2V and the output of the 80 to 110 Hz sounds filter enters on pin BP-2W. These signals go through symmetrical and identical circuitry. The absolute values of the low sounds and high sounds are taken by A1, A2 and by A7, A8, respectively. Transistors Q6, Q7, Q9, and Q10 prevent sound signals from entering the inverter and peak detector amplifiers A3, A4, A9, and A10 unless a SEARCH pulse is simultaneously present. This SEARCH pulse is generated from the QRS PULSE on Board BP-3. Amplifiers A3 and A9 serve as unity-gain inverters. Amplifiers A4 and A10 are operated in the high-input impedance voltage follower connection to charge capacitors C9 and C25 to approximately 1/2 of the voltage of the incoming signal. When the circuitry is

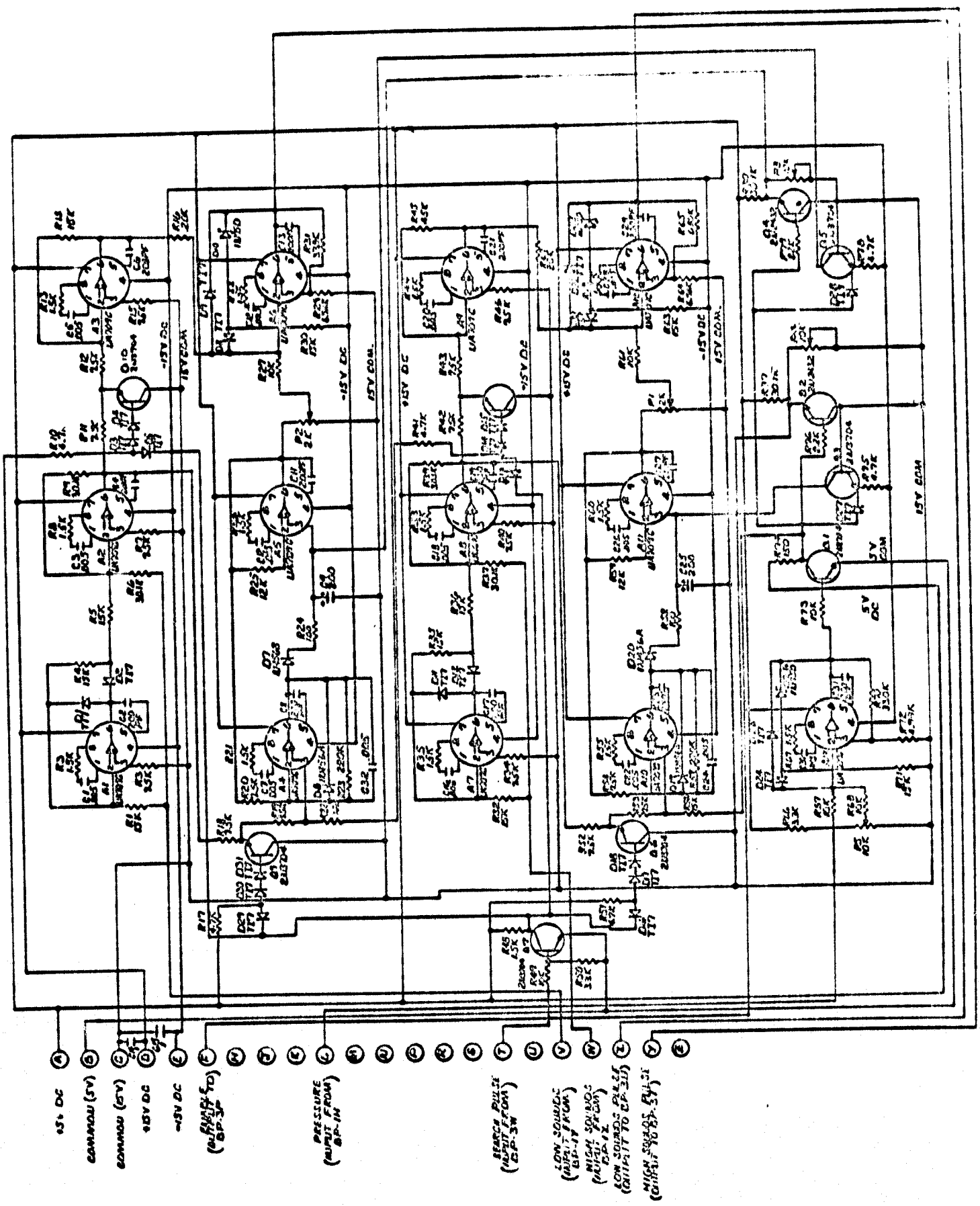


Figure A5 -Sounds and pressure recognition pre-processor (Board BP-2)

enabled, Q2 and Q4 are "ON" and R56 and R22 are connected to Common such that a voltage divider is formed. Amplifiers A5 and A11 are non-inverting and the peak voltage on the storage capacitors appears on P1 and P2. Potentiometers P1 and P2 set the threshold for detection of sounds. Potentiometer P2 sets the ratio of 0.9 and P1 sets the ratio of 0.2. Comparators A6 and A12 pro ide an output whenever the sum of the inverted output of the absolute value of the filtered sounds exceeds the fraction (set by P1 and P2) of the peak value (maximum) stored on capacitors C9 and C25. The comparator outputs go to Board BP-3 through pins BP-2X and BP-2Y.

The transistors Q13 and Q14 on Board BP-3, shown in Figure A6, serve as inverters of the comparator signals from Board BP-2. The negative-polarity pressure analog voltage on pin BP-3K is digitized using the dual-slope integration technique. Field-effect transistor (FET) Q1 turns "ON" and samples the incoming voltage, while Q2 and Q3 are "OFF". Transistors Q7 and Q8 and associated circuitry form an astable multivibrator with a frequency output of 200 kHz. This frequency is divided by two in FF1 and a clock signal of 100 kHz exists on pin 12 of FF1. Amplifier A1 is an integrator which integrates the incoming negative-polarity voltage (pressure analog) until 1000 clock pulses are counted by the decade counters of Board BP-5. The DUMP signal from the decade counters on pin BP-3M causes Q1 to turn "OFF", Q2 to turn "ON" and Q3 to remain "OFF". Thus, the integrator starts to integrate the relatively constant +15VDC power supply voltage and, when the output of the integrator approaches zero volts, amplifier A2 (a comparator) changes state and the decade counters are stopped. The count of the 100-kHz clock which is digitally

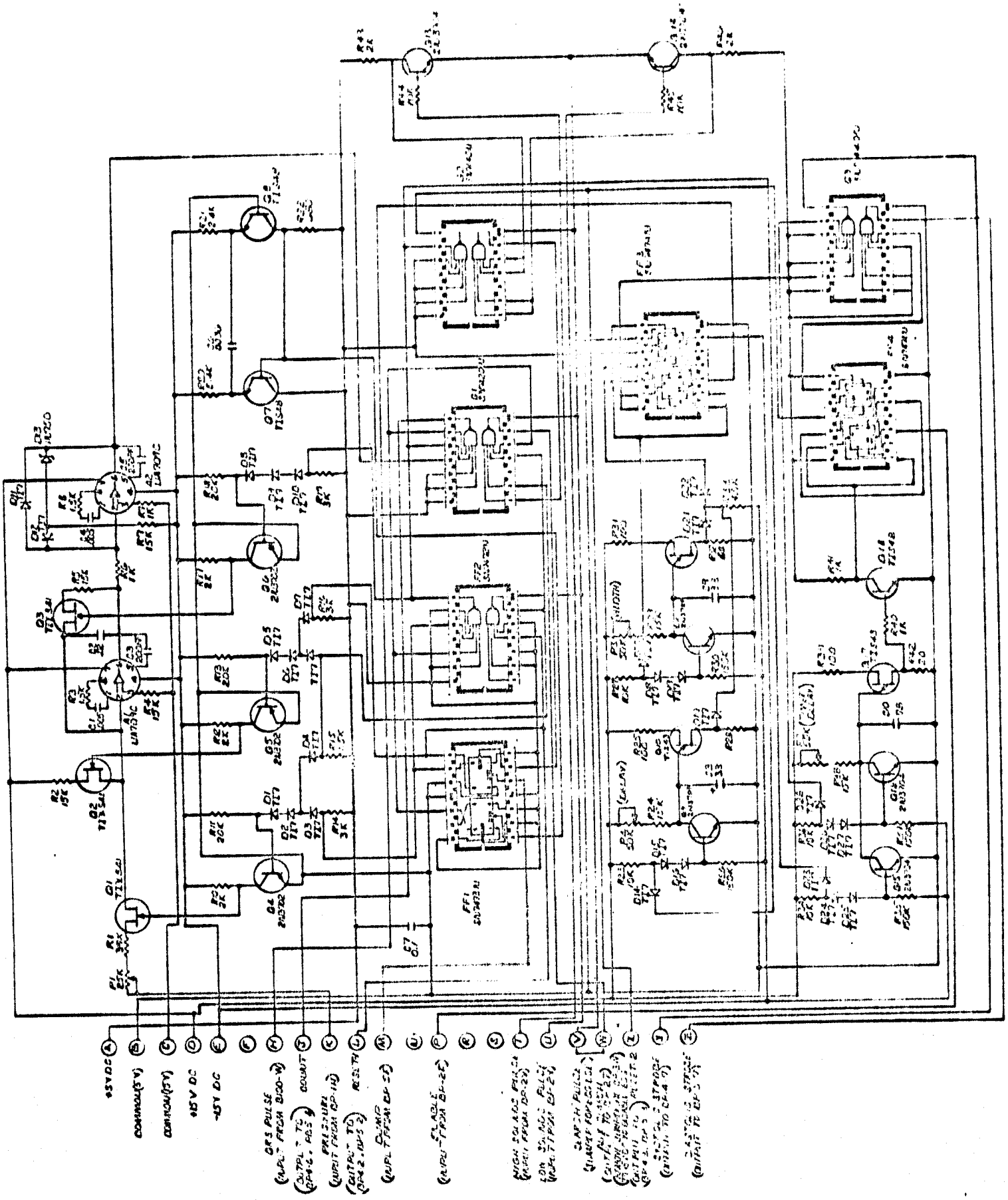


Figure A6 – Analog-to-digital converter, ECG SEARCH generator, and systolic/diastolic recognition logic (Board BP-3)

stored in the storage registers is then proportional to the input voltage (pressure analog). Transistor Q3 is turned "ON" to put R5 in the feedback path of the integrator with an open input to prevent A1 from acting as an integrator except as required during the digitize cycle. The switching FET's Q1, Q2, and Q3 are controlled by transistors Q4, Q5, and Q6 and associated connections with FF1 and FF2. The digitize command is initiated by the inverted form of either the high sounds pulse on BP-3T or the low sounds pulse on BP-3U through G2, and the output of G2 (pin 6) may be considered to be a form of DIGITIZE pulse. The ECG SEARCH pulse is generated by Q9, Q10, Q11, Q12, FF3, and associated circuitry. The QRS pulse on pin BP-3H starts the delay timer comprised of Q9 and Q10. After the delay, the SEARCH pulse goes to a logical 1 state (approximately +5 volts) and returns to a logical 0 state (approximately 0 volts) by the action of the width timer consisting of Q11 and Q12 and associated circuitry. Potentiometers P4 and P3 adjust the delay and width, respectively, of the SEARCH pulse. For use with an ECG input, pins BP-3V and BP-3W must be shorted. When an ECG signal is not available, the unit may be operated by removing the short and by applying +5VDC to pin BP-3 W (and to BP-2T). The nominal 2-second timer for the diastolic decision is effected by the circuitry of Q15, Q16, Q17, Q18, and FF4. Potentiometer P2 adjusts the delay time. Gate G3 is a dual 4-input positive nand buffer used to provide the systolic and diastolic strobe signals to Boards BP-4 and BP-5.

The decade counter, storage register, and decoder/driver circuitry are shown in Figure A7. Two identical boards, designated as BP-4 and BP-5, are used in each system. The decade counters are DC1, DC2, and DC3. The digitized pressure signal

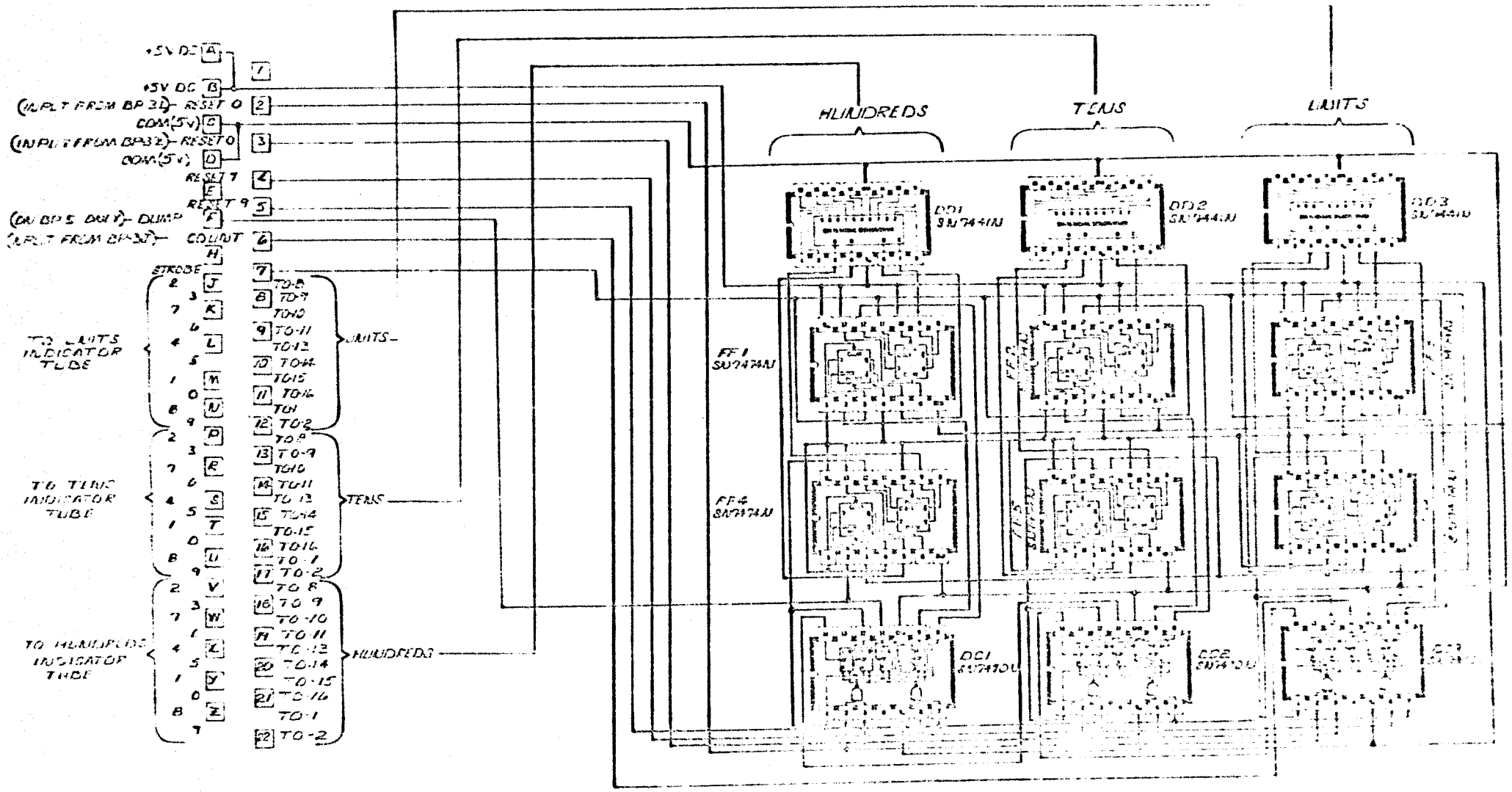


Figure A7 – Decade counter, storage register, and decoder/driver circuitry (Boards BP-4 and BP-5, two required)

is stored in the storage registers FF1, FF2, FF3, FF4, FF5, and FF6 when strobe input on pin BP-4-7 and BP-5-7 occurs. The decoder/drivers (DD1, DD2, and DD3) convert the binary-coded decimal (BCD) signals into decimal form for display of numerals on the gas-filled readout tubes.

In Figure A8 is shown the calibrator unit. Transistors Q1 and Q2 and the associated circuitry are used as an astable multivibrator which generates a square wave with a period of 400 milliseconds. The frequency is divided in half by FF1 and a symmetrical square wave of 400 milliseconds in each state is present on pin 9 of FF1. This square wave is "differentiated" by C3 and R4 and the positive spikes are available as a simulated R wave through D2 (150 b.p.m.) on pin S-100W. The negative spikes, through D3 , are available at pin S-100Z as a simulated sounds signal. Thus, the simulated sounds are synchronized to the simulated R waves and occur 400 milliseconds after the R waves such that the simulated sounds are within the SEARCH gate time interval. The simulated R wave signal of 50 b.p.m. is obtained in a frequency division by three in the connection of FF2. The simulated sounds output is also synchronized to this simulated R-wave output. This card serves as a calibrator for both the cardiotachometer and the sphygmomanometer sections of the Vital Signs Indicator. Known pressure levels, either from the pressure transducer or from magnetic tape, are required as an input for calibration of the sphygmomanometer.

In Figure A9 is shown the systems wiring diagram. All power supply voltages and common connections for all the cards of the system are returned and tied to the same tie-point. Operation of the calibrate and OFF-SUBJECT-TAPE switches are shown on this diagram. Other front-panel controls include the ECG TRIGGER, SOUNDS

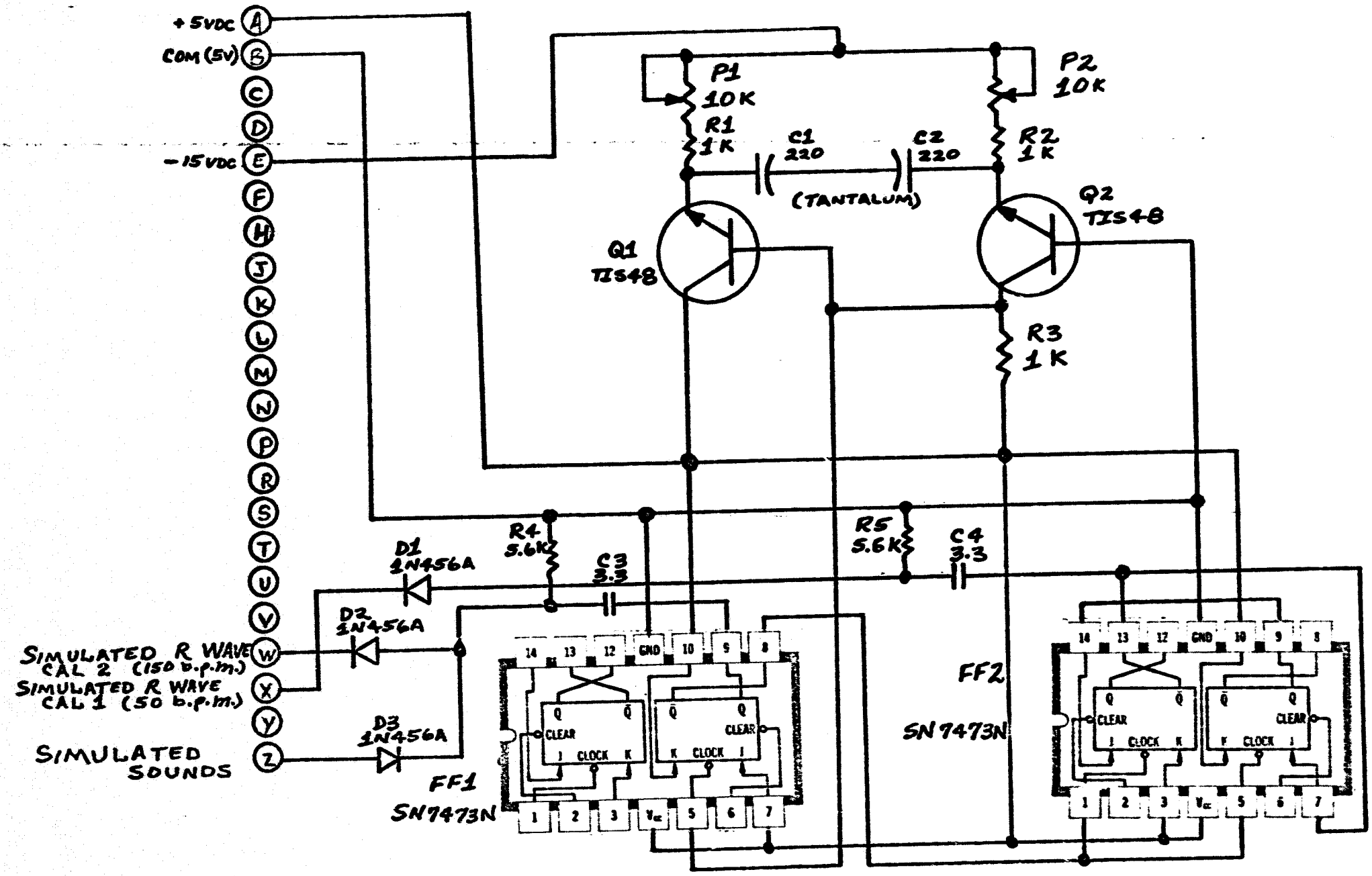


Figure A8 – Calibrator unit (Board S-100)

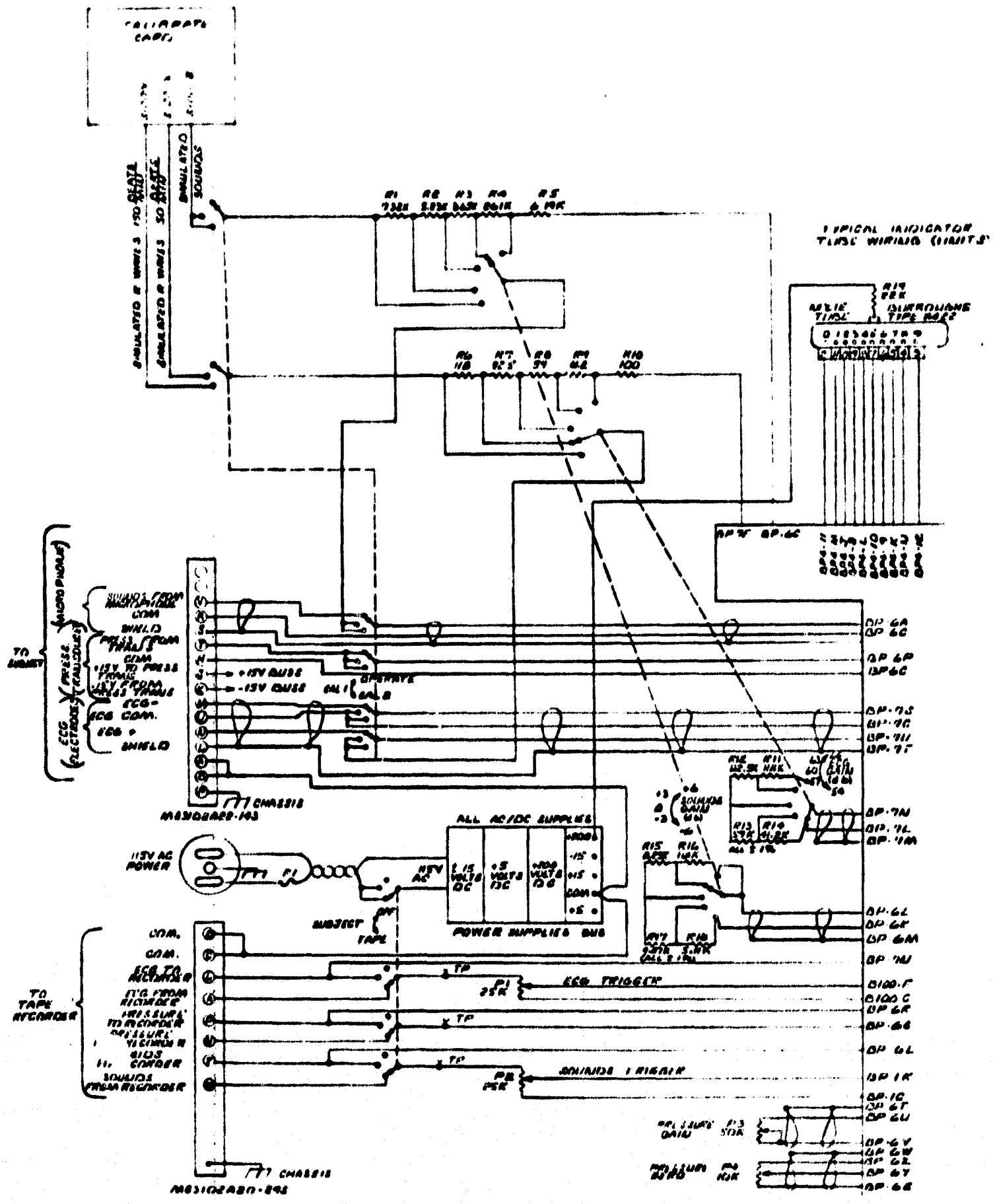


Figure A9 – Systems wiring diagram

TRIGGER, PRESSURE GAIN, and PRESSURE ZERO potentiometers. The gain of the sounds amplifier is controlled by the SOUNDS GAIN switch in 3-db steps from +6 db to -6 db. The gain of the ECG preamplifier is controlled by the ECG GAIN switch in 3-db steps from 54 to 66 db. These gain switches also control the input levels from the calibrate card. A typical indicator tube wiring diagram for the units digit is also shown in Figure A9.

APPENDIX B

BILATERAL DIRECT BLOOD PRESSURE DATA

Bilateral direct (intra-arterial) blood pressure measurements were made on one subject using the previously-described technique. The subject was a 53-year-old Negro male who was a chronic alcoholic with a history of schizophrenia and mild diabetes mellitus. He had been admitted to the hospital for anemia, weight loss, and jaundice. At the time of the measurements, he was 5 feet 7 1/2 inches tall and weighed 125 pounds.

Figure B1 contains the data from a slow cuff inflation. The top tracing (IA_1) is the intra-arterial pressure in the left brachial artery. The middle tracing (IA_2) is the intra-arterial blood pressure in the right brachial artery. The bottom tracing is the cuff pressure with the cuff placed on the right arm. The elevation of the systolic pressure distal to the cuff in the right arm during inflation is obvious. The pressure in the left arm remains essentially constant during cuff inflation.

Figure B2 contains the data from a slow cuff deflation after the inflation shown in Figure B1. Occlusion of the artery caused the intra-arterial pressure distal to the cuff to drop to approximately 40 mm Hg in agreement with the observations of London and London (26). The systolic pressure during cuff deflation is observed to be substantially above the resting systolic pressure at the end of the chart. No appreciable change occurs in the direct blood pressure of the left arm during this deflation.

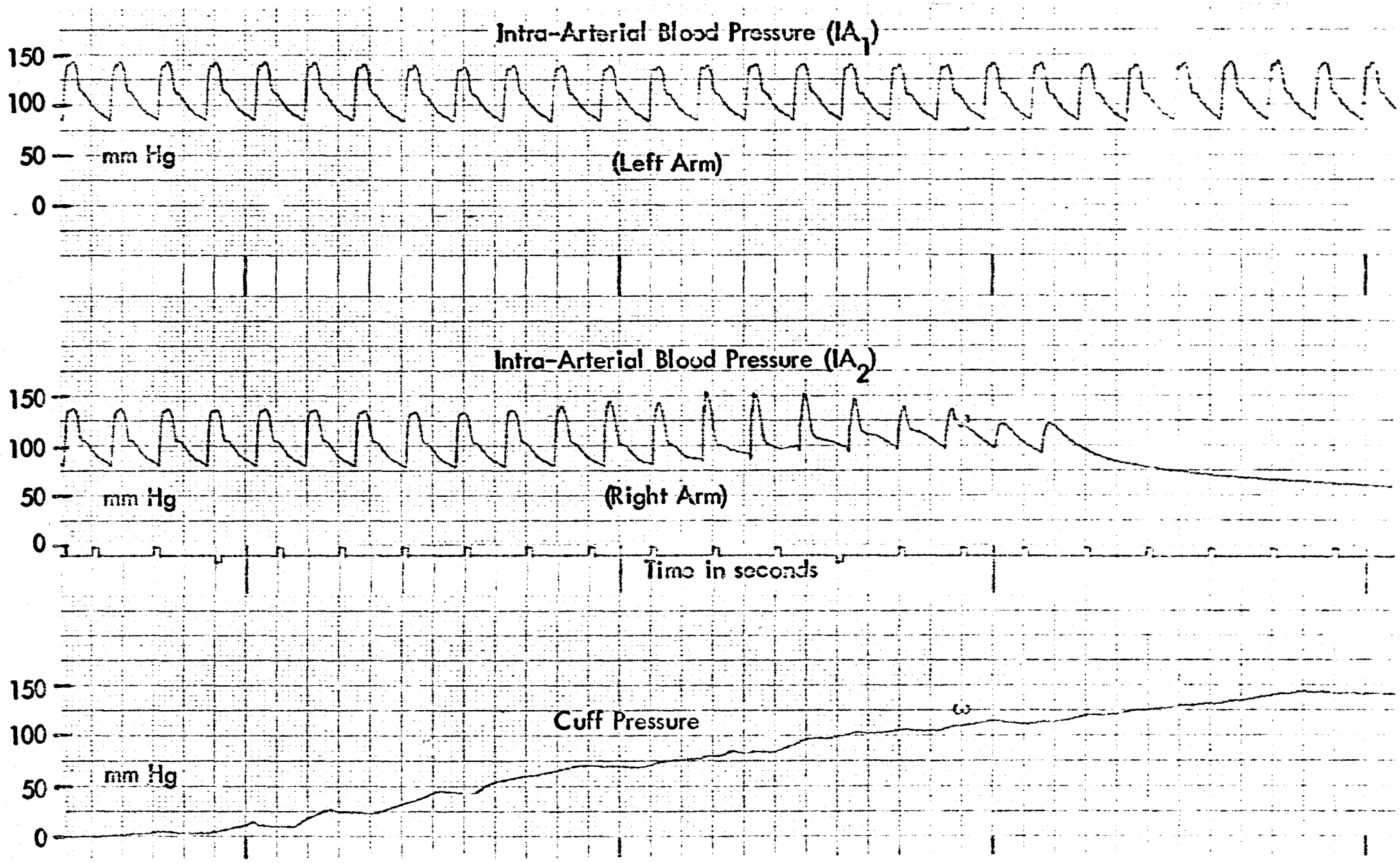


Figure B1 - Bilateral intra-arterial blood pressure during a slow cuff inflation

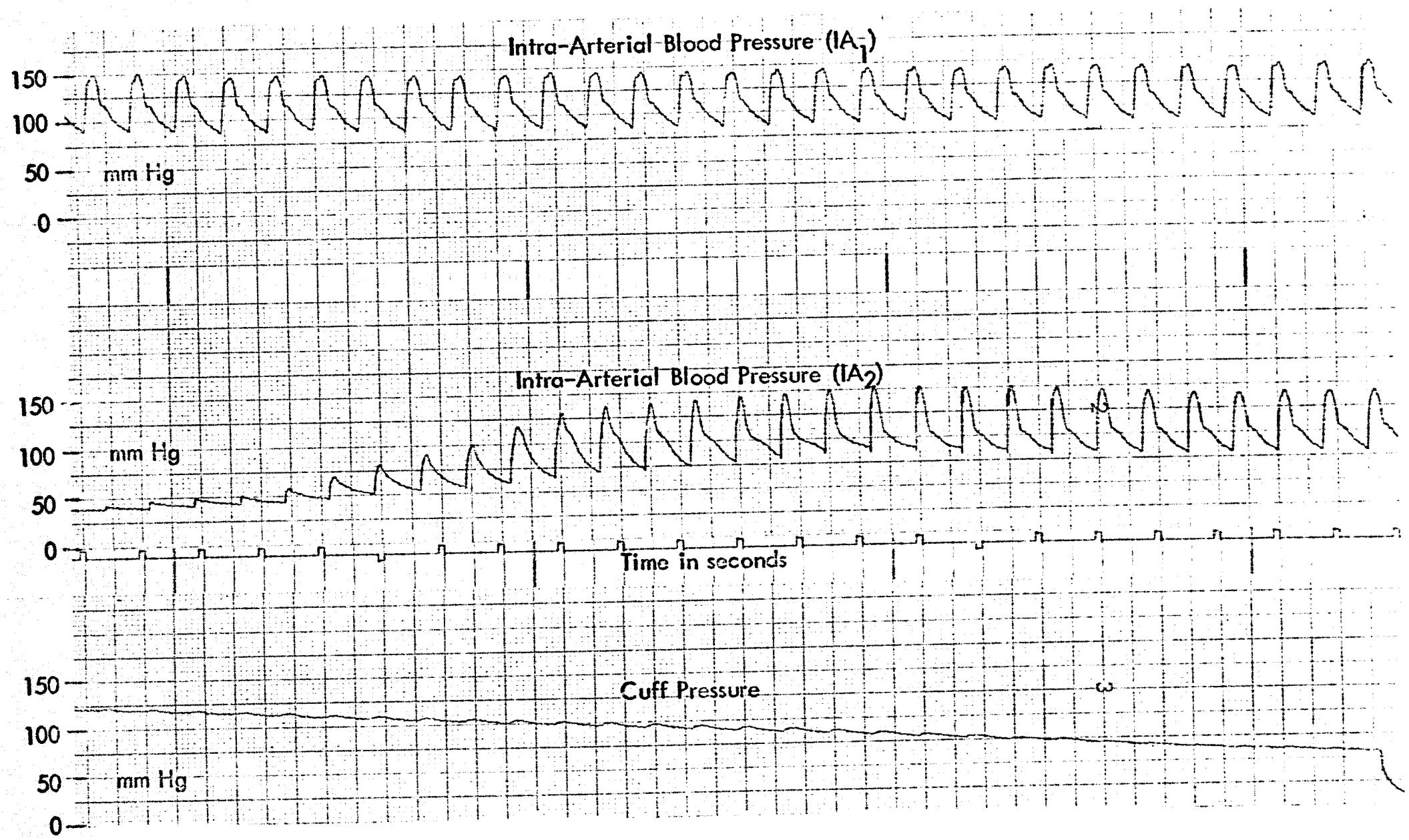


Figure B2 - Bilateral intra-arterial blood pressure during a cuff deflation

Data for a sustained cuff pressure of approximately 100 mm Hg are shown in Figure B3. The change in the shape of the blood pressure pulse as well as the elevation of the systolic pressure is seen in IA_2. The high-frequency notch which is probably indicative of the genesis of Korotkoff sounds is seen on the arm surface pulsations.

The response of the intra-arterial blood pressure (IA_2) to a rapid deflation of the cuff after a sustained pressure in excess of 100 mm Hg is shown in Figure B4. The elevated systolic pressure is observed to return to its resting value with the first heartbeat following deflation of the cuff.

The cuff was then placed on the left forearm such that the cuff was distal to the Cournand needle. Data obtained in this configuration are shown in Figure B5. Alterations in the shape of the intra-arterial pressure pulses (IA_1) are observed as the cuff pressure is varied. Figure B6 contains data gathered in this configuration for a cuff inflation/deflation cycle. It is obvious that changes in pulse shape due to the occlusion and partial occlusion of the artery distal to the Cournand needle do affect the systolic pressure proximal to the cuff.

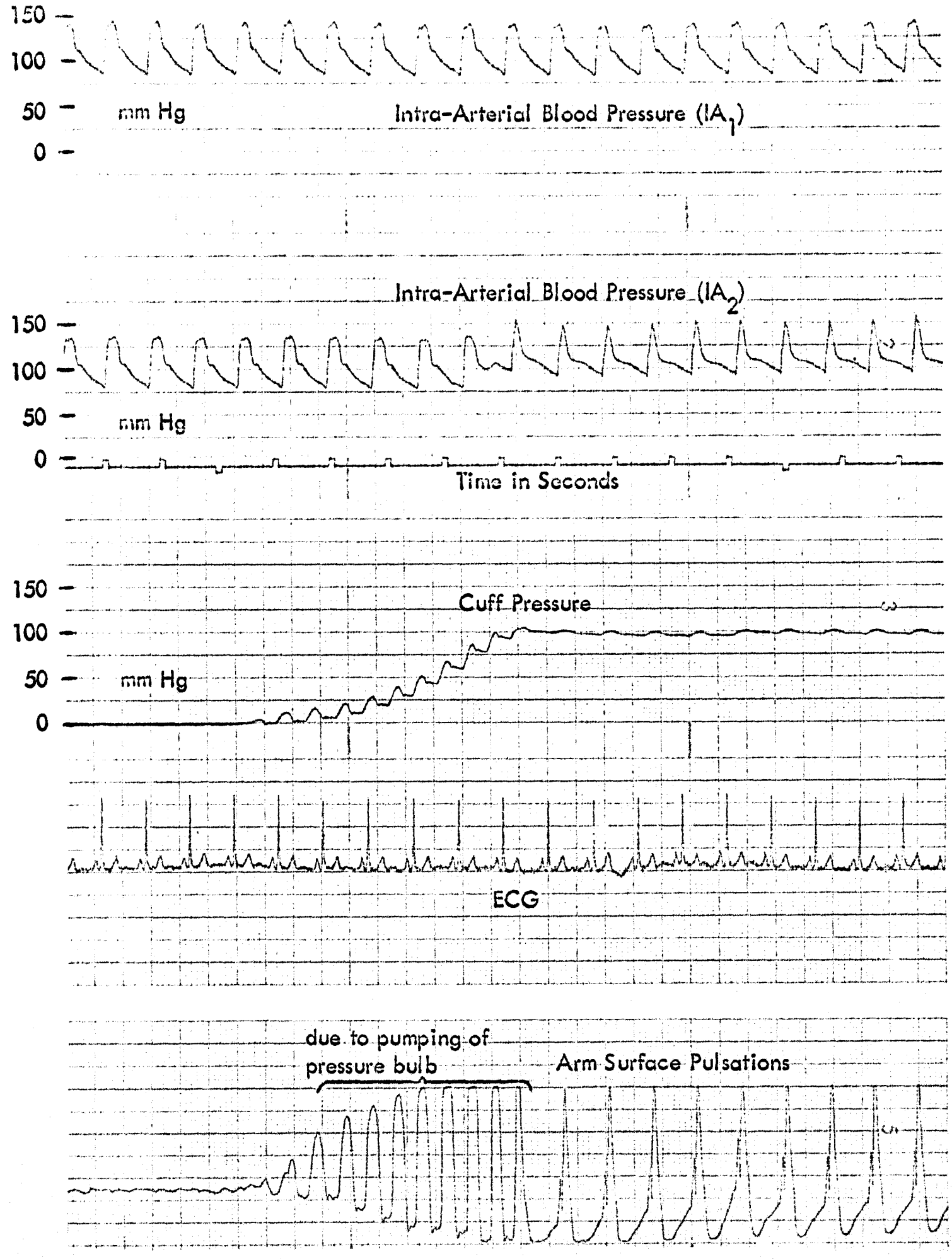


Figure B3 - Bilateral intra-arterial blood pressure during cuff inflation and sustained cuff pressure

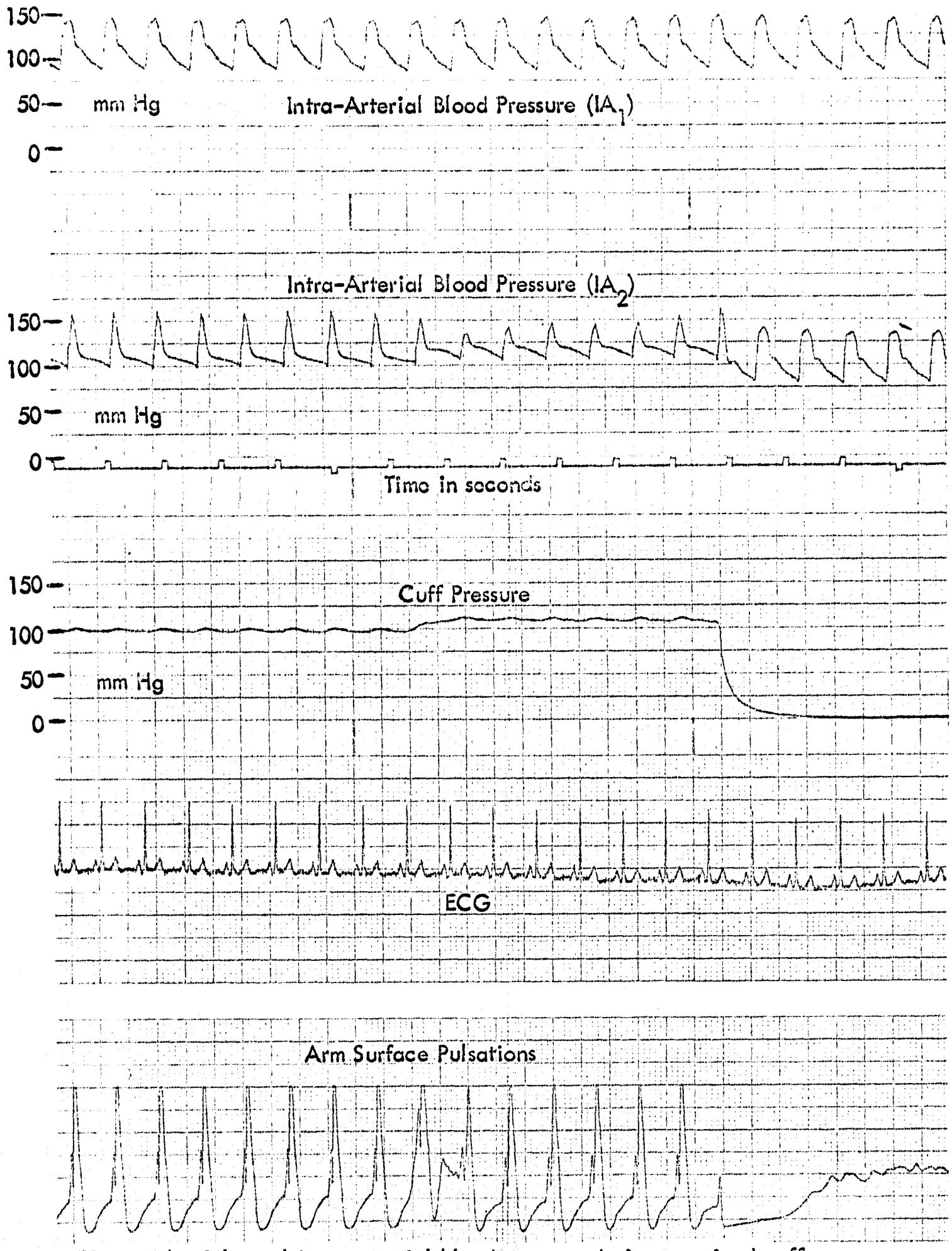


Figure B4 - Bilateral intra-arterial blood pressure during sustained cuff pressure and rapid deflation

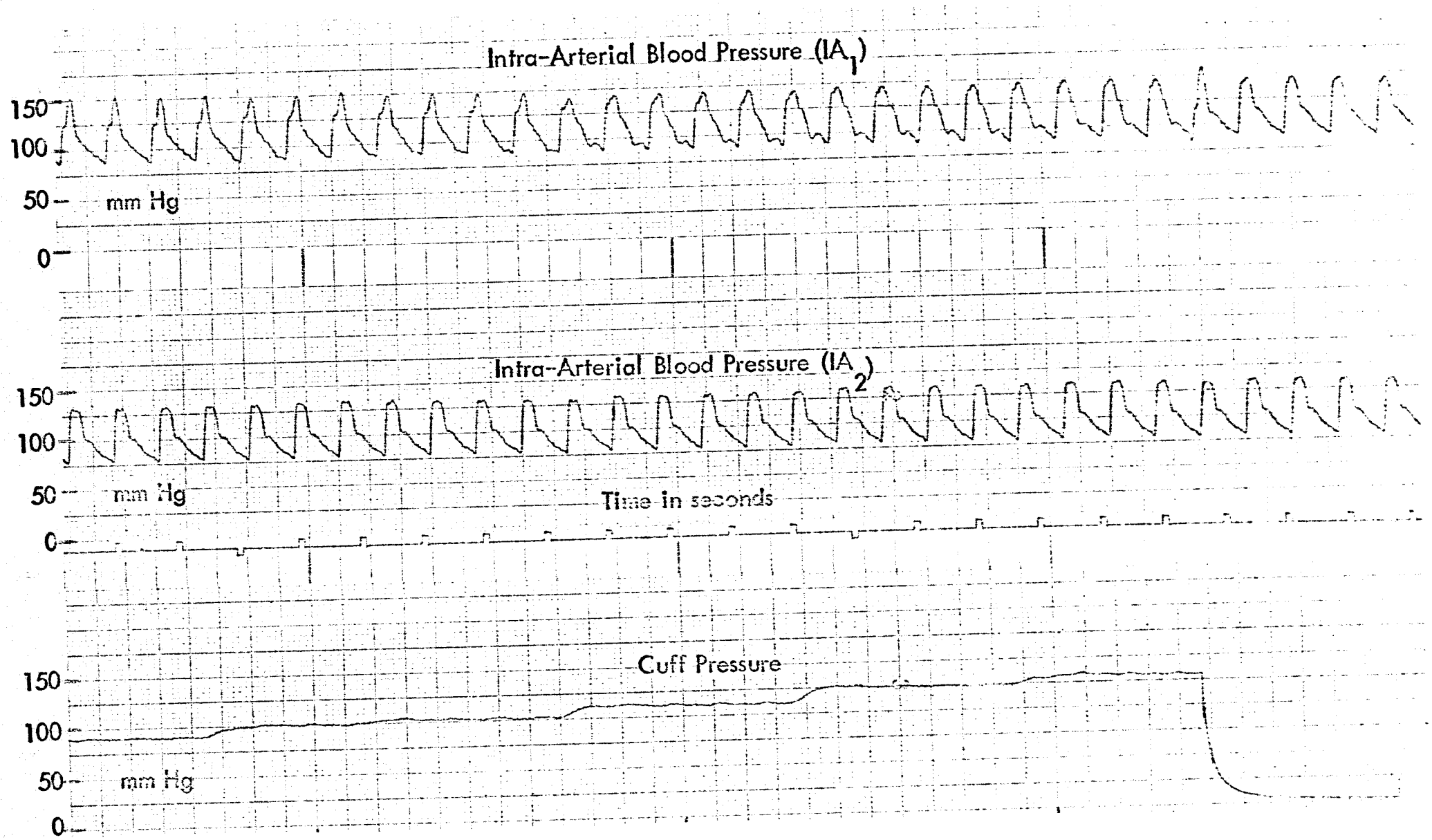


Figure B5 - Bilateral intra-arterial blood pressure with cuff on forearm (distal to IA_1)

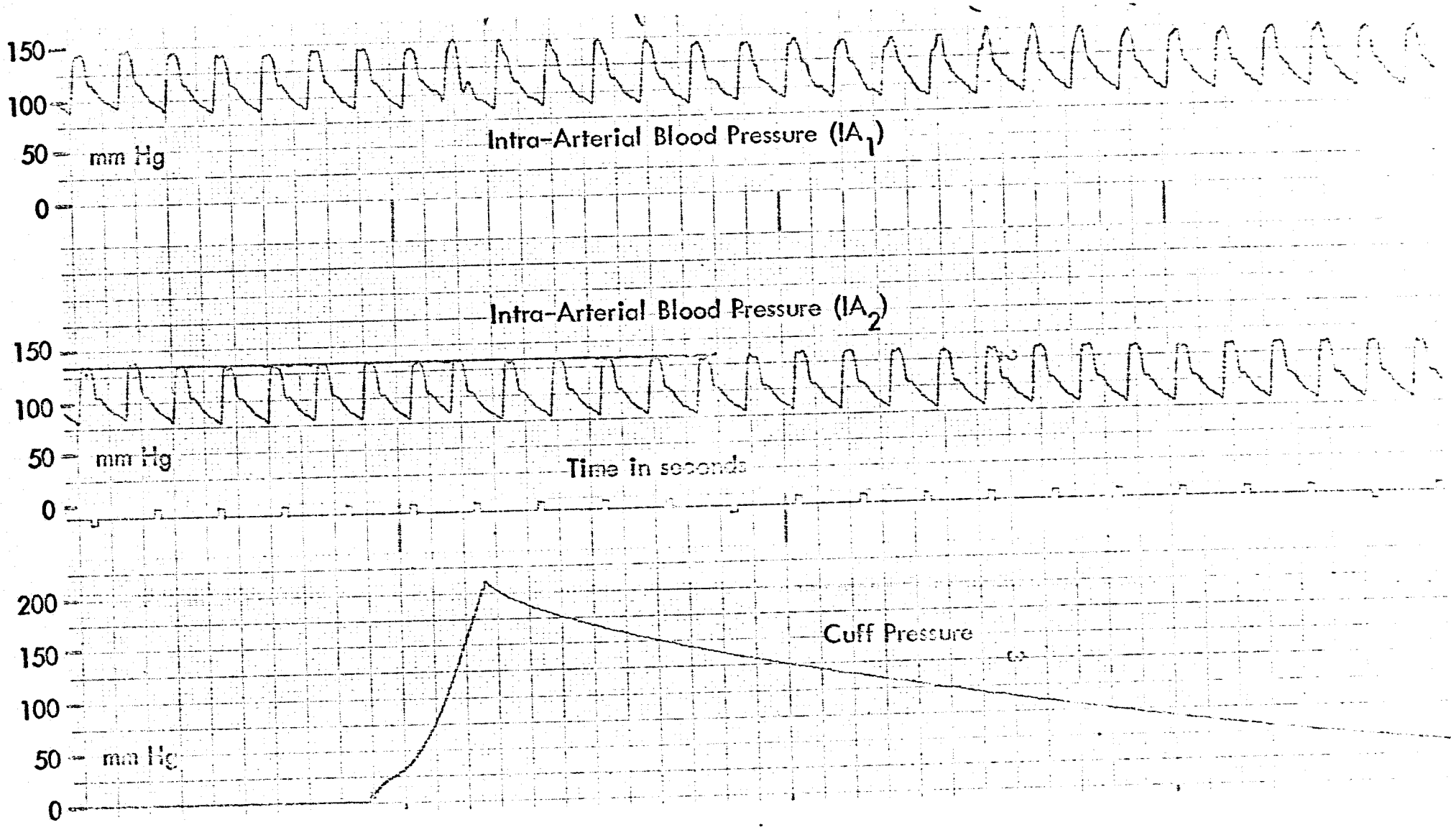


Figure B6 - Bilateral intra-arterial blood pressure during cuff inflation and deflation with cuff on forearm (distal to IA_1)

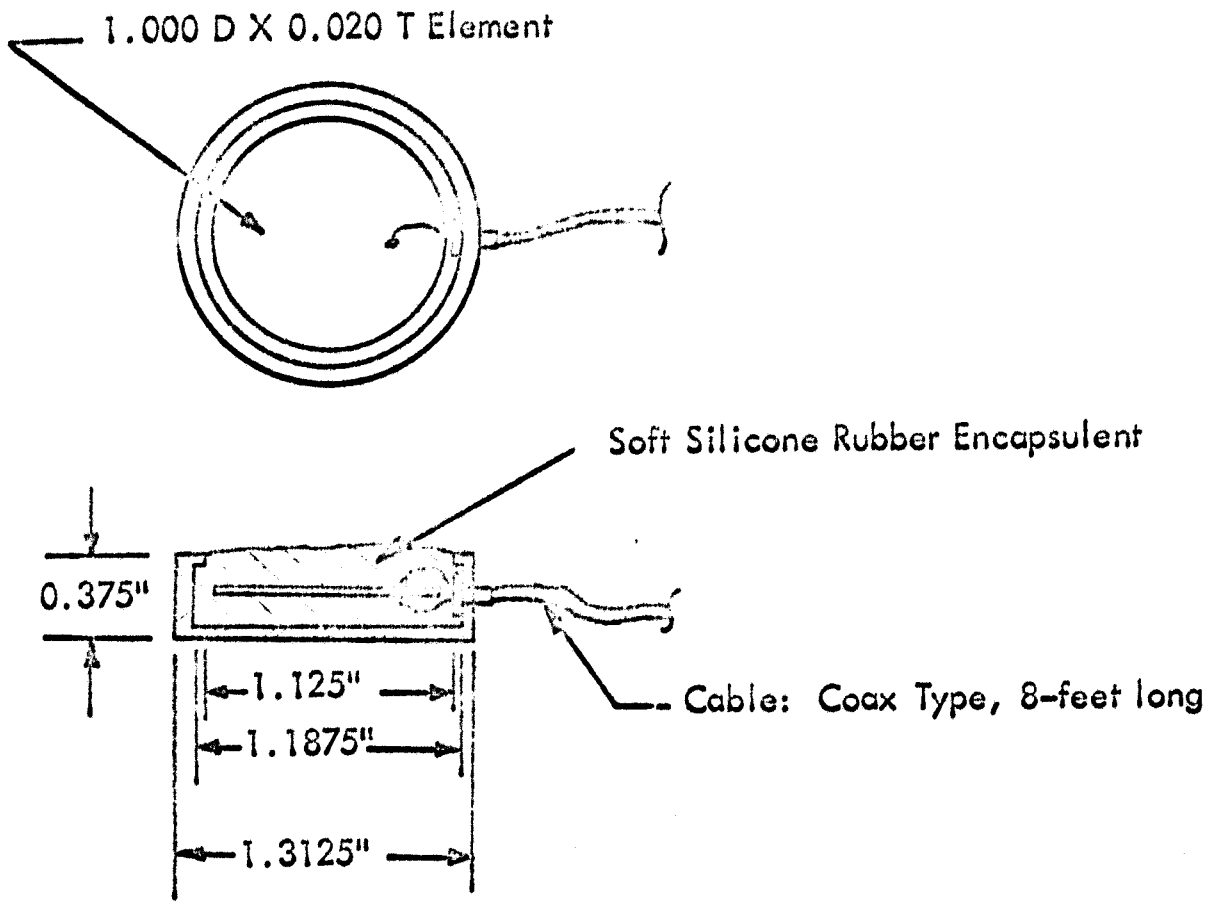
APPENDIX C

CUFF MICROPHONE CHARACTERISTICS

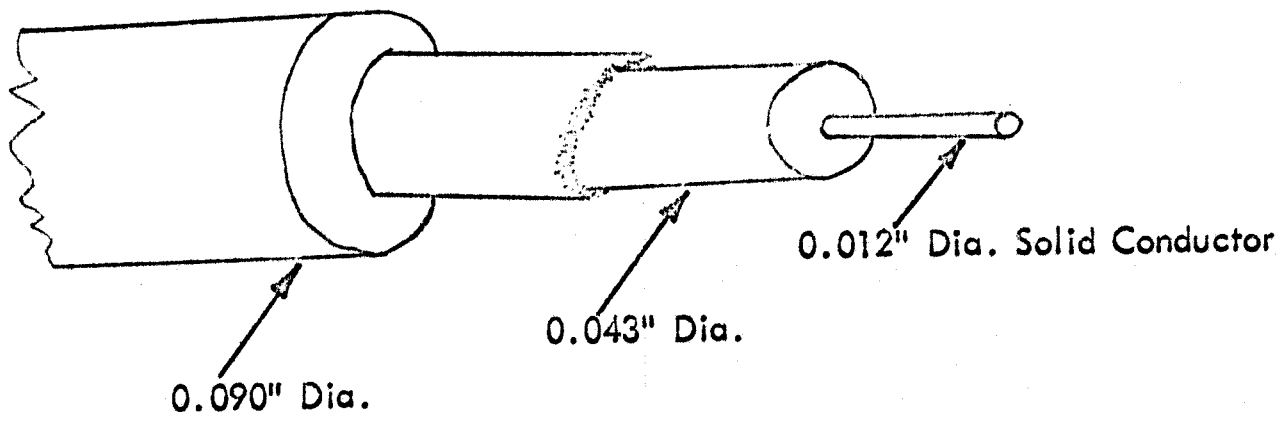
The cuff microphone used during this project was a microphone manufactured for use in the measurement of blood pressure by Air Shields, Inc. The characteristics of the microphone were not available; however, shown in Figure C1 are the measured dimensions and physical characteristics of one of the units. The characteristics vary somewhat from microphone-to-microphone and several microphones were used in the project. The internal dimensions of the microphone were determined from x-ray photographs. It appears that the element is a cylindrical 1.000-inch diameter by 0.020-inch thick disc of piezoelectric material slivered on both ends and is used in the thickness mode. The dimensions of the coaxial cable attached to the microphone are also shown in Figure C1.

The electrical impedance characteristics of the microphone together with the cable were measured using a Hewlett Packard 4260A Universal Bridge (f = 1000 Hz). The equivalent series circuit was found to be a resistor of 207 ohms and a capacitor of 15.4 nf.

(Readings and dimensions courtesy of Dr. Louis S. Meharg)



MICROPHONE



CABLE

Figure C1 - Detailed drawings of cuff microphone and coaxial cable

APPENDIX D

BANDPASS CHARACTERISTICS OF VARIABLE BANDPASS FILTERS

The bandpass characteristics of the Krohn-Hite Model 330M filter were found to vary slightly from unit-to-unit. The exact unit used in this project is not known; however, measured bandpass characteristics on such a filter are shown in Figures D1 and D2. These measurements were taken with a Tektronix 502A Dual-Beam Oscilloscope, Fluke Model 910A RMS Voltmeter, and Wavetek Model 114 Signal Generator. The measured assymptotic slopes are 24 db/octave. For the 80 and 110 Hz dial settings, the 3-db points do not occur at precisely 80 and 110 Hz.

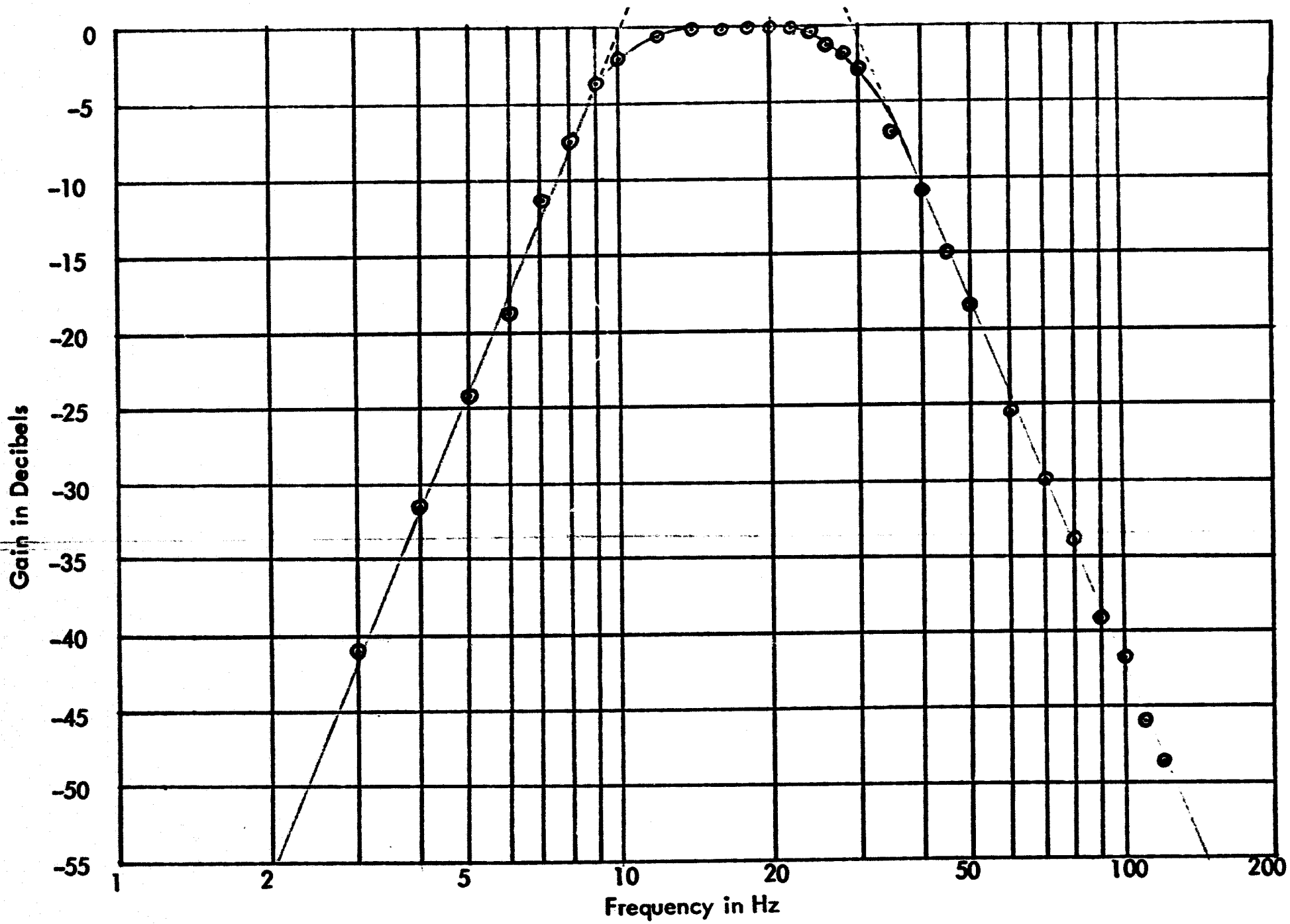


Figure D1 – Measured bandpass characteristics of Krohn-Hite filter for dial settings of 10 and 30 Hz

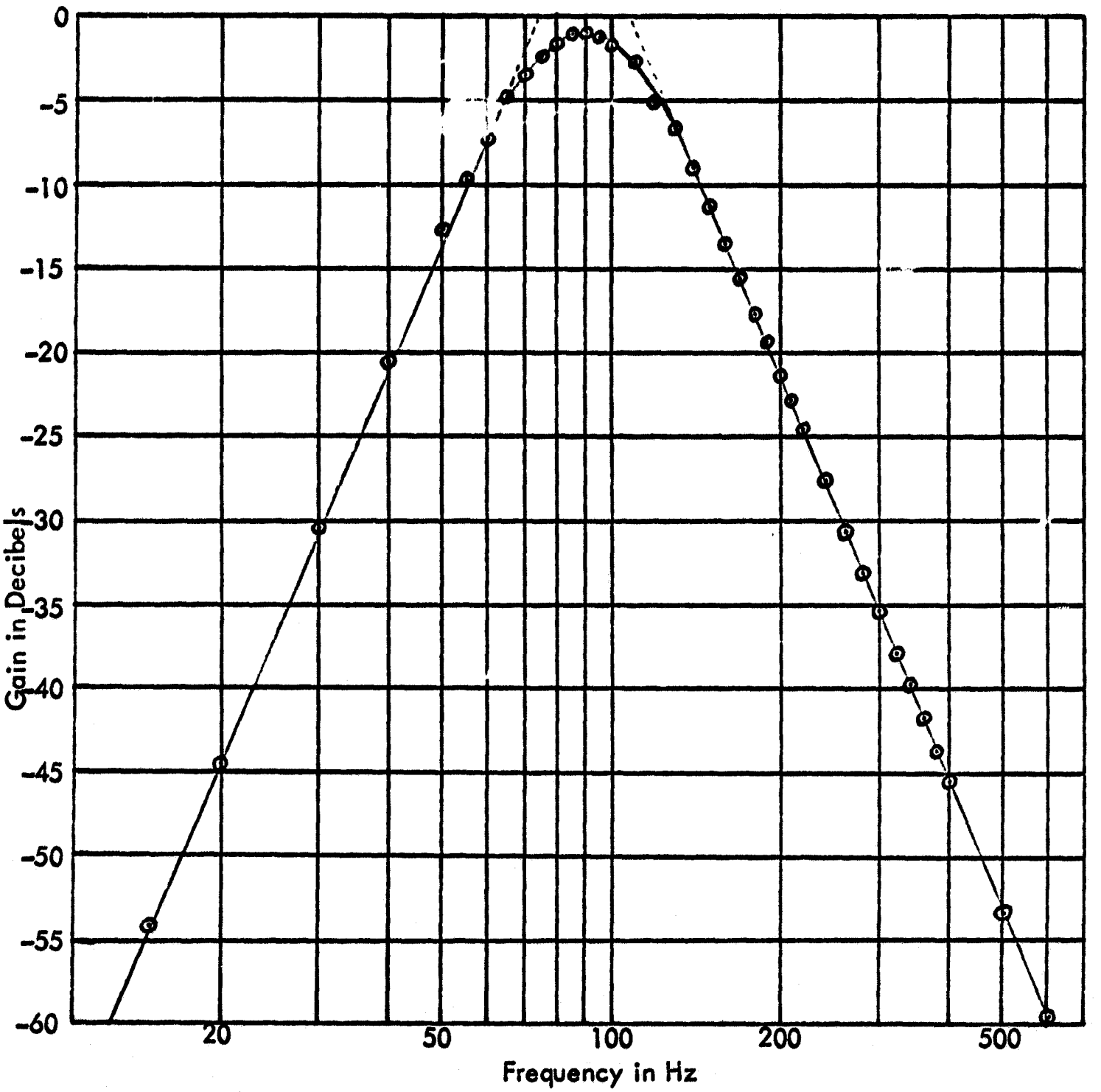


Figure D2 – Measured bandpass characteristics of Krohn-Hite filter for dial settings of 80 and 110 Hz

APPENDIX E

BANDPASS CHARACTERISTICS OF PRE-PROCESSING FILTERS

The bandpass characteristics of the sounds pre-processing filters shown in circuit diagram form in Figure A3 were measured. The test equipment used was the same Tektronix 502A Dual-Beam Oscilloscope, Fluke Model 910A RMS Voltmeter, and Wavetek Model 114 Signal Generator that were used for the measurements reported in Appendix D.

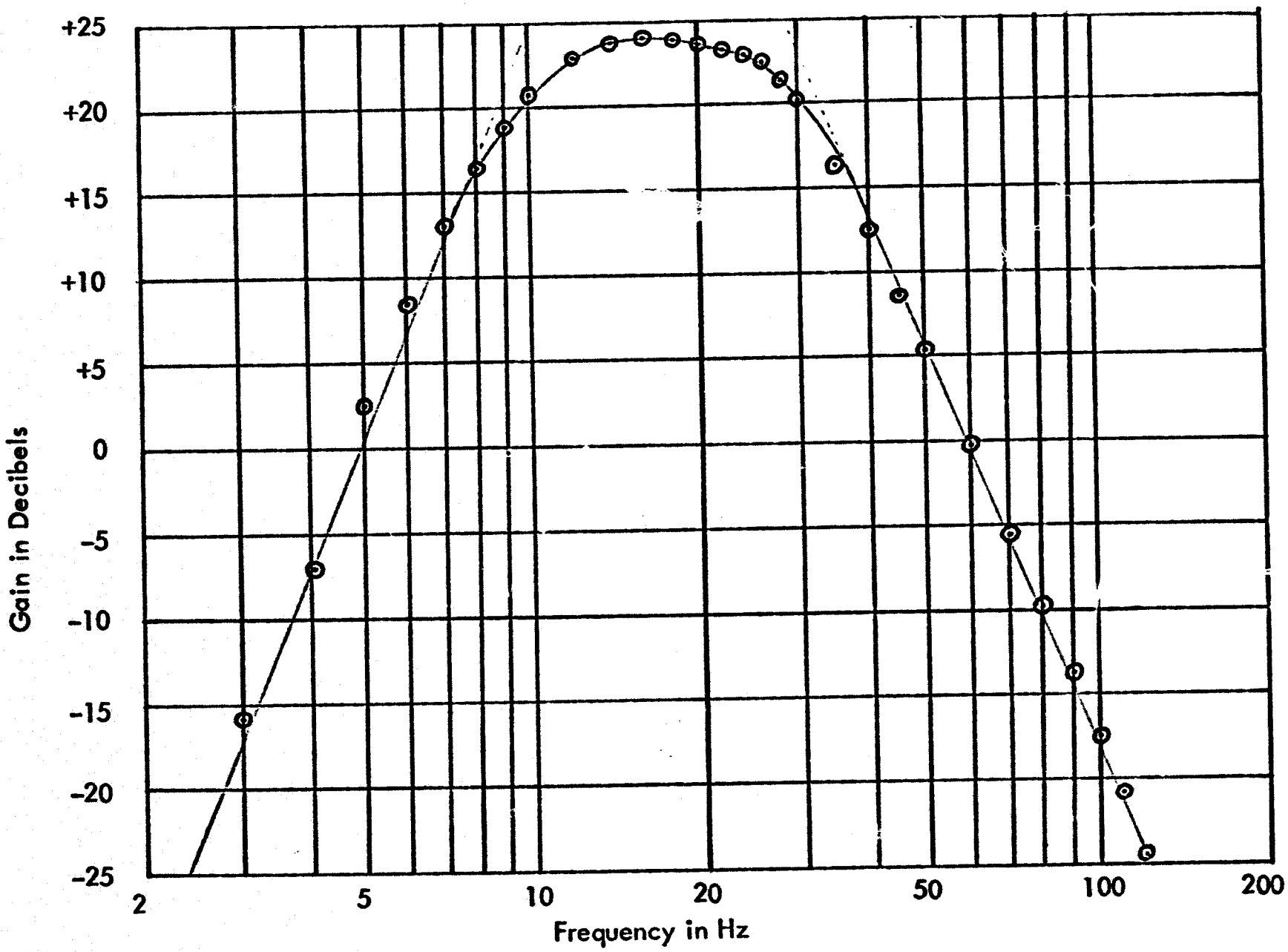


Figure E1 – Bandpass characteristics of low-frequency filter circuit shown in Figure A3

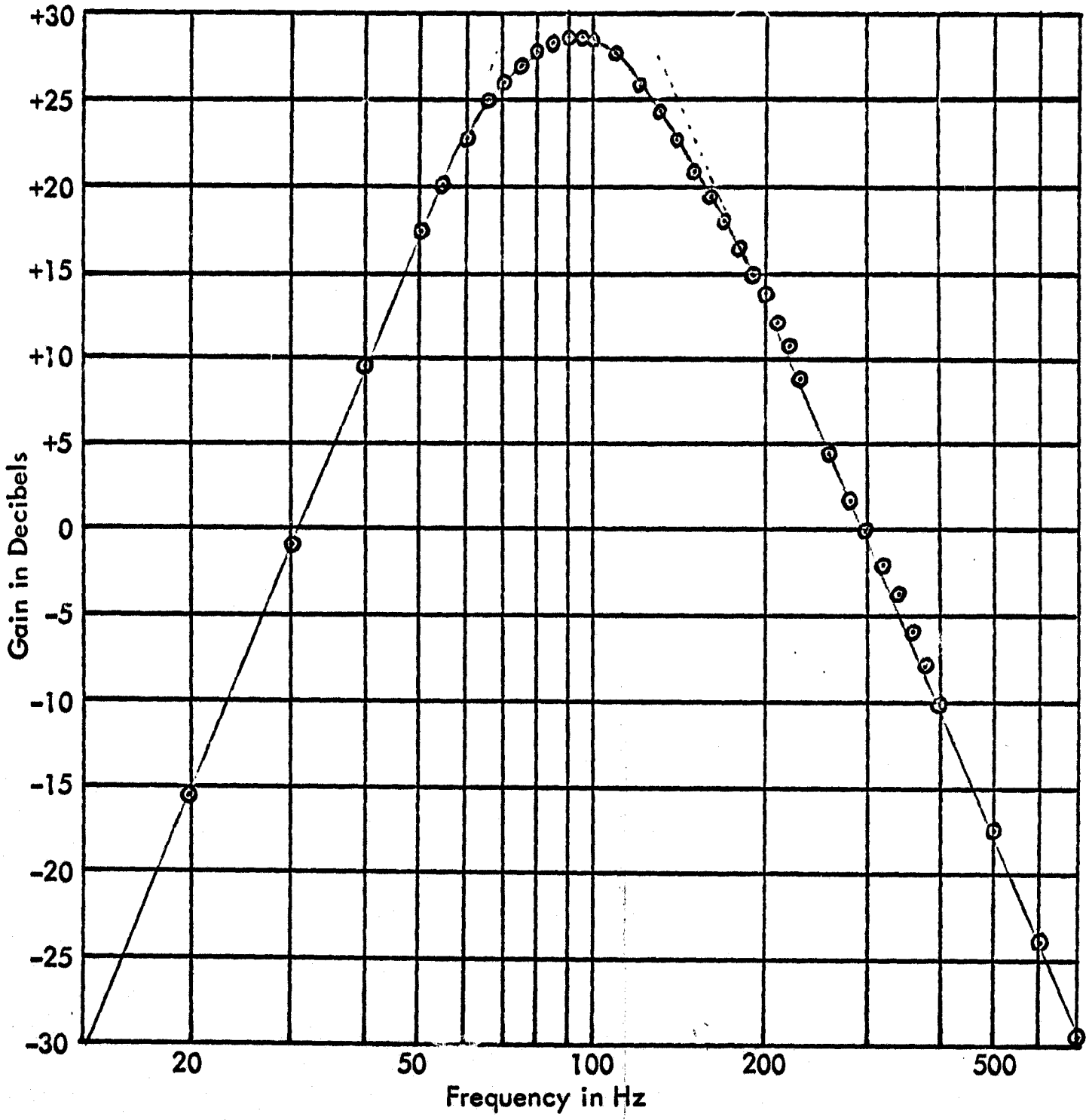


Figure E2 – Bandpass characteristics of high-frequency filter circuit shown in Figure A3

VITA

Arthur Edward Schulze, son of Arthur Dorwin Schulze and Ida Schulze, was born in [redacted] on [redacted]. After graduating from Lamar Consolidated High School, Richmond-Rosenberg, Texas in 1957, he entered Texas Lutheran College at Seguin, Texas. In September, 1959, he entered The University of Texas where he received a Bachelor of Science Degree in Electrical Engineering on June 2, 1962. In June, 1962, he entered graduate school and accepted a position as Research Engineer Assistant II at the Electrical Engineering Research Laboratory, The University of Texas. On September 2, 1962, he married Sharon Havemann of West Point, Texas. After receiving his Master of Science Degree in Electrical Engineering from The University of Texas on August 24, 1963, he accepted a position with the Fort Worth Division of General Dynamics Corporation. In June, 1967, he returned to graduate school and accepted his present position as a Research Associate with The University of Texas Graduate School of Biomedical Sciences at Houston. He is a member of Tau Beta Pi, Eta Kappa Nu, Institute of Electrical and Electronics Engineers, and is a Registered Professional Engineer (State of Texas).

Permanent Address: 8807 Mobud
Houston, Texas 77036

This thesis was typed by Sharon K. Schulze, August, 1968.

MASTER OF SCIENCE DATA SHEET

FULL NAME Arthur Edward Schulze

DEGREE SOUGHT Master of Science

SPECIAL FIELD OF THE THESIS:

Biomedical Engineering

DATE OF GRADUATION January, 1969

EXACT TITLE OF THESIS A System for the Automatic Measurement and Digital Display of Systolic and Diastolic Blood Pressures

PREVIOUS DEGREES:

B.S.E.E. The Univ. of Texas 1962

M.S.E.E. The Univ. of Texas 1963

PERMANENT HOME ADDRESS:

8807 Mobud

Houston, Texas 77036

TOTAL NUMBER OF PAGES (including illustrations and unnumbered pages): 100

NUMBER OF ILLUSTRATIONS 39

Fred B. Vogt, M.D.
Name of Supervising Professor

BRIEF SUMMARY OF THESIS

A system providing automatic, real-time digital display of systolic and diastolic blood pressures, as determined by the occluding cuff technique, has been developed. Design parameters were established from experimental data that included intra-arterial and cuff measurements. The system serves to reliably measure blood pressure by minimizing errors due to noise and patient condition and to reduce inter-observer variations.

PARAMETRIC AND NON-PARAMETRIC ANALYSIS

OF 1964 BEDREST TRIALS

by

Lyle Broemeling

Dr. Broemeling presently is located at the Department of Mathematics and Statistics, Oklahoma State University, Stillwater, Oklahoma.

TABLE OF CONTENTS

	page
1. Introduction	1
2. Parametric Analyses	3
(a) Univariate	3
(1) 9x3x2	3
(2) 9x3	3
(3) 3x2	4
(4) 9x2	4
(b) Multivariate	4
(1) 9x3x2	4
(2) 9x3	5
(3) 3x2	5
(4) 9x2	5
3. Non-Parametric	6
(a) Friedman's AOV	6
(b) Two-Way Layouts	7
4. Comparisons	7
(a) Computing Time	7
(b) Assumptions and Restrictions	8
(c) Sophistication of Analyses	10
5. Tables	
(a) IA: 9x3x2, AOV Variables 1 and 3, MANOVA	13,14,15
(b) IB: 9x3, AOV Variable 1, MANOVA	15, 16
(c) IC: 3x2, AOV Variables 1 and 4, MANOVA	17, 18
(d) ID: 9x2, MANOVA	19
(e) IIA: 9x3, Friedman's AOV, Variable 1	20
(f) IIB: 3x2, Friedman's AOV, Variable 2	20
6. Bibliography	21

PARAMETRIC AND NON-PARAMETRIC ANALYSIS OF 1964 BEDREST TRIALS

1. Introduction

The experimental background of the 1964 summer Bedrest Trials is well outlined by Vogt (1966). The objectives of the Tilt-Table experiments were to provide a means to define the degree of deconditioning for a given test circumstance and allow comparison of various tilt data with control data on the same subjects. The Tilt-Table test evaluates the integrity of the normal adaptive mechanisms and reflexes which regulate heart rate, blood pressure, brain perfusion, vasomotor tone, and a multitude of other changes which occur when a person is changed from a horizontal to a vertical position with respect to gravity. The usual response of a person subjected to a horizontal-vertical change is an increase in heart rate and diastolic blood pressure, but a slight decrease in systolic blood pressure. Various classifications have been applied (1958, 1960) to abnormal responses to Tilt-Table experiments. An abnormal response is usually characterized by a progressive change in blood pressure and heart rate resulting in syncope.

Various derived or direct measurements were taken on each of 11 subjects; however, complete data was recorded for only nine, and of the 32 initial measurements observed or computed, nine were used in the statistical analysis. The reduction to nine dependent variables was accomplished by first computing the principal (32) components of all the measurements. The first and second component accounted for most of the variation (the sum of the characteristic roots of the components),

and the dependence of these components on the nine variables selected was most pronounced, that is, the magnitudes of the regression coefficients corresponding to these nine variables was the greatest in magnitude with comparison to the other variables. The nine variables are:

y_1 = average heart rate before tilt

y_2 = maximum heart rate during tilt

y_3 = average pulse pressure before tilt

y_4 = slope of mean blood pressure

y_5 = maximum during-average pre heart rate

y_6 = time at point of break (hours)

y_7 = heart rate at point of break

y_8 = time at point of break (pp)

y_9 = slope of first regression line

For a definition of the above measurements refer to Vogt (1966).

Baseline data were obtained for in a five-minute control period before tilting the subject to the 70^{o} head-up position, where he remained for 20 minutes unless syncope or impending syncope occurred.

The experiments involved basically three factors; the subject-subject variation, the time the measurements were taken on the subjects, that is, immediately before and after bedrest, and the three sequential bedrest periods. We refer to these factors as subjects, (S) before-after (BA) and treatments (T) respectively.

The purpose of this report is to compare the parametric and non-parametric analyeses of the bedrest data with respect to computing time, assumptions and restrictions of the statistical model, degree of sophistication

in the analysis, and power of the statistical tests.

2. Parametric Analyses

(a) Univariate techniques: The 1964 summer bedrest trials were analyzed using the 9 variables separately with four layouts.

(1) A three-way analysis of variance using the three basic factors subjects (S), BA, and treatments (T). Thus, we have a 9x2x3 factorial with one observation per cell. Since there is no replication (no sub-sampling or repeat observations per cell) there is not valid estimate of experimental error, and the three-factor interaction was used to asses the significance of the main effects and two-factor interactions. Fortunately all two factor interactions were non-significant thus, allowing a less complicated interpretation of the effect of the main factors. The subject-subject variation was significant for the first variable only while the before-after effect was significant ($P \leq .01$) for the first three variables. The treatment effect was non-significant through out. A closer look at the subject variation showed the following pairs significantly different: (5, 6), (1, 2), (2, 7), and (7, 9) by Scheffe's method of parwise comparison.

See Table IA for AOV results.

(2) A two-way layout using treatments and subjects as the main effects and the before-after differences as the observations per cell. This results in a 9x3 factorial with one observation per treatment-subject combination, thus the treatment-subject interaction is used as experimental error. The treatment effect was significant ($P \leq .01$) for variables 1 and 2, but the subject to subject variation is not significant for any of the variables. The data should be analyzed using two observations per cell, that is the before and after measurements as replicates, and then asses the significance of the subject effect. This would allow a way to test for the significance of

the interaction effect which was (and had to be) assumed non-significant for the above analysis. See Table IB.

(3) A two-way layout with before-after versus treatments giving a 5x2 factorial with 9 observations per cell, thus if the assumptions of the model hold (see section 4) a good estimate of experimental error is available from the within-cell variation.

The BA effect was significant for variables 1, 2, and 3; however, the treatment effect was not significant for any variable. The interaction effect was not significant for any variable either. The results of the analysis of variance are given below, Table IC.

(4) A two-way layout with subjects versus B/A with three observations per cell shows the B/A effect significant for the first four dependent variables; however, no subject-subject variation showed up for any variable. This analysis assumed no difference in the observations taken during the sequential bedrest periods because the three observations / cell were treated as replicates in order to obtain a measure of the experimental error. Table ID gives the results from the univariate as well as the multivariate analysis for this layout.

(b) Multivariate Techniques

The nine dependent variables were used simultaneously in a multivariate analysis of variance (MANOVA) with the four designs above to asses the significance of the basic factors.

(1) 9x3x2 factorial with one observation vector per cell shows the two factor interactions non-significant. The Hotelling's Trace Statistic was used to test for significance of the various effects while the discriminant

function and the associated beta statistics test for zero regression coefficients in the discriminant function to show what variables are contributing to the significant effect, if any. We refer to Morrison (1967) for an explanation of the different statistical tests used in MANOVA. For this design all three main effects were significant. The subject effect was significant ($P \leq .001$), and the discriminant function showed variables 1 and 8 contributing to this significance, while for the treatment factor, no one variable appears to be contributing to the significance. Variable 1 is contributing to the significance of the BIA factor.

The MANOVA results somewhat verify the ANOVA because in the latter both the subject and B/A effect were significant for variable 1; but nowhere in the univariate analyses does variable 8 appear as contributing to the significance of any effect. Also, the ANOVA yields no significant treatment effect on any variable. Although the MANOVA does, no variable is apparently contributing. See Table IA for MANOVA of 9x3x2.

(2) The 9x3 factorial gives both subjects and treatments as significant with no variable or variables as contributing to the significance, Table IB.

(3) The 3x2 factorial gives only the B/A effect as significant with variable 1 as the contributing measurement. The univariate procedure somewhat substantiates this since the B/A factor was significant for only variables 1, 2, and 3. Refer to Table IC.

(4) The 9x2 layout with subjects and before-after as the main effects shows variables 1, 5, 7, and 8 as contributing to the significance of the

B/A factor. The univariate analyses produces no significant subject effect for any variable. Table ID gives the pertinent data.

The multivariate analysis of the above data was very sophisticated in that, in addition to the usual MANOVA of testing for the main effects and interactions using all the variables simultaneously, univariate analyses are produced at the same time giving the complete analysis of variance for each variable separately, along with pairwise comparisons between the levels (Scheffe, 1957) of the main effects. Also, included was the multivariate pairwise comparison method of Scheffe using all the dependent variables, unfortunately to test for significance of such a comparison one needs the upper percentage points of the largest characteristic root of the sample covariance matrix. For the data analyzed here, the percentage points are not tabulated for the various combinations of parameters. (Heck, 1960; Pillai, 1967).

3. Non-Parametric Analysis

(a) Univariate analyses of the data involved Friedman's (Siegel, 1956) two-way analysis of variance for significance of the main effects in the 9x3, 3x2, and 9x2 layouts is the non-parametric analog of the usual parametric analysis of variance. A recent univariate non-parametric multiple comparison between levels of the main effects for either a two or one-way layout of McDonald and Thompson (1967) is a non-parametric analog of the Scheffe simultaneous confidence interval approach. A similar procedure is the new method of Rhyne and Steel (1967) that gave the same results as that of McDonald and Thompson.

With regard to multivariate non-parametric methods, significance testing is in the formative stage and is based on so-called asymptotic test

procedures, which involve 'large' sample sizes. In addition the computational aspects are quite complicated in comparison to the univariate methods. Because the bedrest trials provide relatively small sample sizes and the computations are very involved, multivariate procedures from a non-parametric standpoint were not attempted. Sen(1967), Bradley, and Terry (1967) give the theory of some multivariate procedures for a two-way layout.

Note that Friedman's AOV is applicable only for two-way designs because non-parametric methods for evaluating more than two main effects are non-existent. For those two-way designs with more than one observation per cell, namely the 9x2 and 3x2, one must use cell averages (averaged over the number of replications) because Friedman's AOV uses only one observation per cell; thus, one cannot test for interactions, and there is no valid estimate of experimental error. Also, the procedure depends on a balanced designs, and missing values present a problem.

(b) The 9x3 layout with subjects and treatments as the main effects show Friedman's AOV indicating treatments significant ($P \leq .004$) for variable 1 only. The subject variation was not tested for significance. For the 3x2 layout with treatments and before-after as the main factors, B/A was significant with variables 2 ($P \leq .091$), and 8 ($P \leq .0918$), but the treatment effect was non-significant for all variables. See Tables IIA, IIB, and IIC for the analyses of variance.

4. Comparisons

(a) Computing Time

With regard to the parametric analyses, the 9x2 layout involving univariate and multivariate analyses of variance, univariate multiple comparisons and multivariate multiple comparisons involved a total time

of 2.65 minutes including compiling and execution time. The three designs--3x2, 9x3, 9x3x2 were all analyzed with the above techniques in 4.06 minutes total time. An IBM 7094 was used, and Mr. Bob Stein wrote all the programs.

The Friedman's AOV was programmed by Stein using a SSP 360 routine on the 7094. The 3x2 and 9x3 layouts testing treatments along with the multiple comparisons took 0.99 minutes. The 3x2 testing for B/A and the 9x3 testing for treatments ran in 1-04 minutes. Although the computational time for the non-parametric methods is less, the degree of sophistication of the parametric procedures is much greater, and one would expect the computer time to be greater.

Thus with regard to computational time, the time difference between the two programs is negligible, and other considerations for comparison should be taken into account.

(b) Assumptions of Statistical Model

(1) For the univariate parametric analyses all layouts are completely balanced. Cross classification models, such as for the 9x3x2 model, we have

$$y_{ijk} = a + S_i + T_j + B_k + (ST)_{ij} + (SB)_{ik} + (TB)_{jk} + (STB)_{ijk} + e_{ijk}$$

where y_{ijk} is the observation measured or derived on the i-th subject (i = 1, 2, ... a) during the k-th time before or after bedrest (k = 0 or 1 0 = before, i = after) and during the j-th time and k-th bedrest period respectively on the observation. e_{ijk} is the random error associated with the ijk-th observation and reflects the measurement,

technical, and experimental errors involved with this observation.

Now the usual assumptions are that the e_{ijk} are normally distributed, independent, have mean 0, and unknown constant variance σ^2, which is estimated from the AOV. The normality assumption is needed to conduct tests of significance and set confidence intervals on the unknown parameters S_i, T_i, B_k, $(ST)_{ij}$, etc. The assumption of zero mean of the e_{ijk} implies on the average, over repeated experiments, the value of the measurement y_{ijk} is

$$\mu + S_i + T_j + B_k + (ST)_{ij} + (SB)_{ik} + (TB)_{jk} + (BST)_{ijk}$$

where the $(ST)_{ij}$, etc., denote the second order and the one-third order interaction $(STB)_{ijk}$.

Because of one observation per cell, the third-order interaction was assumed negligible. The mean squares in the AOV corresponding to this effect has average value σ^2 and is used as the denominator to test for the significance of the second-order and main effects.

The AOV tests the following hypotheses:

H_1: $(ST)_{ij} = 0$ for all i and j

H_2: $(SB)_{ik} = 0$ for all i and k

H_3: $(TB)_{jk} = 0$ for all j and k

If the above three hypotheses are not rejected (which they are not for the 9x3x2), the texts of significance for the main effects are carried out as

H_4: $S_i = 0$ for all i

H_5: $T_j = 0$ for all j

H_6: $B_k = 0$ for all k

We see from section 2 that H_4 was rejected when y_{ijk} was the average heart rate before tilt (y_1), while H_6 was rejected when y_{ijk} was y_1, y_2, or y_3.

(2) For the non-parametric analysis using Friedman's AOV, we have the following restrictions. First, only two-way layouts may be analyzed, that is, the 9x3, 9x2, and 3x2. One may test for significance of the main effect factors only (the subject, treatment, or time variation) and not for the interaction between two main effects. The reason for this being only one observation per cell is allowed in the Friedman procedure; for example, with the 9x2 we have three observations per cell in the parametric AOV (univariate or multivariate) while we must average these observations to apply the non-parametric procedure. This in turn 'throws away' some of the data by not taking into account the within-cell variability, the estimate of experimental error. If our two-way layout had unequal cell frequencies, the Friedman method would have suspected applicability.

On the other hand, for our non-parametric procedure, it is not necessary to assume the measurements are normally distributed, have constant variance, etc., only that they are samples from a population with a continuous probability distribution, which is a safe assumption for the observations in this study.

Thus, the assumptions of the non-parametric tests are less restrictive than those for the analgous parametric procedures.

(c) Sophistication of the Analyses

We have seem that with regard to computing time, there is little difference between non-parametric and parametric methods, but that

non-parametric procedures, when applicable, are less restrictive with respect to the assumptions of the statistical model. Parametric procedures we have used are all based on the assumption of normality of the observations. When the observations are samples from normal populations, the parametric AOV and MANOVA procedures are much more sophisticated than the corresponding non-parametric procedures.

For example, in the two-way analyses of variance, one may test for interaction effects before proceeding to test the significance of the main effects. The non-parametric test assumes that no interaction is present and immediately tests for the main effects. For the three-way layout, the 9x3x2, no non-parametric procedure exists while the usual AOV tests for significance of the two-factor interactions (using the three factor interaction as error). There are many multiple comparison methods such as Dunnett's, Scheffe, Tukey's, etc., for the parametric, but relatively few for the non-parametric and only used for one-way and two-way models.

The parametric-multivariate analyses are very sophisticated when one remembers multivariate methods for non-parametric procedures are limited.

The parametric multivariate procedures as programmed by Stein are the most sophisticated I have seen. They give the univariate analyses of variance separately for each variable; then, produce the MANOVA using all variables simultaneously. One comment might be in order with regard to the MANOVA as there is no tests for interaction significance, which could be included in the program, see Bargmann. Even so there are two tests for significance of the main effects, namely Hotelling's trace statistic (the program gives an approximate significance level based on the chi-square approximation and the exact significance level based on Heck's tables) and

the likelihood ratio test of Wilk's. Also, the discriminant function is computed which shows along with the beta statistics those variables contributing to significant effect. Another 'good' feature of the MANOVA program is that the correlation matrix between the dependent variables is listed.

It should be pointed out that Heck's charts (1960) are quite limited, in fact, they could not be used for the Tilt-Table data; however, Pillai (1967) has extended the upper percentage points of the largest root of the variance-covariance (sample) matrix of the multivariate normal distribution.

One must pay a price for such a sophisticated MANOVA and that price is that one does not know when the dependent variables are samples from a multivariate normal population, and there are no statistical tests available except for the special case of a bivariate normal.

In comparison the parametric procedures are more sophisticated, thus tell the experimentor much more about his data than the non-parametric analysis of variance.

IA, MANOVA, 9x3x2, B/A

Discriminant Function is: 0.381338 -0.055691 -0.348082 -0.001811 0.322425 0.119790 -0.415989 0.019383

Hotelling's Trace Statistic = 361.8367 is distributed approximately as Chi Square with 9 of

For significance of this effect consult Heck's charts for Theta = 0.957654 S = 1 M = 3 N = 3

Beta Statistics are = 0.08730 0.93944 0.98779 0.95941 0.82545 0.97513 0.99395 0.68362 0.99622

Significance Levels 0.01409 0.99995 1.00000 0.99999 0.99490 1.00000 1.00000 0.94444 1.00000

Likelihood Ratio = 0.04235

IA, AOV, 9x3x2, Variable 1

	DF	SS	MS	FC	FT
TOTAL	53.	0.101319884E 05			
Subjects (9)	8.	0.292900998E 04	0.366126248E 03	5.6897**	2.9730
TRT (3)	2.	0.315063664E 03	0.157531829E 03	2.4481NS	3.2220
Before / After	1.	0.418527969E 04	0.418527969E 04	65.0407**	7.2870
RESIDUAL	42.	0.270264063E 04	0.643485860E 02		

IA, 9x3x2, MANOVA, Subjects

Discriminant Function is: -4.359343 0.688444 5.256241 0.820339 -4.468350 -1.1178283 -1.025172 5.102671 -0.019665

Hotelling's Trace Statistic = 513.1516 is distributed approximately as Chi Square with 72 of

For significance of this effect consult Heck's charts for Theta = 0.956095 S = 8M = O N = 3

Beta Statistics are = 0.12024 0.49536 0.81026 0.32235 0.40601 0.66071 0.41994 0.19303 0.65538

Significance levels 0.00739 0.56118 0.98474 0.19549 0.36089 0.86794 0.39146 0.03904 0.86080

Likelihood Ratio = 0.00022

IA, 9x3x2, MANOVA, Treatments

Discriminant Function is: -0.789396 -0.024087 0.215264 0.205341 -0.348921 -0.250710 0.209881 0.551551 0.323707

Hotelling's Trace Statistic = 38.5722 is distributed approximately as Chi Square with 18 DF

For significance of this effect consult Heck's charts for Theta = 0.596849 S = 2M = 3N = 3

Beta Statistics are = 0.55958 0.99956 0.78425 0.85393 0.93123 0.78219 0.89939 0.94313 0.90242

Significance Levels 0.75835 1.00000 0.98200 0.99633 0.99985 0.98131 0.99924 0.99994 0.99933

Likelihood Ratio = 0.20885

IA, AOV, 9x3x2, VARIABLE 3

		DF	SS	MS	FC	FT
	TOTAL	53.	0.180327744E 03			
Subjects (9)		8.	0.176400982E 02	0.220501232E 01	0.7772NS	0.
TRT (3)		2.	0.139358309E 02	0.696791530E 01	2.4558NS	3.2220
Before / After		1.	0.295851920E 02	0.295851920E 02	10.4272**	7.2870
	RESIDUAL	42.	0.119166623E 03	0.283730060E 01		

IB, 9x3, MANOVA, Subjects

Discriminant Function is: 0.436442 -0.237676 0.184006 0.440336 -0.075506 0.438403 1.134904 -0.386704 0.494872

Hotelling's Trace Statistic = 149.9125 is distributed approximately as Chi Square with 72 DF

For significance of this effect consult Heck's charts for Theta = 0.789466 S = 8M = O N = 3

Beta Statistics are = 0.40699 0.85443 0.64321 0.74342 0.83844 0.63475 0.52177 0.33396 0.55296

Significance Levels = 0.36301 0.99476 0.84368 0.95126 0.99198 0.83113 0.61927 0.21599 0.68476

Likelihood Ratio = 0.00953

IB, 9x3, MANOVA, Treatments

Discriminant Function is: 0.720546 0.104288 -0.958602 -0.130870 0.631071 0.104507 0.262051 -0.169963 0.116725

Hotelling's Trace Statistic = 48.3055 is distributed approximately as Chi Square with 18 DF

For Significance of this effect consult Heck's charts for Theta = 0.697190 S = 2 M = 3 N = 3

Beta Statistics are = 0.46222 0.88011 0.96678 0.72351 0.79837 0.95827 0.92865 0.98936 0.88191

Significance Levels 0.56602 0.99840 0.99999 0.95285 0.98626 0.99998 0.99983 1.00000 0.99850

Likelihood Ratio = 0.17639

IB, AOV, 9x3, Variable 1

	DF	SS	MS	FC	FT
TOTAL	26.	0.289843933E 04			
Subject (9)	8.	0.116646501E 04	0.145808129E 03	2.9142*	2.5900
(B-A) TRT	2.	0.931425095E 03	0.465712547E 03	9.3079**	6.2300
RESIDUAL	16.	0.800549805E 03	0.500343626E 02		

IC, 3x2, AOV, Variable 1

	DF	SS	MS	FC	FT
TOTAL	53.	0.101319884E 05			
TRT (3)	2.	0.315063468E 03	0.157531738E 03	1.3986NS	3.1900
Before / After	1.	0.418527994E 04	0.418527994E 04	37.1586**	7.1950
RESIDUAL	50.	0.563164744E 04	0.112632952E 03		

IC, 3x2, Variable 4

	DF	SS	MS	FC	FT
TOTAL	53.	0.264799215E 04			
TRT (3)	2.	0.616449509E 01	0.308224756E 01	0.0621NS	0.
Before / After	1.	0.159478509E 03	0.159478509E 03	3.2122NS	4.0400
RESIDUAL	50.	0.248235548E 04	0.496471088E 02		

IC, 3x2, MANOVA, Treatments

Discriminant Function is: 0.000894 -0.004166 -0.034607 -0.004830 -0.000108 -0.009323 0.003012 -0.000638 0.006144

Hotelling's Trace Statistic = 19.5134 is distributed appr[illegible]nately as Chi Square with 18 DF

For significance of this effect consult Heck's charts for Theta = 0.224619 S = 2 M = 3 N = 19

Beta Statistics are = 0.94252 0.99592 0.90448 0.98153 0.96389 0.92093 0.99355 0.99681 0.94766

Significance Levels 0.97895 1.00000 0.88640 0.99977 0.99636 0.93708 1.00000 1.00000 0.98503

Likelihood Ratio = 0.69426

IC, 3x2, MANOVA, B/A

Discriminant Function is: 0.013148 0.001852 -0.022227 0.008886 0.010303 -0.001846 -0.003819 -0.007956 -0.001007

Hotelling's Trace Statistic = 56.0232 is distributed approximately as Chi Square with 9 DF

For significance of this effect consult Heck's charts for Theta = 0.538565 S = 1 M = 3 N = 19

Beta Statistics are = 0.55243 0.97481 0.93294 0.94830 0.99860 0.99168 0.99386 0.98442 0.99963

Significance Levels 0.00289 0.99922 0.96649 0.98685 1.00000 0.99999 1.00000 0.99990 1.00000

Likelihood Ratio = 0.46144

ID, 9x2, MANOVA, Subjects

Discriminant Function is: -0.633963 0.130824 2.647609 0.244134 -1.338018 -0.183073 -0.407812 0.779871 -0.177622

Hotelling's Trace Statistic = 253.7696 is distributed approximately as Chi Square with 72 DF

For significance of this effect consult Heck's charts for Theta = 0.720247 S = 8 M = 0 N = 17

Beta Statistics are = 0.50746 0.66448 0.87510 0.65801 0.58273 0.86376 0.59720 0.55827 0.83435

Significance Levels 0.00162 0.06556 0.81162 0.05811 0.01178 0.76297 0.01647 0.00647 0.62367

Likelihood Ratio = 0.02719

ID, 9x2, MANOVA, B/A

Discriminant Function is: 0.035457 -0.001622 -0.092793 0.008252 0.051760 0.007313 0.001662 -0.043700 0.005181

Hotelling's Trace Statistic = 115.3031 is distributed approximately as Chi Square with 9 DF

For significance of this effect consult Heck's charts for Theta = 0.723797 S = 1 M = 3 N = 17

Beta Statistics are = 0.41895 0.96184 0.87657 0.99013 0.94029 0.99634 0.99703 0.84993 0.99478

Significance Levels 0.00012 0.99719 0.82940 0.99999 0.98431 1.00000 1.00000 0.71578 1.00000

Likelihood Ratio = 0.27620

FRIEDMAN'S TWO WAY AOV IIA, 9x3, Variable 1

RANK MATRIX HAS

2.00000	3.00000	3.00000
3.00000	2.00000	3.00000
3.00000	3.00000	3.00000
3.00000	2.00000	2.00000
1.00000	3.00000	2.00000
2.00000	1.00000	2.00000
1.00000	1.00000	1.00000
2.00000	1.00000	1.00000
1.00000	2.00000	1.00000

Friedman's Statistic (Chi Square SUBR) = 10.88889DF = 2 PValue = 0.00481198

FRIEDMAN'S TWO WAY AOV IIB, 3x2, Variable 2

RANK MATRIX HAS

2.00000	2.00000	2.00000	2.00000	1.00000	2.00000

Friedman's Statistic (Chi Square SUBR) = 2.77778DF = 1 PValue = 0.09182956

BIBLIOGRAPHY

1. Bargmann, R. E., (1962). Representative Ordering and Selection of Variables, Parts A and B. Virginia Poletehnic Institute.

2. Bradley and Davidson, (1966). Multivariate Paired Comparisons. Florida State University, Department of Statistics. Report m121 ONR technical report 22.

3. Heck, D. L., (1960). Charts on some Upper Percentage Points of the Distribution of the Largest Characteristic Root. Annals of Math.-Stat. 31: 625-41.

4. McDonald, B. J. and Thompson, W. A., (1967). Rank Sum Multiple Comparisons In One a Two-Way Classifications. Biometrika 54: 487-98.

5. Morrison, D. F., (1967). Multivariate Statistical Methods, McGraw-Hill Book Company, New York.

6. Pillai, K. C. S., (1967). Upper Percentage Points of the Largest Root of a Matrix in Multivariate Analysis. Biometrika, 54: 189-194.

7. Scheffe, H., (1959). The Analysis of Variance, John Wiley and Sons, Inc., New York.

8. Sen, P. K., (1966). On a Class of Non-Parametric Tests for MANOVA in Two-Way Layouts. Proceeding of the 12-th Conference on the Design of Experiments in Army Research, Development and Testing.

9. Siegel, S., (1956). Non-Parametric Statistics for the Behavioral Sciences., McGraw-Hill Book Company Inc., New York.

10. Rhyne, A. L. and Steel, R. G. D., (1967). A Multiple Comparisons Sign Test: All Pairs of Treatments, Biometrics, 23: 539-50.

11. Vogt, F. B., (1966). An Objective Approach to the Analysis of Tilt-Table Data, Aerospace Medicine, 37: 1195-1204.

12. Vogt, F. B., (1967). The Use of Tilt-Table Studies to Evaluate Cardiovascular Deconditioning of Space Flight. NASA Contract Report, NSR 44-024-006.

AUTOMATED ESTIMATION OF THE DEPTH OF SLEEP

by

STEPHEN MICHAEL SLOAN, B.S., B.S.E.E.

THESIS

Presented to the Faculty of The University of Texas
Graduate School of Biomedical Sciences at Houston

in Partial Fulfillment

of the Requirements

For the Degree of

Master of Science

THE UNIVERSITY OF TEXAS

Houston, Texas

August, 1968

AUTOMATED ESTIMATION OF THE DEPTH OF SLEEP

APPROVED:

Fred B. Joyt, M.D.
Supervising Professor

_____

_____

_____

ACKNOWLEDGMENT

The research reported was supported in part by National Aeronautics and Space Administration Contract NAS-9-7029 to The University of Texas Graduate School of Biomedical Sciences. Computer time and services were provided by the Department of Biomathematics of The University of Texas M. D. Anderson Hospital and Tumor Institute and the Common Research Computer Facility supported by National Institute of Health Grants FR00258 and FR00254 respectively.

I would like to thank Dr. James D. Frost, Jr. of the Baylor University College of Medicine for his cooperation and advice on the EEG aspects of this study and for providing data that was collected under support of National Aeronautics and Space Administration Contract NAS-9-1200 to the Baylor University College of Medicine and the Methodist Hospital.

I would also like to express my appreciation to Dr. Fred Vogt, my supervising professor, and to my committee, Dr. Stuart Zimmerman, Dr. Louis Meharg, and Dr. Donald Kroeger, for their guidance in the preparation of this thesis.

August 16, 1968

ABSTRACT

This report describes a system designed to aid in the investigation of relationships that may exist between physiological variables and the depth of sleep. Analog computer circuitry was developed to preprocess electrocardiogram (ECG) and respiration (ZP) signals to provide several characteristics of the cardiovascular and respiratory systems which have previously been shown to be related to the depth of sleep. The relationship of these variables (heart rate, variance of the heart rate, respiration volume, respiration rate, and the variance of the respiration rate) to the electroencephalogram (EEG) derived depth of sleep is computed by calculating the appropriate correlation coefficients and forming a linear additive model of the variables. This model can be investigated to gain insight into possible functional relationships between the variables and to provide a basis for future consideration of more meaningful predictive models.

The system has been designed to provide flexibility for future consideration of other measurements that may contain sleep-wakefulness information, as well as for alteration of the linear model.

TABLE OF CONTENTS

I. Introduction 1

II. Physiological Indications of Sleep 6

III. EEG Determination of Depth of Sleep

A. Electroencephalographic Classification of the Depth of Sleep 13

B. Automated Analysis of EEG Determined Depth of Sleep 21

IV. Preprocessing and Analysis of Data 29

V. System Testing and Sample Output 48

VI. Discussion 46

APPENDIX 59

Bibliography 61

Appendix A (Analog Preprocessing Circuits) 63

Appendix B (Digital Program) 68

Appendix C (Sample Matrix Inversion) 73

LIST OF FIGURES

Figure 1, Occipital-Parietal Bipolar EEG Samples Depicting Various Stages of Sleep 16, 17

Figure 2, Typical Sleep Profile 19

Figure 3, System Block Diagram 33

Figure 4, Block Diagram and Typical Wave Forms EEG Depth of Sleep Analyzer 36

Figure 5, EEG Filter Frequency Response 37

Figure 6, Comparison of Automatically Analyzed and Visually Scored Depth-of-Sleep Records . 38

Figure 7, Respiration Rate Filter Frequency Response 40

Figure 8, Block Diagram of Respiration Rate Detection Circuit 40

Figure 9, Respiration Volume Filter Frequency Response 41

Figure 10, Block Diagram of Heart Rate Detection Circuit 43

Figure 11, ECG Filter Frequency Response 43

Figure 12a, Standard Variance Circuit 44

Figure 12b, Altered Derivation of Variance 45

Figure 13, Processed Data - Subject #1 49

Figure 14, Processed Data - Subject #2 50

LIST OF TABLES

Table I, Statistical Analysis for Sample Data of Figure 13 54

Table II, Statistical Analysis for Sample Data of Figure 14 55

AUTOMATED ESTIMATION OF THE DEPTH OF SLEEP

I. Introduction

Volumes have been written and compiled solely on the various aspects of sleep. The subject has been broached from philosophical, psychological, and physiological viewpoints, but introductory remarks in the literature frequently concede that very little is known about sleep. Although this may have been true in even the recent past due to an unreasonable lack of scientific investigation, the last decade has witnessed a renewed interest in sleep research that is providing pockets of information based on sound experimental design. However, a theory explaining the mechanism of the cycle of sleep and wakefulness is still lacking.

In the last one hundred years, and particularly since the advent of the electroencephalogram (EEG) in 1929, the concept of depth of sleep has evolved. This concept has permitted quantification of sleep, and though by no means absolute, the quantification has produced a frame of reference for the researcher. An interesting aspect of this quantification was that it caused reconsideration of the significance of many conventional indicators of sleep such

as slow, even respiration and reduced heart rate. In fact, on recent Gemini orbital space flights, physicians charged with the responsibility of monitoring the vital functions of the astronauts attempted to estimate whether or not the astronauts were asleep by observation of heart rate and respiration depth and rate as revealed in the telemetered electrocardiogram (ECG) and impedance pneumogram (ZP).

The criteria used for the estimation was straightforward. If the heart rate was low and the respiration relatively low in amplitude and regular in rate, the astronaut was judged to be asleep. The exact time of falling asleep and the level of sleep at any one point of time were difficult, if not impossible, to judge by visual observation of the raw data. Periods of arousal from sleep were interpreted by noticing sudden increases in heart rate and could usually be well defined in time. However, the adequacy of a given sleep period was judged by the subjective reports of the astronauts in combination with the monitoring physicians' interpretation of the data during the supposed sleep period. In order to (a) optimize work-rest cycles during flights, (b) make any necessary readjustments of sleep or work periods,

and (c) to render opinions as to whether a clinically significant sleep deficit may exist in an astronaut, it is necessary that a more objective measure of sleep be available for use during orbital flights.

The only clinically acceptable method of determination of the depth of sleep that is available at the present time is through the interpretation of the EEG, which itself contains all the required information regarding sleep. Its use in space flight, however, has three disadvantages:

(a) The monitoring physicians would require several months of training in EEG interpretation.

(b) Presently available EEG electrodes present problems in application and durability. They must be applied to prepared sites and are easily dislodged and uncomfortable to the wearer, thus presenting critical problems in long duration space flights.

(c) The telemetry of the EEG to ground receiving stations would require additional bandwidth and on-board hardware.

The primary objective of this research was to design a flexible hybrid computer routine which could be used in the investigation of experimental models which relate various physiological variables to the sleep-wakefulness states of an individual. The ultimate use of such a system would be to provide a reliable, simplified on-line monitoring technique to determine the depth of sleep. The potential for extending such technology into clinical situations such as bedside monitoring, multiphasic screening, and surgical monitoring could then be explored using similar techniques.

Indications that such a study might yield positive results have been obtained from previous reports in the literature and a limited analysis of data from the Gemini VII orbital flight. A qualitative relationship between EEG sleep level and heart rate and respiration on Astronaut Frank Borman has been described by Maulsby (19), and further preliminary studies were proposed and conducted by Maulsby and Vogt (20).

Chapter II consists primarily of a review of recent literature that reports studies directly related to the

special interests of this project. For general information on the various aspects of sleep see reports by Kleitman (15), Oswald (21), and Jouvet (13), all of which contain comprehensive bibliographies. Kleitman, for example, lists 4,337 references. Chapter III includes a limited review of automated EEG analysis techniques. Burch (6) and Brazier (4) have published accounts considering the more general aspects of the subject. Chapter IV describes the system and Chapter V describes the system testing and sample results. Documentation of the system is included in the appendices.

II. Physiological Indications of Sleep

The concept of sleep lacks a concise definition due to the lack of an accepted theory on the mechanism of the sleep-wakefulness cycle and to the confusion between the state of sleep and that of unconsciousness. Even so, sleep is a familiar, naturally occurring phenomena, and throughout the history of its investigation there has been general agreement on the more obvious characteristics of sleep. Some of the most ancient and widely accepted characteristics have a written history dating back to the time of Aristotle (2). The observation that respiration becomes slow and regular during human sleep has been documented by early studies (15) as well as the daily (or nightly) experience of persons observing sleep. The observation that the heart rate is reduced during sleep also has a long history and has been supported, although refined and qualified, by more recent studies (5, 14, 27). These two observations comprised the major portion of the earliest physiological study of sleep.

Kleitman (15) has traced the history of attempts to quantify the depth of sleep dating from the first reported effort over one hundred years ago. The concept of depth of

sleep is usually expressed (a) as a function of the intensity of stimulus required to evoke some criterion response, or (b) in terms of the magnitude of change of some continuously recorded physiological or behavioral variable. There are many problems with these various measurements of the depth of sleep, the most serious being that the different indications of depth of sleep do not run synchronously during a sleep period so that the estimation of the depth of sleep varies with the measurement used to quantify it. H. L. Williams (29) discussed many additional problems associated with quantifying the depth of sleep.

In spite of these problems and the belief by many (15, 29) that it is inadequate to determine the depth of sleep from a single variable, the EEG determination of the depth of sleep (7, 10, 17) has gained such wide acceptance that it has become the sole criteria used in most recent investigations. EEG definitions of the depth of sleep have undergone changes of an evolutionary nature, but presently the definition by Dement and Kleitman (7) is the most often quoted in the literature. Several aspects of these EEG definitions of depth of sleep will be discussed in the next

chapter. The acceptance of this central criteria for quantifying sleep, coupled with the discovery by Aserinsky and Kleitman (3) of the rapid eye movement (REM) phenomena of sleep, was instrumental in initiating the renewed interest in sleep research.

The development of a definition of depth of sleep and the revelation of the cyclical nature of normal sleep reopened investigation on the relationship of common physiological variables to the sleep-wakefulness cycle. Significant to this project are those studies of the effect of sleep on the respiratory and circulatory systems.

Brooks et al (5) in 1956 reported a study in which the relationship of changes in heart rate and the depth of sleep were investigated. In their study one-minute samples of EEG, ECG, and heart rate were collected at 17-1/2 minute intervals. The EEG was visually scored for depth of sleep according to the criteria of Gibbs and Gibbs (10). The statistical presentation of the data in this report was rather inadequate, since only a few graphs and data from selected subjects were presented. Their conclusions, however, seemed to be based on the total experience of the investigation, and

they stated that the data presented was representative of that collected in the experiment. By visually observing scatter plots of average nightly heart rate and average estimated depth of sleep and by calculating changes in heart rate or cardiac acceleration associated with changes in depth of sleep they stated:

> These results suggest that changes in sleep depth are reflected more in the lability of the cardiac cycle length than in changed average heart rate.

Also,

> When different subjects are compared, it is seen that there is no relationship between the average heart rate and depth of sleep.

Based on the high incidence of cardiac rate increases corresponding to changes in level of sleep, they concluded:

> One of the best justifications for using the EEG to identify the depth of sleep is the fact that independently-made measurements of heart rate changes show such exact correlation with EEG identified sleep changes.

In 1964 Snyder et al (27) reported on the changes in respiration rate, heart rate, and systolic blood pressure in human sleep. The EEG was recorded (continuously) and visually scored for EEG stage according to the criteria of Dement and Kleitman. (Refer to pages 14 and 15 of this thesis.)

From this data all acceptable five-minute samples were selected representing the various levels of sleep, and from these sections of data the heart and respiratory rates were manually counted on the basis of thirty-second averages. In addition, systolic blood pressure was recorded for each minute of the samples. A variability index was calculated for each of the above three variables for the five-minute intervals. The data was then pooled, and the Scheffe (25) multiple comparison procedure was used to test the significance of the differences between stages of sleep. Stages III and IV were grouped "in order to provide a body of data comparable to that for the other stages." They found that:

> All three measurements and their variability indices showed consistent and significant changes over the whole night of sleep and periodic variation concomitant with the EEG cycle within each night of sleep.

Their conclusion, however, was that the periodic variation of the measured variables was due only to the stage I-REM sleep and that significant differences of these changes were not consistent with relation to stages II and III-IV sleep.

The hemodynamic changes associated with sleep were studied by Khatri and Freis (14). In addition to

various measurements related to hemodynamics, the heart rate and respiration were monitored throughout the periods of sleep. The significance of the changes of the mean of the measures between levels of sleep was calculated, and their results concur with those reported by Snyder et al.

The studies described above represent the most significant and recent investigations of the relationship of the heart rate and respiration rate to the depth of sleep. The most significant results reported in each of the studies were those reflecting the changes of the variables from their basal or presleep values. These changes were shown to have a significant relationship to the sleep profile, whereas the absolute values of the variables seemed to depend on other factors such as those affecting the metabolic rate of the subject. Even though a significant relationship had been shown to exist among the variables, it had not been found to be a sensitive enough indicator to yield a quantification of the sleep levels. Snyder et al (27) concluded:

> If EEG patterns are reliable indicators of sleep depth, then it appears that [heart rate, respiration rate, blood pressure, and their variances] . . . are not.

The previously reported attempts to identify a relationship between these variables are lacking in that (a) there are no reported studies designed to investigate the phase or temporal relationships of the variables, and (b) there have been no attempts to find a "new" indication of depth of sleep based on the combined information from several variables. The use of hybrid computation, as reported herein, allows such an approach as well as permitting the use of preprocessing circuitry which continuously derives the variables of the study from the raw data.

III. EEG Determination of Depth of Sleep

A. Electroencephalographic Classification of the Depth of Sleep

As mentioned in the previous chapter, definitions of the depth of sleep based on the EEG have produced a common reference criteria that allows comparison of the work of different researchers on the various aspects of sleep. The appeal of the method is that investigation has verified its reproducibility of interpretation within relatively narrow limits, both between and within observers, and the EEG is now included as a portion of most studies involving sleep.

Following Berger's discovery of the EEG, the condition of altered cerebral states during sleep was detected, and several methods of classifying these states were developed (7, 10, 17). All such methods have depended in some way on the alterations of the amplitude, frequency, and pattern complexes that are considered to be characteristic of the altered cerebral states. Loomis et al (17) and Gibbs and Gibbs (10) developed two of the earlier classification schemes, but the discovery of the REM phase of sleep and the Dement and Kleitman (7) classification of four stages of sleep combined to produce the most unified and widely

accepted definition of sleep levels. Samples of EEG signals typical of the categories described by Dement and Kleitman, in addition to the characteristic EEG patterns corresponding to full wakefulness and the resting or eyes closed rhythm, are shown in Figure 1 as follows:

Awake (Figure 1a): A desynchronized, low voltage, high frequency EEG characterizes the normal alert state.

Resting (Figure 1b): The assumption of a relaxed state by the subject with his eyes closed results in the characteristic alpha rhythm. These very regular waves occur at frequencies between 8 and 14 cps with the frequency relatively stable in an individual. Specific mental activity or opening of the eyes results in cessation of the alpha rhythm and the assumption of the low voltage desynchronized wave form.

Stage I (Figure 1c): The first stage of sleep is characterized by the absence of the alpha rhythm and the presence of relatively low voltage theta wave forms (4 to 8 cps). The appearance

of "sleep spindles" (short bursts of 14 cps activity superimposed on low frequency waves) terminates stage I sleep.

Stage II (Figure 1d): This stage comprises that portion of the record that consists of spindles with a low voltage background and intermediate segments of low voltage theta activity.

Stage III (Figure 1e): This stage is described as an intermediate stage characterized by the appearance of high voltage delta waves (less than 4 cps) with some superimposed spindles.

Stage IV (Figure 1f): In this case at least half of the record must be dominated by high voltage delta waves.

A considerable amount of judgment on the part of the investigator is incorporated into the interpretation of the stage of sleep from EEG records. Usually the decision is made on the basis of evaluation of one-minute segments of the record, but this length may vary among investigators. Each consecutive segment is given a value corresponding to the stage of sleep it represents. When an

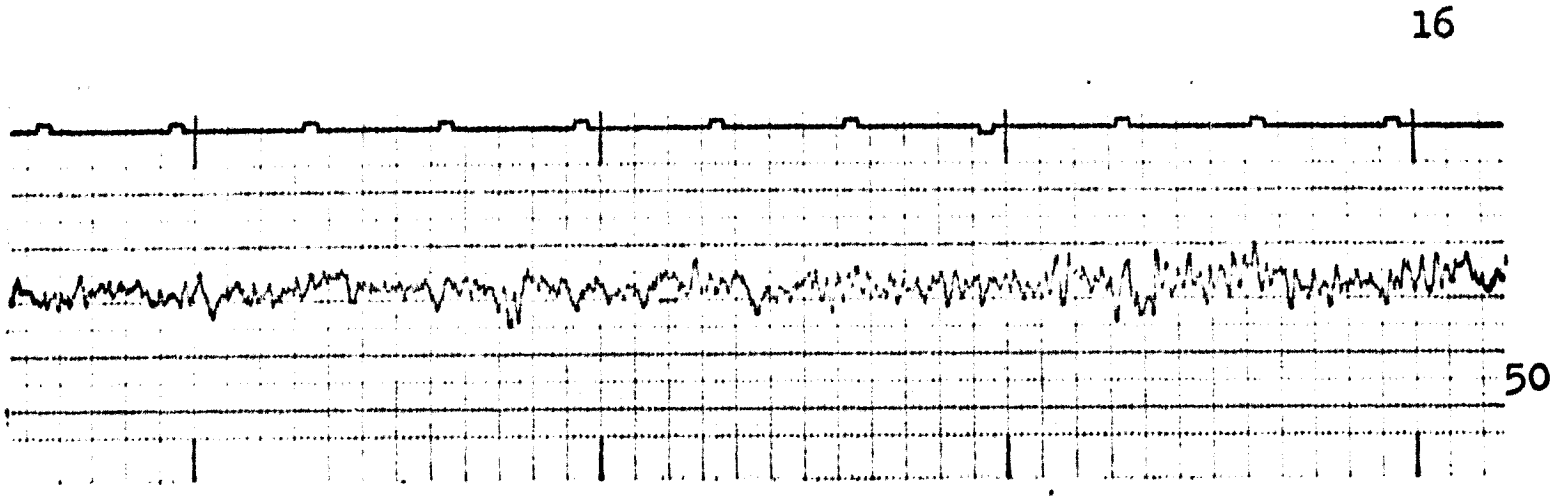


Figure 1a Awake

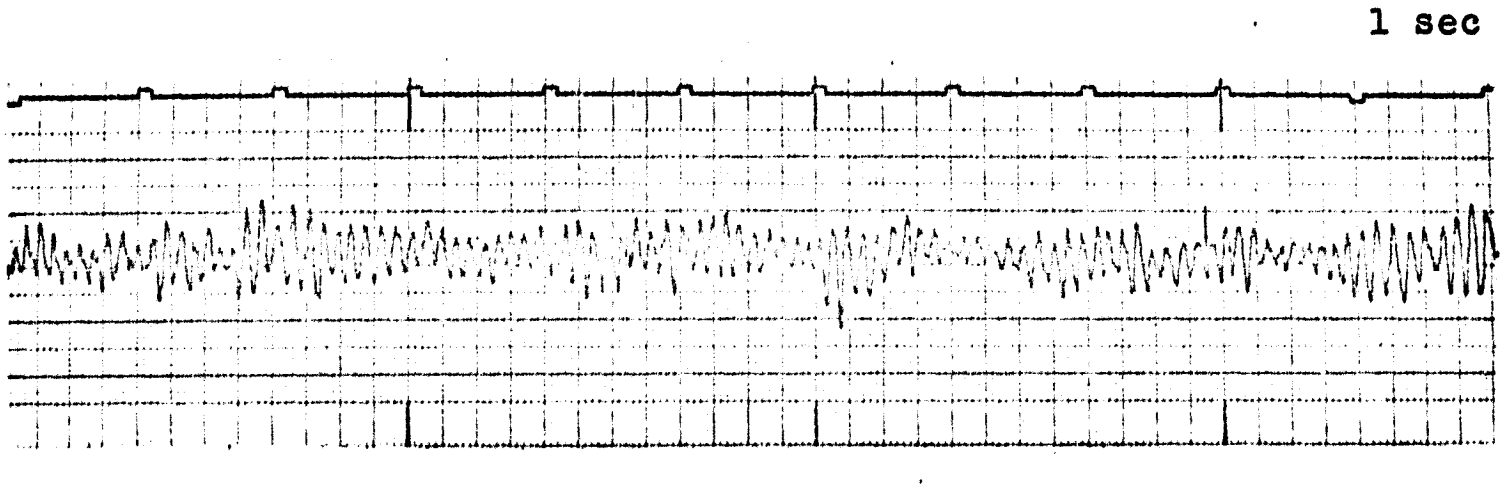


Figure 1b Eyes Closed (Alpha Rhythm)

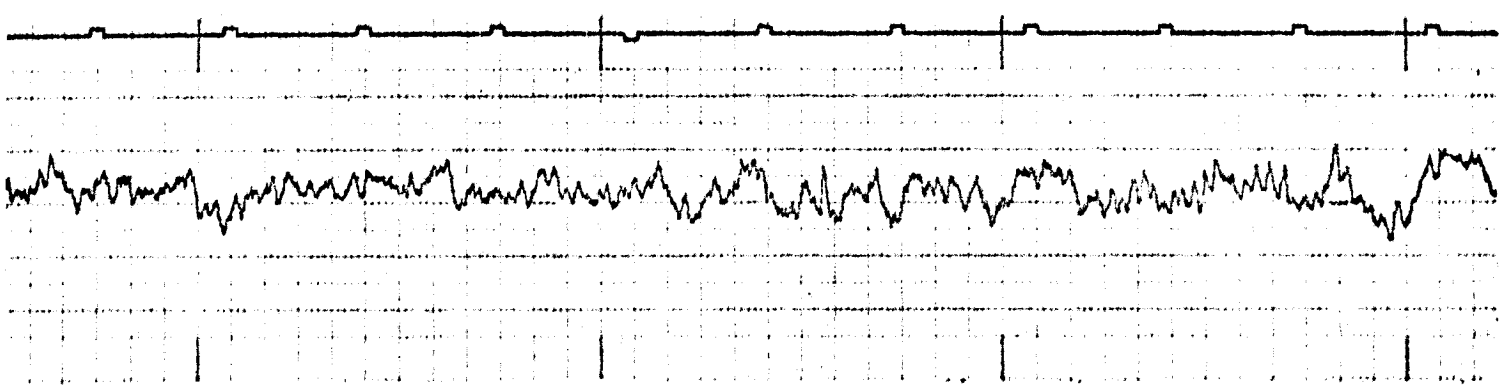


Figure 1c Stage I Sleep

Figures 1a, 1b and 1c

Occipital-Parietal Bipolar EEG
Samples Depicting Various Stages of Sleep

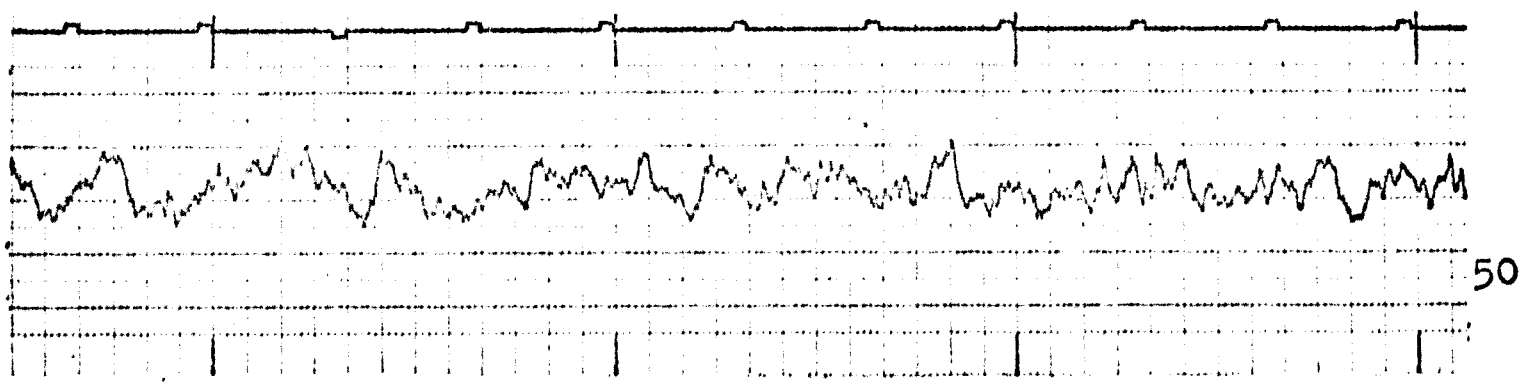


Figure 1d Stage II Sleep

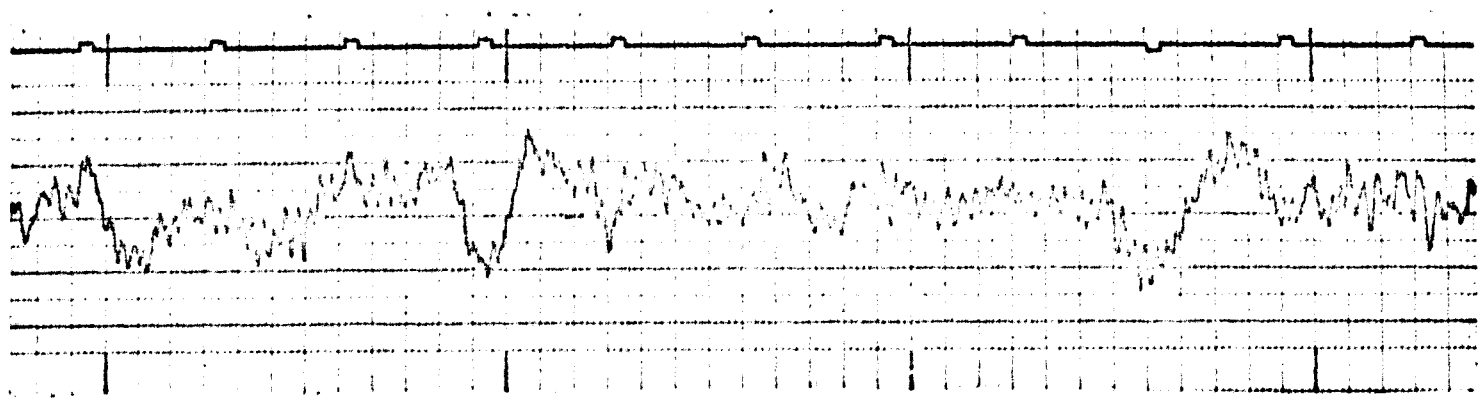


Figure 1e Stage III Sleep

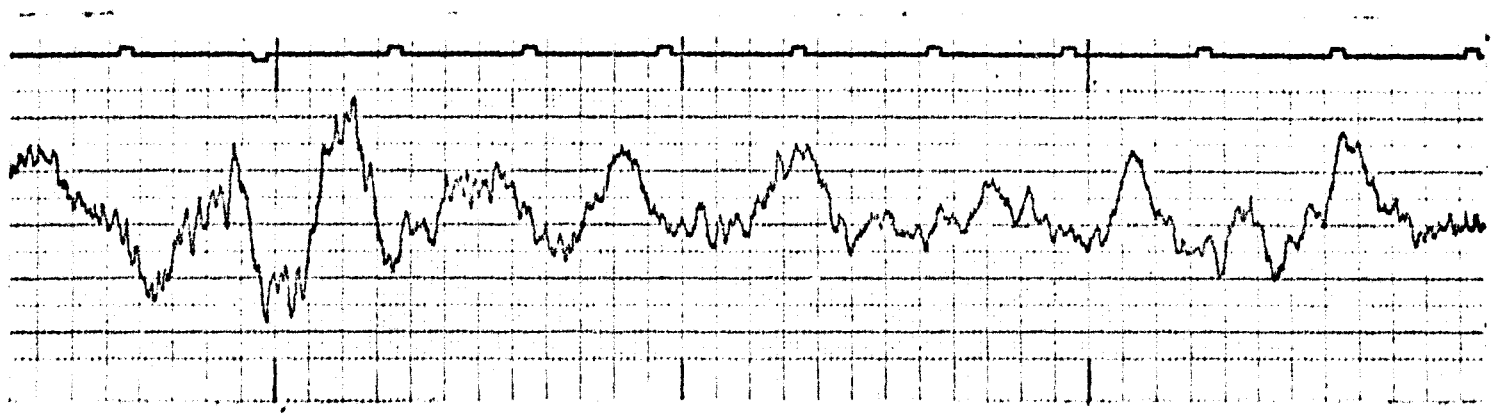


Figure 1f Stage IV Sleep

Figures 1d, 1e and 1f

Occipital-Parietal Bipolar EEG
Samples Depicting Various Stages of Sleep

entire record has been interpreted in this manner, the information can be presented as a continuous profile of the sleep period such as shown in Figure 2. This typical record illustrates the cyclical nature of the depth of sleep. Except for the stage I period at the initial onset of sleep, all subsequent stage I periods are accompanied by REMs (7) and the associated variability of heart rate and respiration variables mentioned in the last chapter. These periods are known as the stage I-REM periods of sleep.

Since the production of a profile of sleep requires a continuous graphic record of the EEG with a chart speed sufficient to allow detailed inspection of the wave form, large quantities of the record are accumulated. The visual interpretation of the record is usually described as tedious and time consuming and requires trained personnel to obtain reproducible results, thus indicating that there are practical as well as academic reasons for pursuing alternate methods of analysis. Numerous means of automatic analysis of sleep from EEG have been investigated, but none of the proposed methods have gained widespread acceptance. To gain

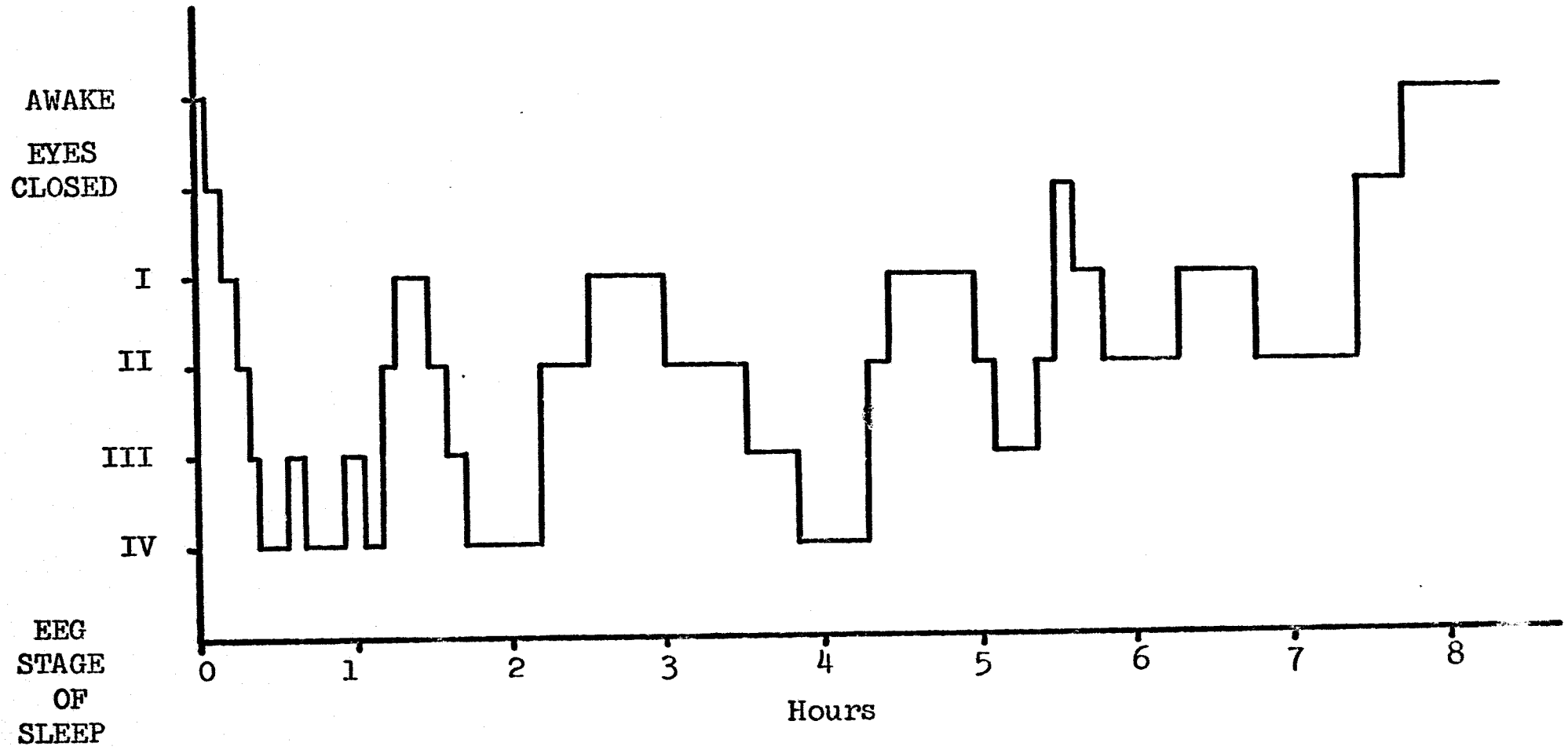


Figure 2

Typical Sleep Profile

such acceptance, a method for automatic analysis of the EEG should meet a basic set of requirements which might be stated as simply as the following:

(a) The ability to reproduce records that differ from human interpretation by no larger a margin than that expected between independent human interpreters is desirable.

(b) In addition to being a measure of economy, the ability to analyze data at real time or faster than real time rates is necessary to prevent the accumulation of data in large studies. Although inexpensive hardware versions might be made available for analysis during the collection of data and would be required to operate no faster than real time, methods requiring the services of large scale computers should have the ability to operate much faster than real time.

(c) Another factor of relative importance is that simple, easy-to-operate equipment is desirable over that which requires lengthy training of personnel to properly establish and maintain.

(d) In many instances the acceptability of such an analysis would depend on the form of the output information. It is desirable that such information would not require subsequent interpretation, and the most convenient output would be the sleep profile itself or some form which is adaptable to this type of presentation.

B. Automated Analysis of EEG Determined Depth of Sleep

The following few paragraphs are a brief review of the field of automatic depth-of-sleep analysis. The intent is to describe some of the more familiar methods of depth-of-sleep analysis to provide background information pertaining to the method of analysis chosen for this study.

The amplitude change of the EEG signal which accompanies alteration in the level of sleep has been the focal point of several approaches to automated depth-of-sleep analysis. One very direct approach is simply to measure the energy content of the EEG by integration of the rectified voltage wave form. An integrator designed specifically for EEG analysis was presented by Drohocki in 1948, as cited by Goldstein and Beck (11). Drohocki's

method was to charge a capacitor through a high gain pentode and to discharge the capacitor through a thyratron tube at a preselected limiting voltage. The large plate resistance of the pentode and the amplification of the capacitor value (due to the Miller effect) allowed time constants sufficiently long to extend the linear portion of the charging curve to a practical value. The capacitor discharge triggered a monostable multivibrator which produced a pulse as the output of the circuit. This train of pulses, representing the energy content of the EEG, could then be subjected to statistical analysis or processed by additional circuitry to derive or enhance the desired information.

Goldstein and Beck (11) indicated computations based on the mean energy content (MEC) of the EEG as derived from the train of pulses and the coefficient of variation (CV) of the MEC determination to distinguish between differing subject populations. They also suggested that these measures may be used to define a normal population of EEG values to serve as a basis for studies of abnormal EEGs. Many clinical studies of the various EEG populations are referenced in their paper.

Agnew et al (1) used the amplitude measurement of Goldstein and Beck in a preliminary study of its application to scoring the sleep EEG. By forming a histogram of the mean energy measurement (MEC) based on one-minute averages, they displayed a sleep profile approximating that of the visually scored record. Based on fourteen subject-night records they reported correlations between visually scored sleep stage and the MEC value ranging from 0.72 to 0.96 with all but four coefficients above 0.85. They did not indicate which portion of the record contributed the most error, but the histograms displayed in their paper suggest that it was probably present in the lighter stages of sleep (stages I and II) and in the discernment of wakefulness and stage I sleep. They did not indicate values based on pooled data but stated that intrasubject differences were "insignificant" and that intersubject differences were "significant at the 0.05 level."

Maulsby et al (18) achieved similar results by replacing the integrator and multivibrator of the circuit with a simple RC filter. This replacement combined the integration and averaging of pulses of the previous method and, most

important, replaced the need for manual plotting of the record. Although no comparative data was presented, visual inspection indicates that they may have gained resolution of the lower levels of sleep by selectively filtering the input EEG signal to attenuate all but the delta and theta frequencies.

In addition to analysis based on the amplitude of the EEG, there have been continuous efforts to characterize the signal by using frequency analysis techniques (6). Early attempts to derive specific information seem to have resulted in frustration, as exemplified by Grass and Gibbs (12) after their experiences.

> Much experimentation with the data finally leads to the conclusion that, although frequency analysis has advantages for revealing certain general features of the EEG, it is not satisfactory for clinical purposes. No index, either simple or complex, based on one or on many spectra from a given case, can express the highly specific detailed information contained in the EEG.

The limited success of these early attempts with frequency analysis probably can be related to three factors as follows:

(a) The attempts were made at a time when many of the more objective criteria for present-day sleep analysis were still unknown.

(b) The lengthy computation characteristic of frequency analysis techniques (such as the Fourier series) had to be accomplished without the benefit of high speed computers.

(c) The filter circuits that were used for early analysis would be considered primitive by present standards.

The more specific criteria available when the analysis is limited to the detection of sleep levels and the usage of rapid computation have permitted additional progress of such analyses, but only to the point where problems inherent in the frequency aspects of definitions of depth of sleep have intervened. Specifically, the criteria pertaining to frequency alone do not seem to be restrictive enough for concise discrimination of the depths of sleep. Walter et al (28) used a digital spectral analysis routine to segment EEG samples of varying states of consciousness (not sleep) into four bandwidths (delta, 0.5-3.5 cps; theta, 3.5-7.5 cps; alpha, 7.5-12.5 cps; and beta, 12.5-25.5 cps). On each frequency band three parameters were derived: the power, or mean-square intensity; the mean frequency within the band;

and the predominant bandwidth within the band. A discriminant analysis routine was used to select the most descriptive of those parameters for discrimination between the various samples. Their conclusions were that those parameters which were selected for the pooled data did not correspond in each case to the parameters selected for individual data. Because they were unable to include experimentation to test the individual results for consistency, this is possibly another case of intrasubject consistency and intersubject variability.

Riehl (23, 24) reported a method of automatic analysis of the EEG that was based on the ratio of frequency and amplitude measures of the EEG but was not specific in defining or showing the derivation of his variables. The ratio that he developed (frequency/voltage) was defined as the "unit of activity" and fluctuated in relation to the various states of cerebral activity. Riehl showed data indicating that this ratio changed in mean value and variability in relation to changes in the level of sleep, but no experiment designed to verify and quantify the relationship has been found in the literature.

Another method, devised by Frost (9), combining both frequency and amplitude measures of the EEG was selected for further study in conjunction with this project. In his method the frequency/voltage relationship may be described as:

$$F(f,v) = G(f) - H(f,v)$$

where G(f) is proportional to the fundamental frequency of the EEG and H(f,v) is proportional to the frequency of excursions of the signal above a fixed amplitude. The rationale for selecting this type of relationship is that the appearance of high voltage wave forms will emphasize the reduction of signal frequency in the defined relationship. Unpublished studies by Frost indicate a good correlation between visually scored depth-of-sleep records and those produced by Frost's method. The major reason this method was selected for use in this research was the conformance with all portions of the criteria listed on pages 20 and 21 of this report.

The circuitry required to implement the system is incorporated into the analog signal processing portion of the hybrid routine described in the following chapter. The analog

circuit diagram and the coefficient values are shown and listed in Appendix A.

IV. Preprocessing and Analysis of Data

Most previous investigations of the relationship between various physiological measurements and the EEG determined depth of sleep have been characterized by manual processing and interpretation of the raw data. In exploratory studies the time and expense involved in such data processing could well be a limiting factor in the initiation or extension of a research project. A definite aid in such projects would be an automated system to derive the variables of the study from the raw data and to calculate the relationships that exist among the data on high speed digital computers. Such a system would allow the principal efforts of the research to emphasize the collection of sufficient data to test the premises of the study followed by the initiation and testing of hypothesis based on the accumulated information.

The characteristics of a hybrid computation system are particularly suited to a flexible analysis procedure such as that desired. The development and use of signal preprocessing circuitry on the analog portion of the system permits the derivation of signal variables such as rates and variances on

a continuous basis either in on-line applications or at multiples of real time. This involves the extraction and emphasis of characteristics of a signal that may otherwise be obscured by noise or artifact or not apparent in the standard presentation of the signal. As information is transferred through the interface (analog to digital converter), the digital portion of the system can accomplish such derivations of additional parameters and measures of the data that are more suited to digital computation. Coinciding with the derivation of variables, statistical analyses can be performed on the digital computer, and utilizing the interface and peripheral equipment (digital to analog converter, plotter, etc.), wave forms can be reconstructed for visual interpretation and further analog processing.

In applying these hybrid techniques to the study of physiological variables relating to the depth of sleep, limitations are necessary but should not be construed as fundamental to the system. Alteration of the proprocessing circuitry will allow the study of variables other than those selected, and additional digital programming will allow alteration or extension of the statistical analysis.

The hybrid routine reported in this chapter may be described as a system which accepts EEG, ECG, and respiration data from analog tape at real time or multiples thereof and utilizing analog circuitry derives six variables as follows:

(a) The EEG determined depth of sleep using the method devised by Frost;

(b) An average of the beat-by-beat heart rate;

(c) An indication of the variance of the heart rate;

(d) A qualitative measure of the respiration volume;

(e) An averaged respiration rate; and

(f) An indication of the variance of the respiration rate.

As these variables are determined, they are digitized, and correlation coefficients and a regression analysis are computed on the digital computer. Following the computation of the regression coefficients, a second pass of the analog tape results in the reconstruction of the estimated variable and analysis of the residuals. For the initial studies a model was used in which a linear combination

of the five independent variables is regressed against the dependent variable, depth of sleep. This is of the form:

$$Y = b_0 + b_1x_1 + b_2x_2 + b_3x_3 + b_4x_4 + b_5x_5 + e$$

where

Y = depth of sleep

x_1 = respiration volume

x_2 = respiration rate

x_3 = variance of the respiration rate

x_4 = heart rate

x_5 = variance of the heart rate

$b_0, b_1, \ldots, b_5$ = regression coefficients

e = error of the regression

A block diagram illustrating the information flow through the system is shown in Figure 3. Detailed analog computer circuits and the digital computer program are documented in the appendices.

The general features of each of the component blocks will be considered in the following paragraphs. The resulting voltage levels are not calibrated to absolute parameter values due to the previous reports (5, 14, 27) that these absolute values were not significant when related

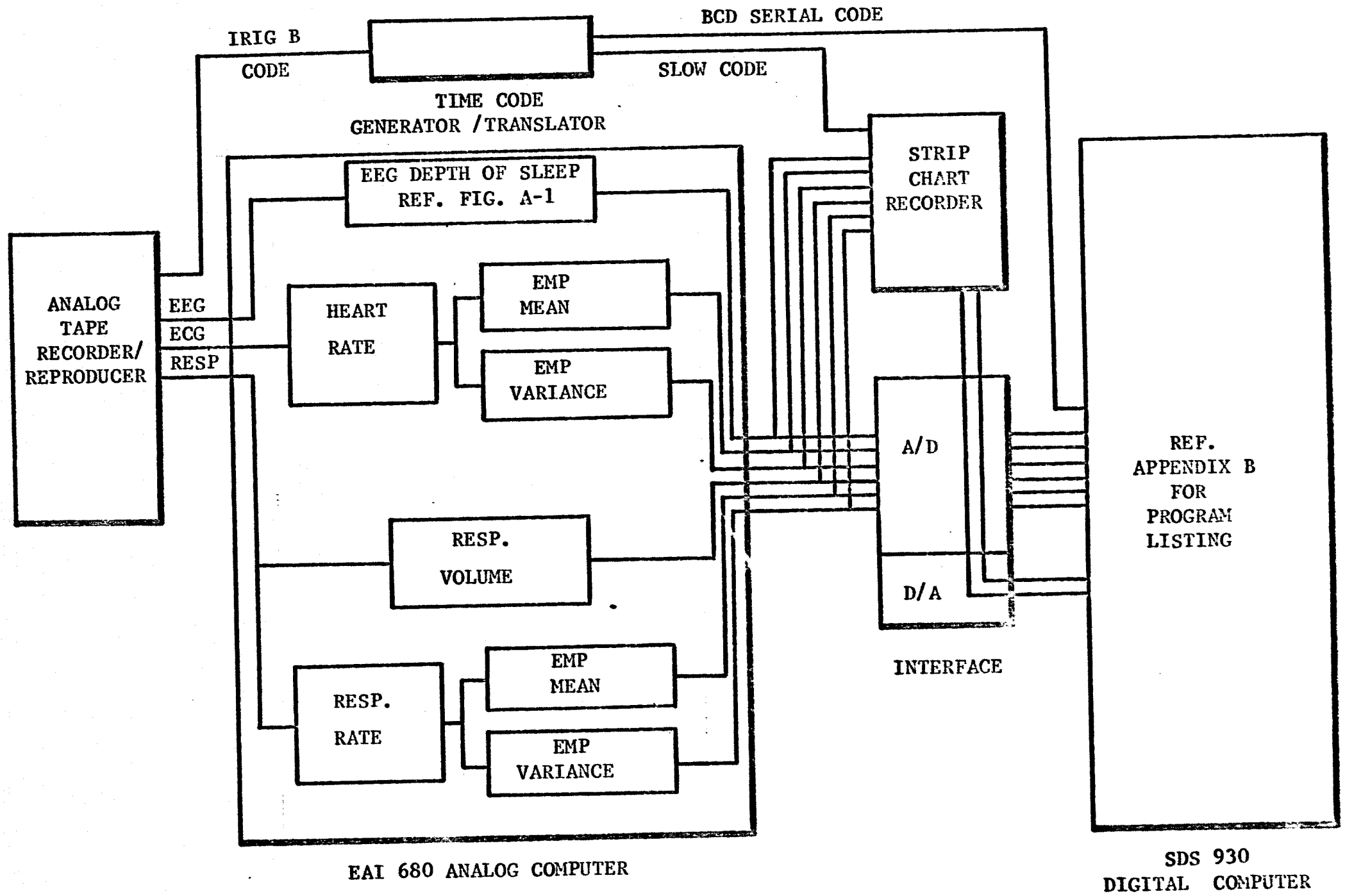


Figure 3

System Block Diagram

to the depth of sleep. Significant information relating to the depth of sleep has been found in base line trends and changes from the basal values. A measure more sensitive to these fluctuations around the base line can be devised if the absolute value of the signal is not retained allowing the amplification to be increased.

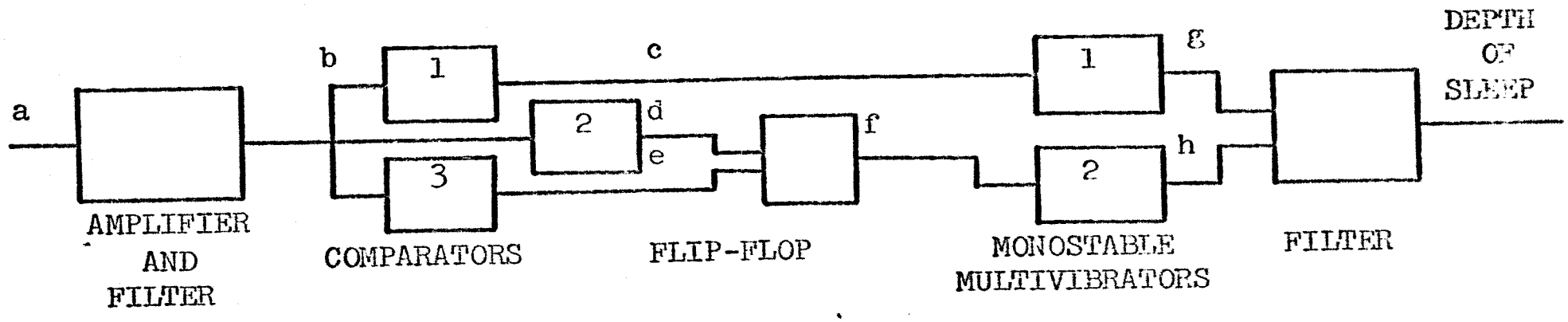
EEG Preprocessing

The method used to derive the depth of sleep from the EEG was briefly described in the previous chapter. The block diagram and idealized wave forms of Figure 4 illustrate its general operational features as described below.

The raw EEG signal (Figure 4a) (occipital-parietal bipolar lead) is initially amplified and passed through a 1-11 cps bandpass filter (Figure 5). This filtering removes many of the slow wave artifacts in the delta band as well as eliminating any DC offset voltage that may be present. As mentioned earlier, the removal of the higher frequencies seems to help discriminate between stage I sleep and wakefulness. The filtered signal (Figure 4b) is then presented to the comparator portion of the circuit. Comparator 1 in the block diagram switches when the input rises above a

a preselected value. This value is empirically derived for each subject and is set to a voltage level just above the dominant alpha rhythm amplitude. Comparators 2 and 3 are set to indicate the dominant frequency of the filtered EEG by detecting excursions across the base line of the signal. Comparator 2 switches when the signal amplitude has a small positive value and its output (Figure 4d) sets a flip-flop which is reset by the output of comparator 3 (Figure 4e). This comparator is set to detect small negative signal values. By biasing the comparators off the base line in this manner, the common problems of zero signal detection in noisy signals can be minimized. In addition, this biasing allows indication of abnormal EEG conditions since extremely small amplitudes or noise levels will not trigger the circuit.

The leading edge of the output pulses of the comparator circuitry triggers the monostable multivibrators. The output of comparator 1 (Figure 4c) triggers a train of negative pulses, and the output of the flip-flop (Figure 4f) triggers a train of positive pulses. These fixed duration and amplitude pulses (Figures 4g and 4h) are combined and



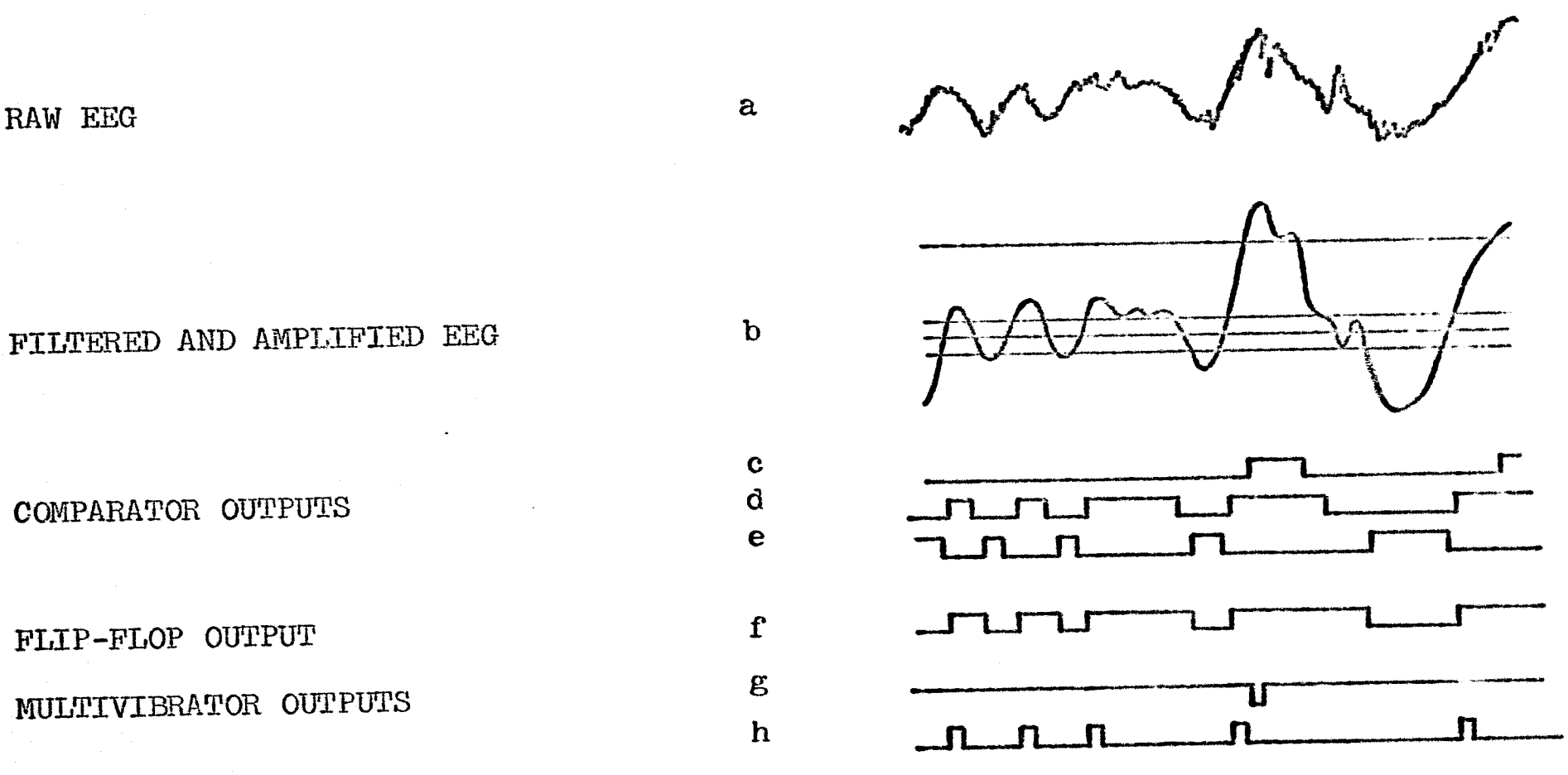
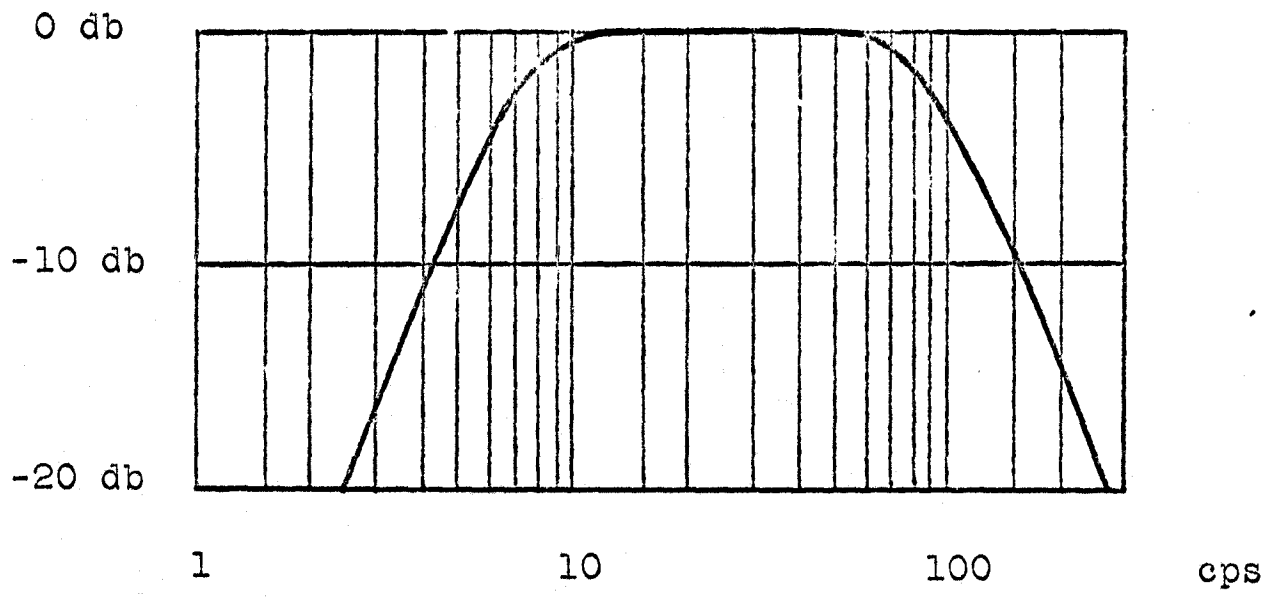


Figure 4

Block Diagram and Typical Wave Forms
EEG Depth of Sleep Analyzer

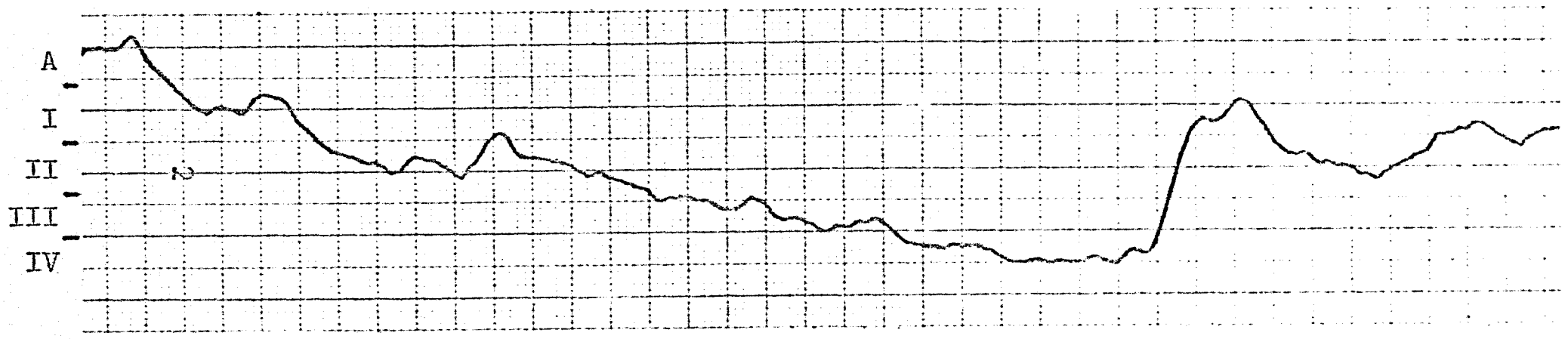
processessed by the final stage, which includes averaging of the pulse train with a second order filter and scaling the output signal to the desired amplitude. In Figure 6 the results of the analysis of a sample sleep EEG and the associated visually scored record of the raw data are illustrated.



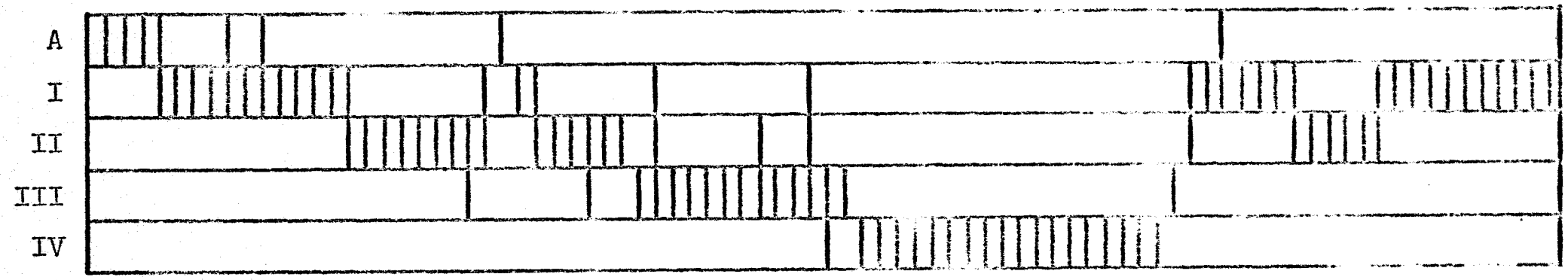
8-88 cps for operation at eight times real time.

Figure 5

EEG Filter Frequency Response



Automatically Analyzed EEG Depth of Sleep



Visually Scored EEG Depth of Sleep

Figure 6

Comparison of Automatically Analyzed and Visually Scored Depth-of-Sleep Records

Respiration Signal Preprocessing

Methods used to transduce respiration into an electrical signal can be susceptible to the inclusion of various artifacts. Band pass filtering can aid in reducing much of the artifact, but since slow wave artifact may also be present in the range of frequencies that comprise normal respiration signals, the possibility of disturbances remains. After experimenting with various techniques under noisy signal conditions, it was found that the most reasonable method of rate determination is achieved by narrowing the pass band from the high frequency end so that the signals representing the highest desired respiration rates are attenuated but still detectable. In combination with this reduction, the signal can be made more insensitive to remaining artifact by employing an averaging technique in the circuit. The pass band cannot be narrowed significantly from the low frequency side, since slow and held breaths are quite common, and the attenuation of their fundamental frequency components can lead to erroneously high rate determinations. The pass band used in this circuit was approximately 0.05 to 0.7 cps as described by Figure 7. The circuit shown in Figure 8

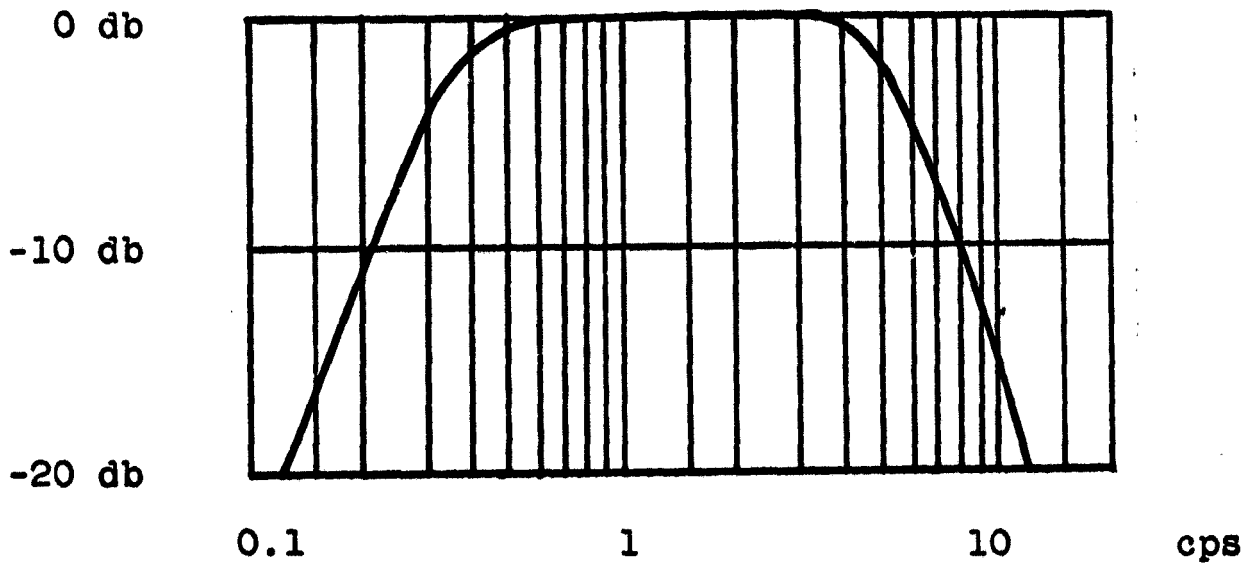


Figure 7

Respiration Rate Filter Frequency Response

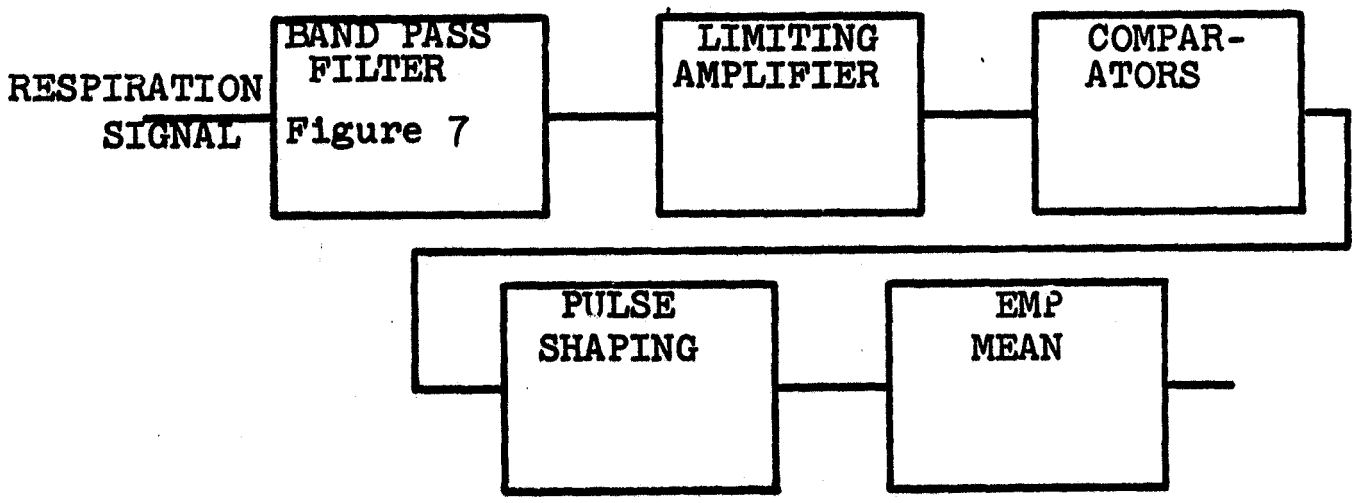


Figure 8

Block Diagram of Respiration Rate Detection Circuit

allows detection of breathing rates ranging from 4 to 50 breaths per minute. The method is not insensitive to the detection of all artifact and is not applicable to breath-by-breath studies, but it is adequate for applications that do not require those features.

Using the same basis for judgment, a qualitative determination of the respiration volume can be made by first filtering the respiration signal to remove DC voltage levels and slow wave artifact with the filter described by Figure 9 and then full wave rectifying the signal and averaging it

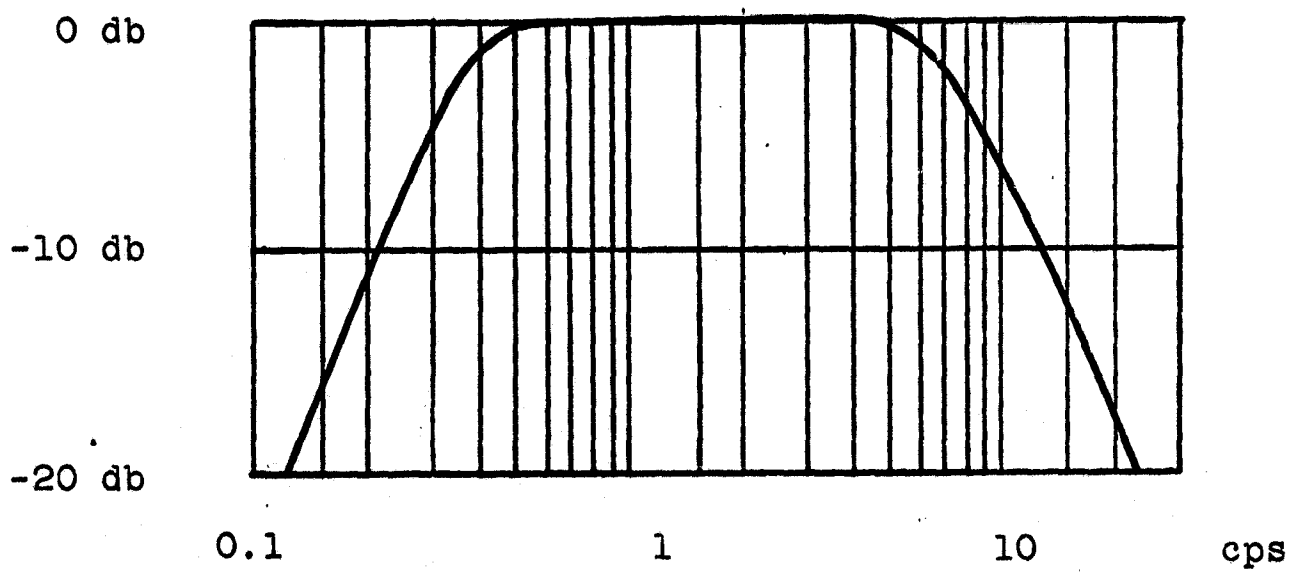


Figure 9

Respiration Volume Filter Frequency Response

with a long time constant filter. This method is applicable to the derivation of volume from respiration signals which are transduced as qualitative indicators of respiration information. As an example, the impedance pneumogram, which is used in space flight applications, is not easily calibrated to yield a quantitative respiration volume signal (16).

ECG Preprocessing

Detection of the cardiac rate can also be hindered by artifact, but the effects of the artifact can be eliminated in all but the most severe cases. The block diagram of Figure 10 illustrates a circuit that has proven satisfactory for the determination of the beat-by-beat heart rate. A band pass filter (Figure 11) which spans the predominant QRS complex frequencies and a dead time after the detection of the QRS complex accomplishes the elimination of most slow wave and high frequency artifact and prohibits T wave triggering. The absolute value circuit permits detection of inverted R waves.

After determining the heart and respiration rates by these circuits, additional circuitry is employed to

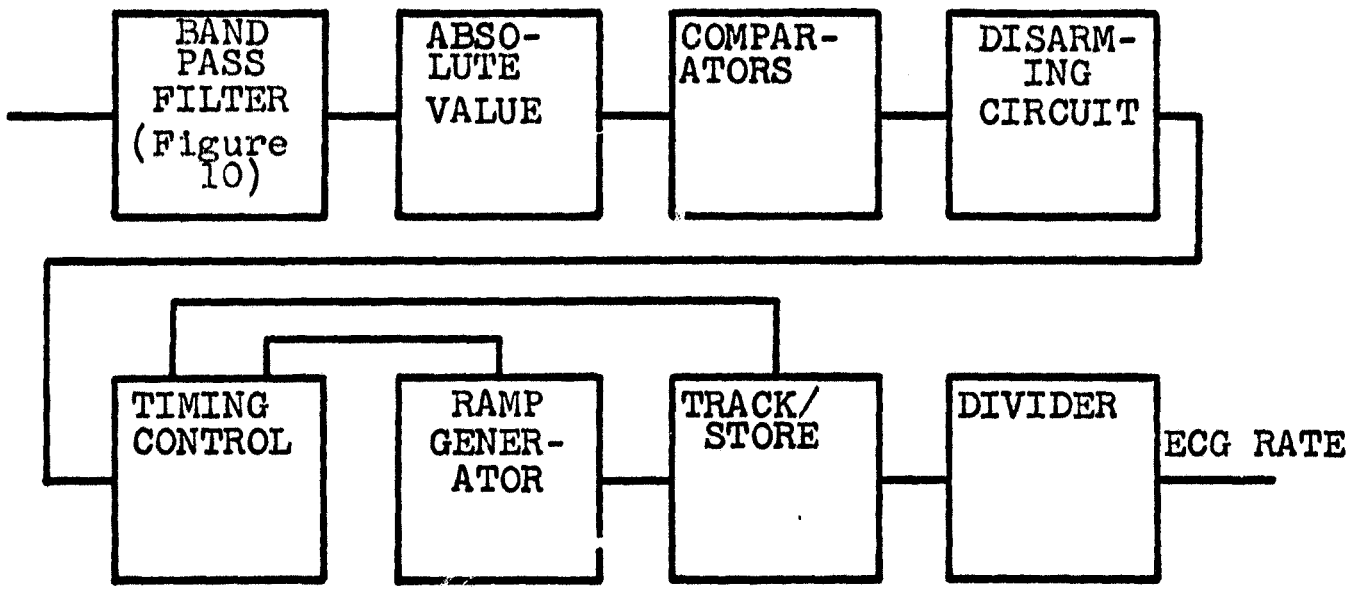


Figure 10

Block Diagram of Heart Rate Detection Circuit

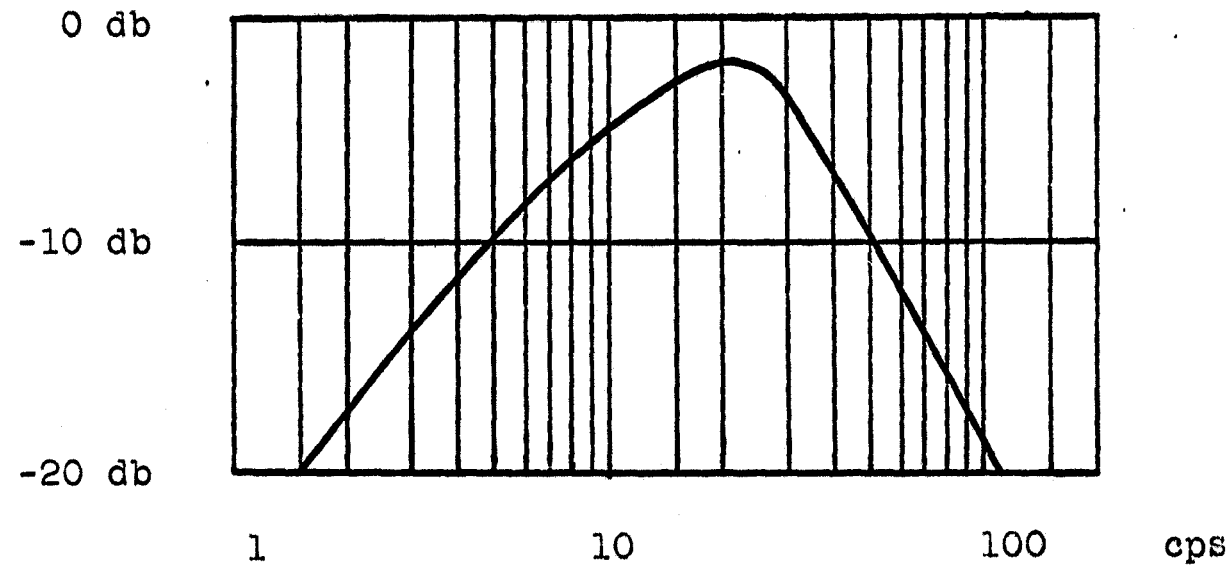


Figure 11

ECG Filter Frequency Response

compute the means and approximate variances of these signals. This is accomplished on the analog computer since the objective is to obtain these parameters on a continuously up-dated basis. The process involves the exponentially mapped past (EMP) estimation of the mean and variance. The derivation of the method is shown by Otterman (22) and has become standard procedure in analog computation. For this study, however, the derivation of the EMP estimates of the rate variances has been altered to increase the sensitivity for the display of small variances. This was accomplished by replacing the squaring operation of the standard variance circuit (Figure 12a) with an absolute value determination (Figure 12b).

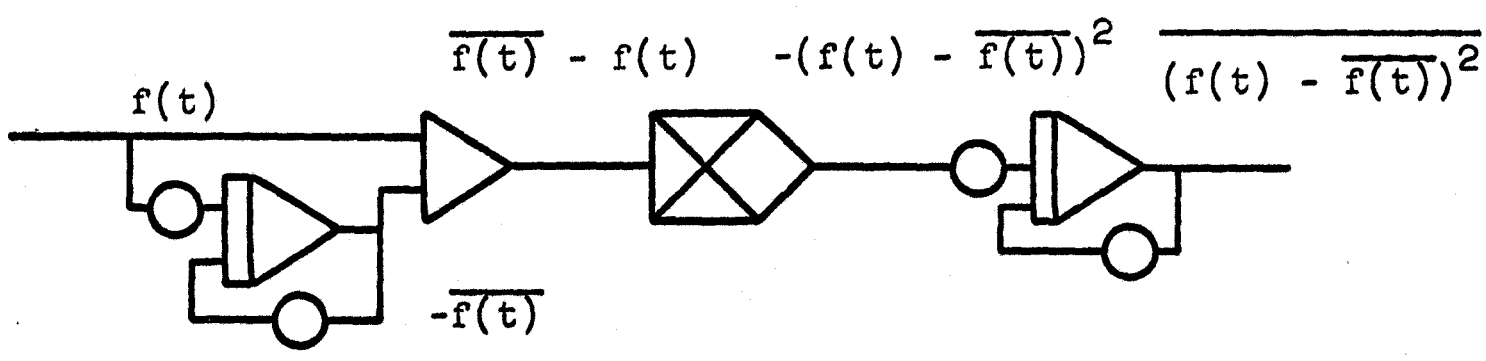


Figure 12a

Standard Variance Circuit

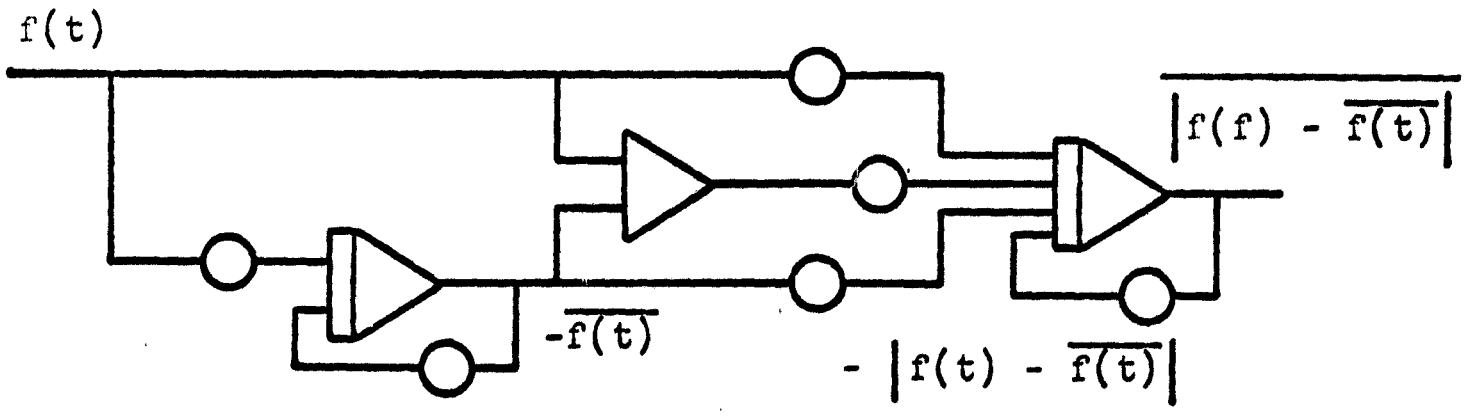


Figure 12b

Altered Derivation of Variance

The complete circuit diagrams and associated coefficient values for the analog portion of the hybrid routine are shown in Appendix A. However, it should be noted that the time constants of the various filtering circuits could well become variable parameters in future studies.

The method used to perform the regression analysis is described by Draper and Smith (8). As implemented in this system, the routine includes a variable time delay in the data sampling loops which allows adjustment of the sampling frequency to compensate for changes in the time constants of the averaging filters and resulting changes in the

frequency components of their output signals. Due to the inclusion of floating point operations in the sampling loop, the minimum sampling period is 27 msec. This is adequate for operation at eight times real time, even allowing for averaging filters with short time constants. Operation faster than eight times real time must be accompanied with consideration of the frequency content of the sampled variables.

As the variables are sampled, the necessary summations are accumulated, and when the input of data is terminated, the correlation coefficients between all variables are calculated and placed in matrices. Inversion of the principal correlation matrix and subsequent multiplication results in scaled versions of the correlation coefficients which are readily converted to those desired.

To ascertain the accuracy of the inversion routine, the product of the matrix and its inverse is printed out after processing the data. However, the centering and scaling of the data involved in the formation of the correlation matrix yields a well-formed matrix for inversion in regression analyses of this type (8), and the sample inversions shown in

Appendix C illustrate that the error of inversion is negligible.

Following the computation of the regression coefficients, an analysis of the variance table is computed to aid in evaluating the regression, and a plot of the residuals versus time is produced on a subsequent pass of the analog data tape.

A program listing for the digital routine is located in Appendix B. By varying the summation statements in the data collection loop, the model can be altered from the linear form shown on page 32.

V. System Testing and Sample Output

The system described in the previous chapter and shown in Appendices A and B was implemented on a hybrid computer. The system has been tested with simulated as well as actual data as described in the following paragraphs.

Testing of the analog preprocessing circuits was accomplished with data from two sources. Initial tests were made with data transcribed from the biomedical tape recorder aboard the spacecraft on the Gemini VII orbital space flight. This data included extensive interference and artifact on the respiration signal (ZP) which was in part due to deteriorating electrode connections. Failure of the respiration parameter derivations under these conditions was not surprising.

Subsequent tests were accomplished with data collected under controlled laboratory conditions. This data was collected from healthy Air Force Pilots in afternoon recording sessions during which each subject passed through a period of sleep. The data was accompanied by visually scored interpretations of the depth of sleep during the sleep period. In Figures 13 and 14 the wave forms resulting from the

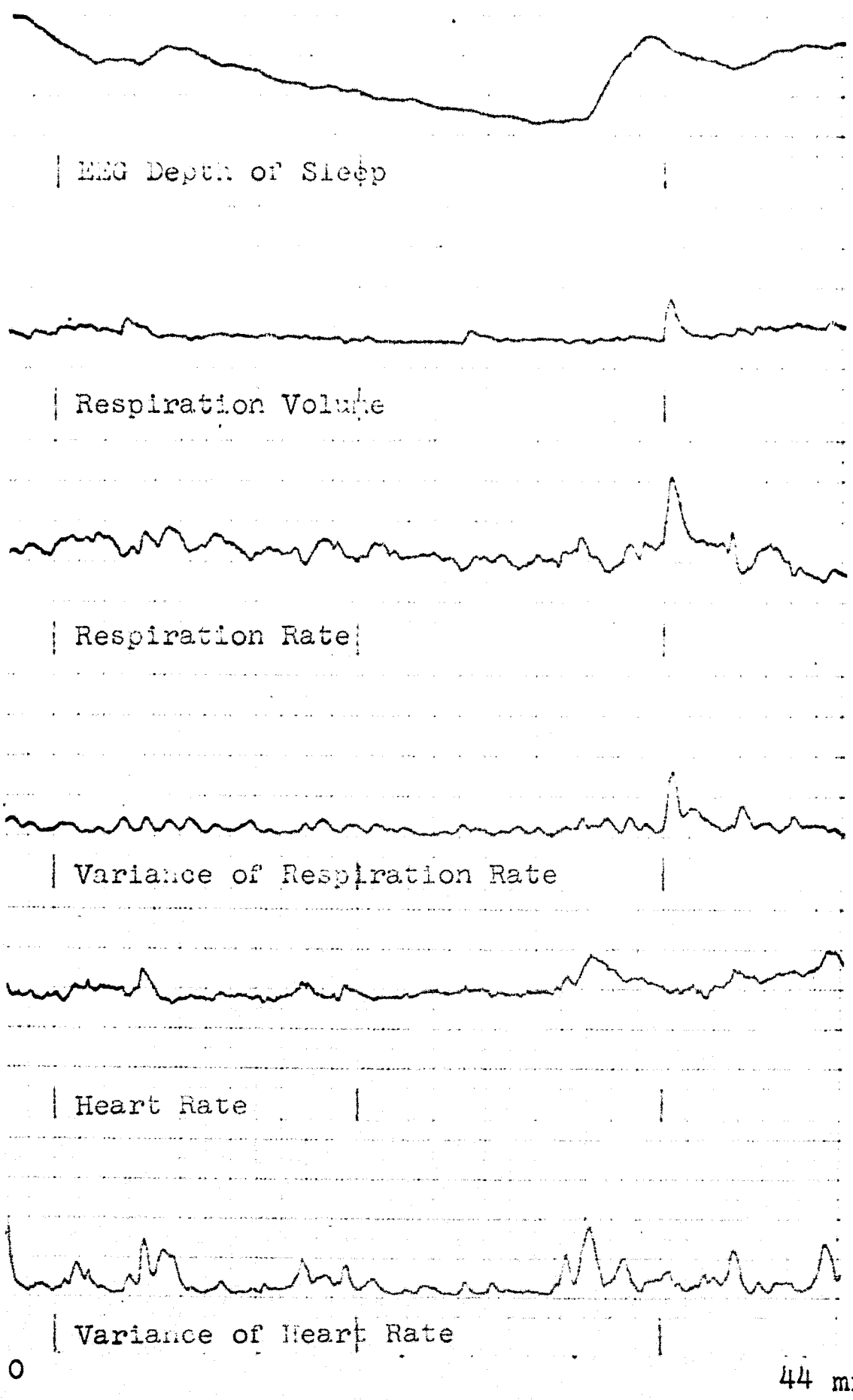


Figure 13
Processed Data - Subject #1

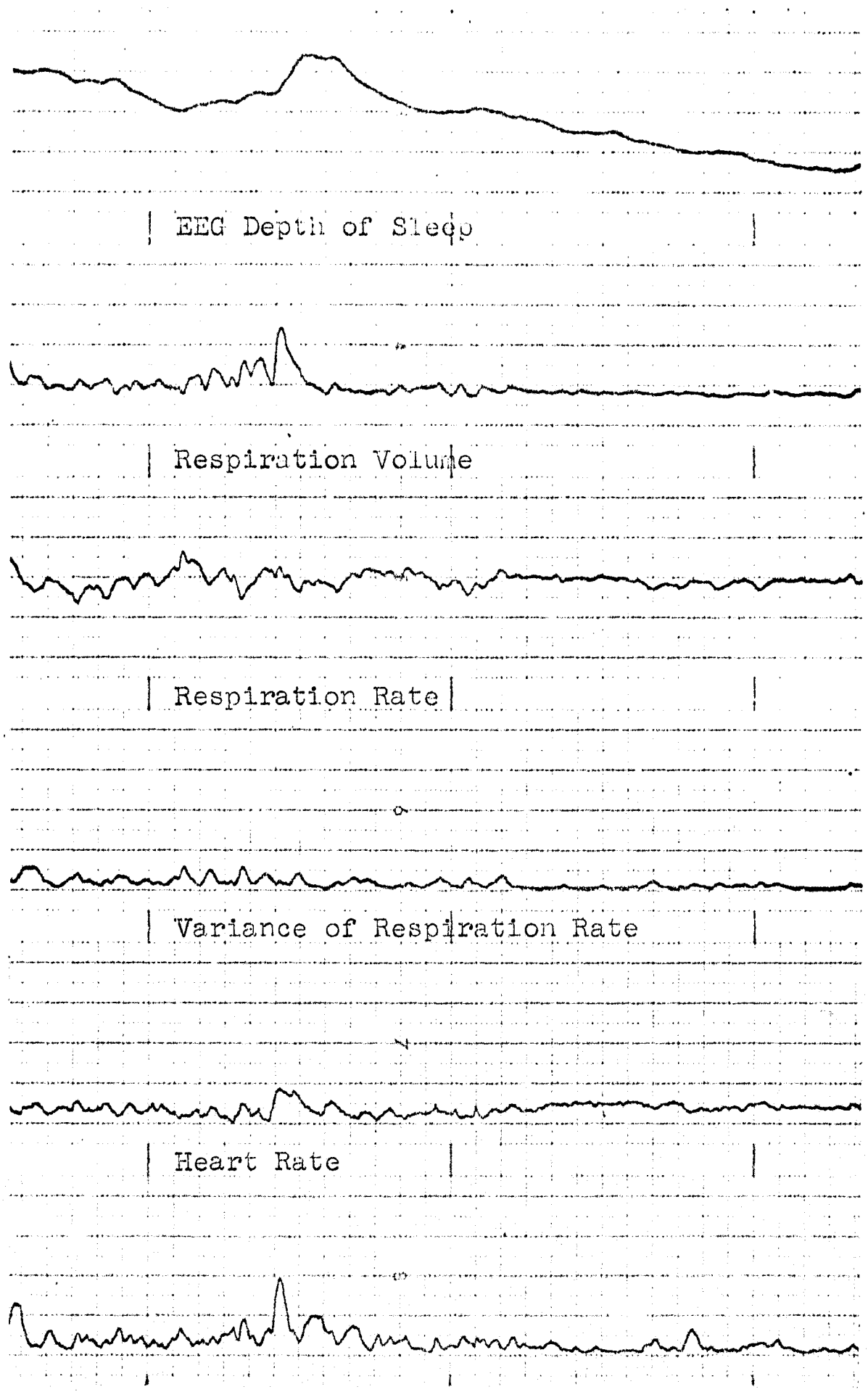


Figure 14

Processed Data - Subject #2

preprocessing of the data are shown and illustrate some of the types of relationships that can exist between the variables.

The depth-of-sleep derivation in Figure 13 indicates that the subject initially progressed from light stages to deeper stages of sleep followed by a sharp arousal and a subsequent period of light (stage I) sleep. The derived variables all indicate a progressive regularity of function as the sleep became deeper. In addition, the respiration rate and volume signals indicate a positive relationship between their base line values and the depth of sleep. The period of arousal was accompanied by transients in the respiration variables and increases in the level of the heart rate and its variance. The segment of stage I sleep following the arousal is indicated primarily by the increased variability of both the heart and respiration rates and the increased respiration volume. The increased variability of the rate signals indicates stage I-REM sleep according to the report by Snyder et al (27), and in fact, this period of sleep was recorded as stage I-REM by the investigators who collected the data.

Figure 14 illustrates a sleep profile in which an initial period of stage I sleep is followed by a segment of stage II sleep, a brief period of arousal, and a progressive deepening of sleep throughout the remainder of the record. The arousal is indicated in the derived variables by a transient in the respiration volume signal and in the heart rate and its variance. The deepening of sleep is associated with decreased variance signals, but in this record the heart rate, respiration rate, and respiration volume show no change of level associated with the deeper stages of sleep. Another observation is that the stage I period at the onset of sleep does not show the high rate variances that are associated with the stage I-REM portion shown in Figure 13. It is therefore possible that the derivation of either the heart or respiration rate variance alone might be adequate to determine REM periods of sleep, thus eliminating the need for transduction of ocular movements in studies requiring REM sleep information.

The time constants of the various analog averaging circuits were selected on an empirical basis with primary consideration being given to the appearance of the output

variables as they relate to the time varying characteristics of the EEG derived depth-of-sleep signal. Those values in Appendix A were chosen to average out the more dynamic changes which could include the effects of artifact and yet to emphasize the short term fluctuations of the measures from their basal values. The circuitry has been operated in real time as well as multiples thereof. The coefficient values given in Appendix A are for operation at eight times real time and are easily converted for operation at other speeds.

The regression analysis routine was tested with simulated data taken from an exercise problem in Draper and Smith's text (8). The routine proved to work satisfactorily and was applied to the variables illustrated in Figures 13 and 14. Tables I and II which were obtained by sampling at the maximum rate available (approximately 4.6 samples per second related to real time), illustrate the type of information that is produced by the computer analysis.

Independent Variable	Correlation x vs. Depth of Sleep	Regression Coefficient For Centered Model	Standard Regression Coefficient
x_1, Respiration Volume	0.160	0.045	0.109
x_2, Respiration Rate	0.129	0.023	0.050
x_3, Variance of Respiration Rate	0.594	0.576	2.409
x_4, Heart Rate	0.256	0.141	0.287
x_5, Variance of Heart Rate	0.267	-0.085	-0.312

Intercept for Standard Regression 10.277

$R^2 = 0.366$

Analysis of Variance for the Regression

Source	Sum of Squares	Degrees of Freedom	Mean Square Error	F Ratio
Regression	48881.7	5	9776.3	
Residual	84800.7	10957	7.7	1270.
Total	133682.4	10962		

Table I

Statistical Analysis for Sample Data of Figure 13

Independent Variable	Correlation x vs. Depth of Sleep	Regression Coefficient For Centered Model	Standard Regression Coefficient
x_1, Respiration Volume	-0.129	-0.270	-1.540
x_2, Respiration Rate	0.500	0.310	0.850
x_3, Variance of Respiration Rate	0.421	0.236	0.650
x_4, Heart Rate	0.015	-0.166	-0.648
x_5, Variance of Heart Rate	0.494	0.279	1.635

Intercept for Standard Regression 12.311

$R^2 = 0.424$

Analysis of Variance for the Regression

Source	Sum of Squares	Degrees of Freedom	Mean Square Error	F Ratio
Regression	81949.3	5	16389.9	
Residual	111118.8	11777	9.4	1744.
Total	193068.1	11782		

Table II

Statistical Analysis for Sample Data of Figure 14

VI. Discussion

The ability to process and analyze data at multiples of real time using the system described in this paper will permit the emphasis of future research to shift from tedious data processing techniques to the evaluation and interpretation of results obtained from experiments designed to test different hypotheses. The system should be used as a means to more precisely determine the relationships that exist between the EEG depth of sleep and the variables derived for analysis. Data should be evaluated which is adequate to test intersubject and intrasubject consistency of derived relationships. The studies using the system must include the analysis of data from both the sleeping and waking states to permit the derivations to be based on physiological changes as the subject passes through periods of sleep. Consideration also must be given to the distinction that may exist between normal sleep periods and naps (15). Ultimately it would be desirable to test any proposed model for estimating the depth of sleep with data collected under conditions that stress the model, such as those existing during space flight, sleep deprivation, and administration of drugs.

After processing the above types of data, it may prove to be desirable or necessary to include additional analysis routines or to alter or delete some existing features of the system. It is anticipated that the time constants of the various averaging circuits will have some effect on the results of the data analysis and will suggest investigations of these effects on different experimental designs. In addition, a preliminary investigation of these phase relationships that exist among the derived variables should be made to determine whether or not appropriate time leads or lags should be included in the derivation of regression models. To achieve these phase relationships, a program which computes and plots auto-correlation and cross-correlation functions of its input variables can be used in conjunction with the routine developed in this project.

Besides possible alterations in the derivation of the variables, examination of the residuals from the regression analysis would be helpful in determining the need for nonlinear terms or other suitable alterations of the regression model. In addition, certain variables may prove to yield consistently insignificant contributions

to the regression and should therefore be deleted from the model.

Quantification of the EEG depth-of-sleep derivation into discrete levels of sleep might prove to aid in establishing consistent relationships between the levels of sleep and the various physiological variables. In such a study discriminant analysis techniques, such as those used by Walter et al (28), could replace the regression analysis to provide the functional relationship.

If future experimentation yields a consistent intersubject relationship between the variables derived from the EEG and respiration signals and the depth of sleep, a hardware version of the preprocessing circuitry and an appropriate model could be developed to provide an on-line monitoring system for displaying the depth of sleep. If only intrasubject consistency is found, the ability to monitor sleep levels would be limited to situations where prior knowledge of the subjects' sleep characteristics are available.

APPENDIX

BIBLIOGRAPHY

1. Agnew, H. W. Jr., J. C. Parker, W. B. Webb, and R. L. Williams. "Amplitude measurement of the sleep electroencephalogram." Electroenceph. clin. Neurophysiol., 1967, 22:84-86.

2. Aristotle. "On Sleep and Sleeplessness," trans. by J. I. Beare, in The Works of Aristotle, ed. by R. M. Hutchins. William Benton, Publisher, Chicago, 1952, pp. 673-689.

3. Aserinsky, E., and N. Kleitman. "Regularly occurring periods of eye motility, and concomitant phenomena, during sleep." Science, 1953, 118:273-274.

4. Brazier, M. A. B. (ed.). "Computer techniques in EEG analysis." Electroenceph. clin. Neurophysiol., 1961, Suppl. 20.

5. Brooks, C. McC., B. F. Hoffman, E. E. Suckling, F. Kleyntjens, E. H. Koenig, K. S. Coleman, and J. J. Treumann. "Sleep and variations in certain functional activities accompanying cyclic changes in depth of sleep." J. Appl. Physiol., 1956, 9:97-104.

6. Burch, N. R. "Automatic analysis of the electroencephalogram: A review and classification of systems." Electroenceph. clin. Neurophysiol., 1959, 11:827-834.

7. Dement, W., and N. Kleitman. "Cyclic variations in EEG during sleep and their relation to eye movements, body motility, and dreaming." Electroenceph. clin. Neurophysiol., 1957, 9:673.

8. Draper, N. R., and N. Smith. Applied Regression Analysis. John Wiley and Sons, Inc., New York, 1966.

9. Frost, J. D. Jr. Personal communication, January, 1968.

10. Gibbs, F. A., and E. L. Gibbs. Atlas of Electroencephalograph. I. Methodology and Normal Controls. Addison-Wesley Press, Cambridge, 1950, 2d ed., p. 324.

11. Goldstein, L., and R. A. Beck. "Amplitude analysis of the electroencephalogram." International Review of Neurobiology, 1965, 8:266-279.

12. Grass, M. A., and A. F. Gibbs. "A Fourier transform of the EEG." J. Neurophysiol., 1938, 1:521.

13. Jouvet, M. "Neurophysiology of the states of sleep." Physiol. Rev., 1967, 47(2):117-177.

14. Khatri, I. M., and E. D. Freis. "Hemodynamic changes during sleep." J. Appl. Physiol., 1967, 22(5): 867-873.

15. Kleitman, N. Sleep and Wakefulness. The University of Chicago Press, Chicago, 1963.

16. Kubicek, W. G., E. Kinnen, and A. Edin. "Calibration of an impedance pneumograph." J. Appl. Physiol., 1964, 19(3):557-560.

17. Loomis, A. L., E. N. Harvey, and G. A. Hobart. "Electrical potentials of the human brain." J. Exp. Psychol., 1936, 19:249-279.

18. Maulsby, R. L., J. D. Frost, Jr., and M. H. Graham. "A simple electronic method for graphing EEG sleep patterns." Electroenceph. clin. Neurophysiol., 1966, 22:109-117.

19. Maulsby, R. L. Personal communication, 1967.

20. Maulsby, R. L., and F. B. Vogt. Unpublished Project Proposal, Personal communication, January, 1966.

21. Oswald, I. Sleeping and Waking. Elsevier, Amsterdam, New York, 1962.

22. Otterman, J. "The properties and methods for computation of exponentially mapped past statistical variables." IRE Trans. on Automatic Control, 1960, AC-5(1):11-17.

23. Riehl, J. L. "Analog analysis of EEG activity." Electroenceph. clin. Neurophysiol., 1963, 15: 1039-1042.

24. Riehl, J. L. "Analysis of the frequency/voltage ratio of the EEG in intracranial diseases." Electroenceph. clin. Neurophysiol., 1966, 21: 325-334.

25. Scheffe, H. The Analysis of Variance. Wiley, New York, 1959.

26. Snyder, F. "Autonomic nervous system manifestations during sleep and dreaming." Functions of Varied Experiences, ed. by D. W. Fiske and S. R. Maddi. Dorsey, Homewood, Illinois, 1961.

27. Snyder, F., J. A. Hobson, D. F. Morrison, and F. Goldfrank. "Changes in respiration, heart rate, and systolic blood pressure in human sleep." J. Appl. Physiol., 1964, 19(3):417-422.

28. Walter, D. O., J. M. Rhodes, and W. Ross Adey. "Discriminating among states of consciousness by EEG measurements. A study of four subjects." Electroenceph. clin. Neurophysiol., 1967, 22:22-29.

29. Williams, H. L. "The problem of defining depth of sleep." Functions of Varied Experiences, ed. by D. W. Fiske and S. R. Maddi. Dorsey, Homewood, Illinois, 1961.

APPENDIX A

Analog Preprocessing Circuits

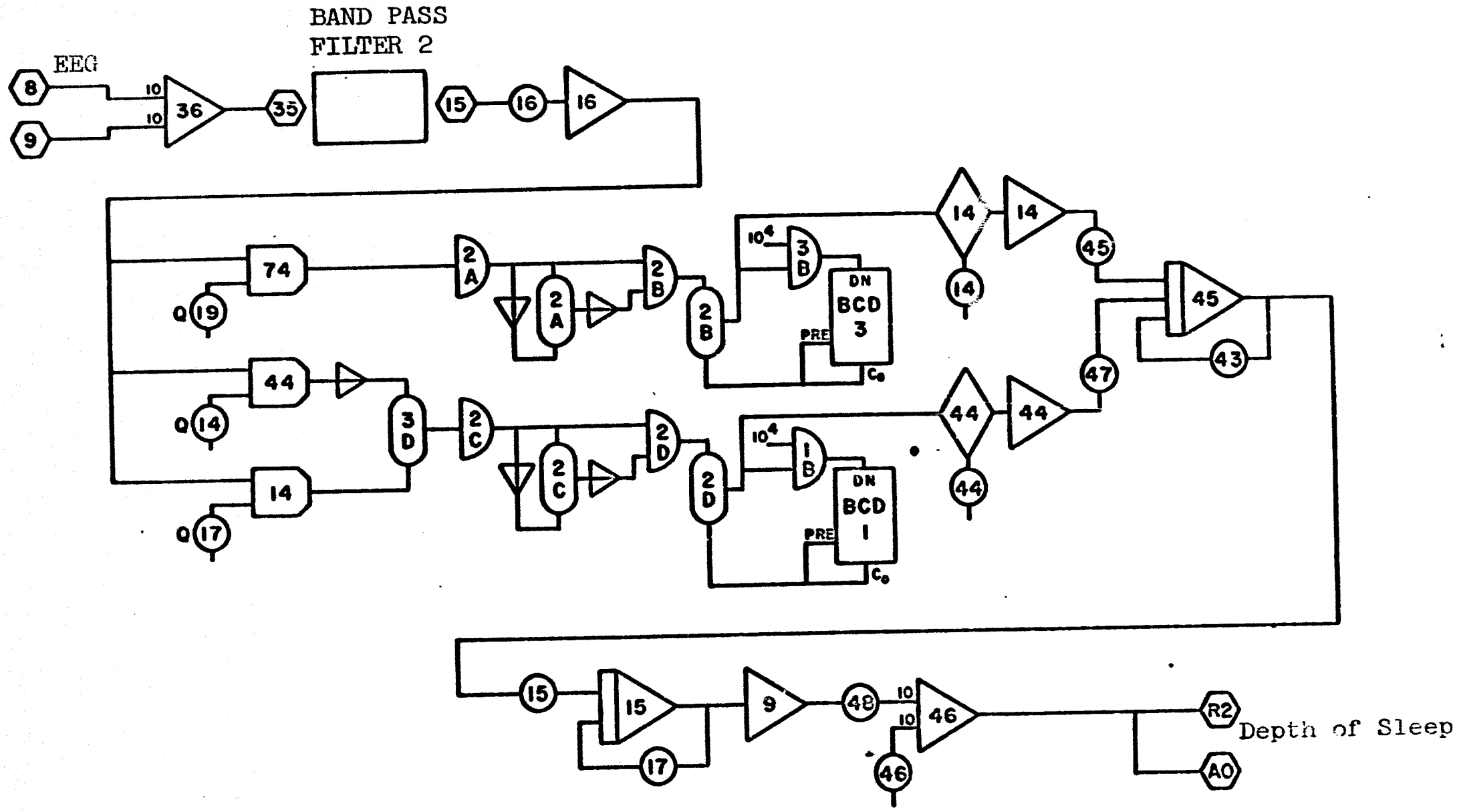


Figure A-1

EEG ANALYZER

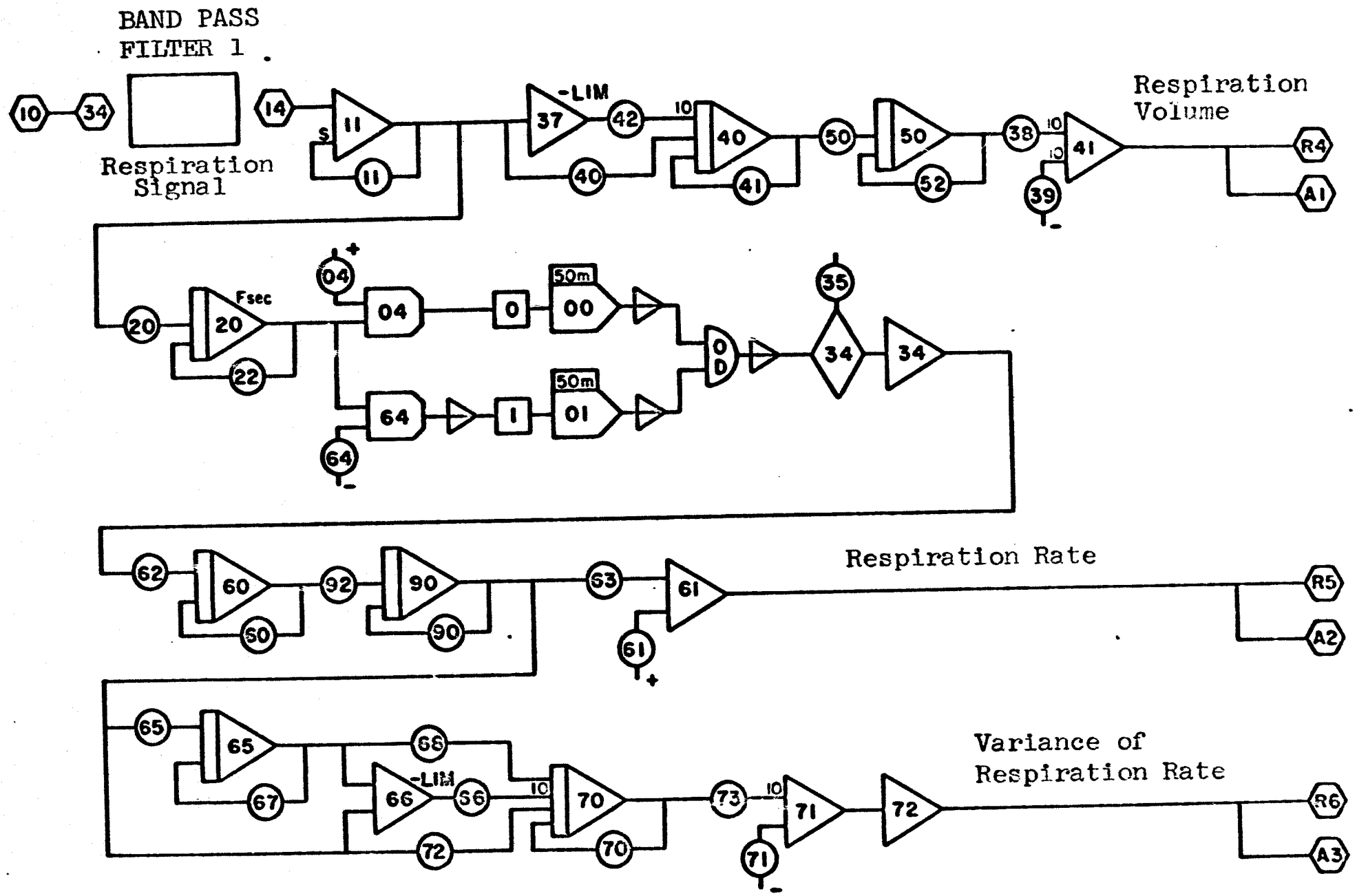


Figure A-2

RESPIRATION PREPROCESSOR

ECG

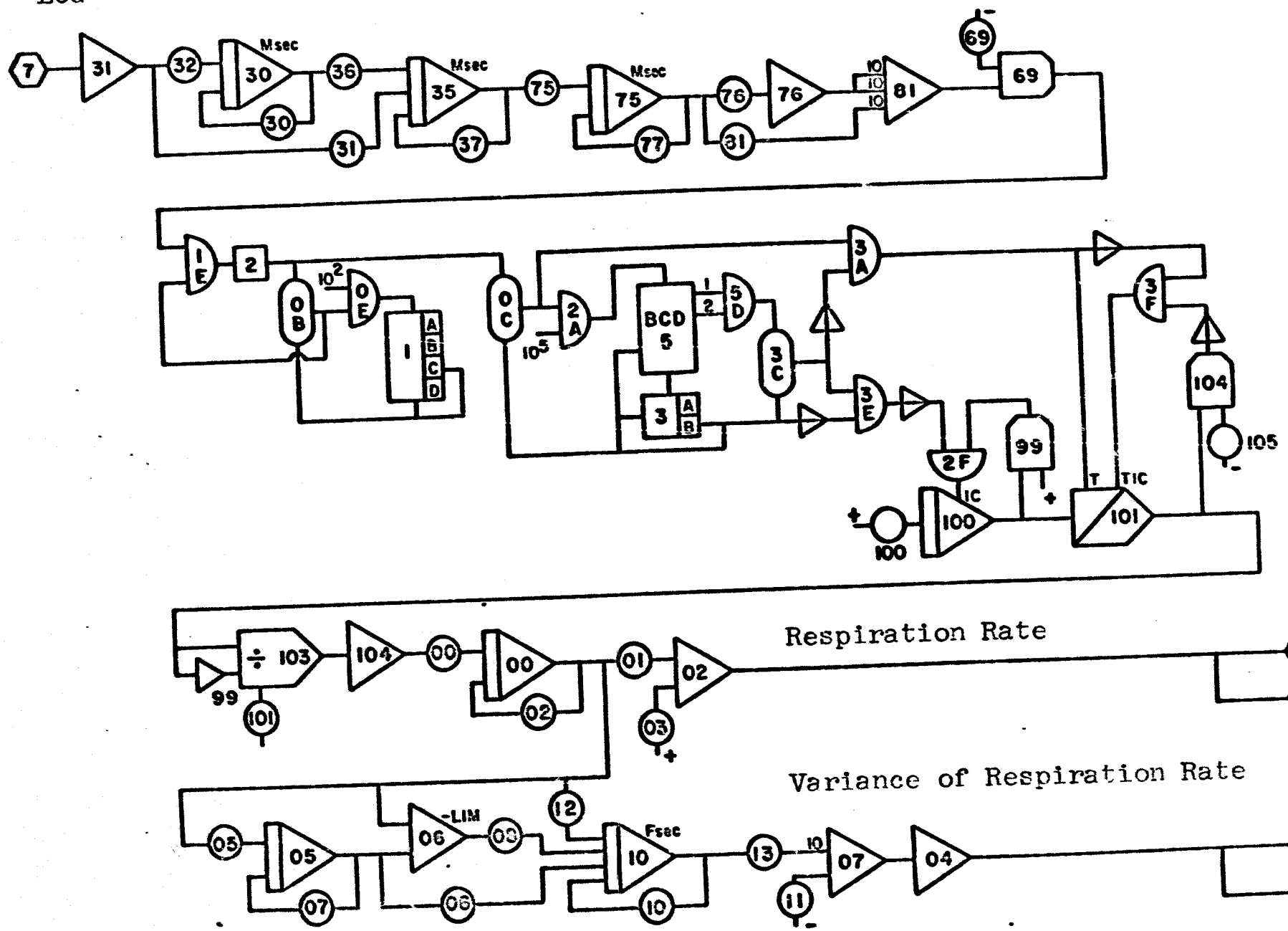


Figure A-3

ECG PREPROCESSOR

COEFFICIENT VALUES FOR ANALOG COMPUTER
Eight Times Real Time Operation

Potentiometer Number	Coefficient	Potentiometer Number	Coefficient
00	1.0000	47	.1110
01	.5000	48	.2000
02	1.0000	50	.3366
03	.6250	52	.1150
04	.0400	60	.5000
05	.2000	61	.4000
06	.6250	62	.0200
07	.2000	63	.1000
08	.1250	64	.0400
10	.6250	65	.1250
11	.3000	66	.0200
12	.7720	67	.1250
13	.5000	68	.1000
14	.5000	69	.1500
15	.1410	70	.0750
16	.1600	71	1.0000
17	.7720	72	.1000
20	1.0000	73	.5000
22	.2000	75	.8540
30	.9540	76	.7140
31	.8150	77	.8540
32	.9540	81	.7140
35	.1000	90	.5000
36	.8150	92	.5000
37	.8540	100	.2665
38	.2000	101	.1110
39	.5000	105	.1110
40	.7500		
41	1.0000	Q 14	.0120
42	.2000	Q 17	.0120
43	.1333	Q 19	.1500
44	.5000		
45	.1110	BCD #1	050
46	.1550	BCD #2	050

APPENDIX B

Digital Program

Digital Program

```
      ▲JOB.
      ▲ASSIGN S.DF1Y,X1.DF1Y,X2.DF1Y,SI.CR,LO.LP,BO.DF1Y,BI.DF1Y.
      ▲REWIND BO.
      ▲RTFTRAN BO,LO.
            DIMENSION R(15,15),A(5),B(5),   IX(0/5),X(5),SUMX(5),SUMYX(5),
           1SUMXX(5,5),RYX(5),EX(5),S(5,5),SYX(5),KP(0/119)
            DIMENSION RINV(15,15),CHK(5,5)
            DIMENSION IV(0/5),IR(0/1)
        198 CONTINUE
            DO 1 I=1,15
            DO 1 J=1,15
          1 R(I,J)=0.
            DO 2 I=1,5
            R(I,I)=1.
            A(I)=0.
            IX(I)=0.
            X(I)=0.
            SUMX(I)=0.
            SUMYX(I)=0.
            RYX(I)=0.
            EX(I)=0.
            SYX(I)=0.
            DO 2 J=1,5
            SUMXX(I,J)=0.
          2 S(I,J)=0.
            IX(0)=0.
            SUMY=0.
            SUMYY=0.
            N=0
            NV=5
            TYPE 102
            ACCEPT 103,K
      C
      C     DATA SAMPLING LOOP
      C
            PAUSE
      S     EOM 033412                          /DIGITAL MODE
      S     POT =0400                           /RUN.
           10 IF(SENSE SWITCH 2) 11,30
           11 N=N+1
      S     EOM 033421
      S     POT=0100000
            CALL ADCS (IX,0,1,2,3,4,5)
            Y=IX(0)/1638.3
            SUMY=SUMY+Y
            SUMYY=SUMYY+Y*Y
            DO 20 I=1,5
            X(I)=IX(I)/1638.3
            SUMX(I)=SUMX(I)+X(I)
            SUMYX(I)=SUMYX(I)+X(I)*Y
            DO 20 J=1,5
            X(J)=IX(J)/1638.3
           20 SUMXX(I,J)=SUMXX(I,J)+X(I)*X(J)
            CALL TIMER(K)
            GO TO 10
      C
      C     COMPUTATION OF MEANS AND VARIANCES
      C
           30 EY=SUMY/N
```

```
      DO 31 I=1,5
   31 EX(I)=SUMX(I)/N
      SYY=SUMYY-2.*EY*SUMY+N*EY*EY
      DO 40 I=1,5
      DO 40 J=I,5
   40 S(I,J)=SUMXX(I,J)- X(J)*SUMX(I)-EX(I)*SUMX(J)+N*EX(J)*EX(I)
C
C     FORMATION  OF CORRELATION MATRICES
      DO 41 I=1,5
      DO 41 J=I+1,5
   41 R(I,J)=S(I,J)/SQRT(ABS(S(I,I)*S(J,J)))
      DO 42 I=2,5
      DO 42 J=1,I-1
   42 R(I,J)=R(J,I)
      DO 43 I=1,5
      SYX(I)=SUMYX(I)-EX(I)*SUMY-EY*SUMX(I)+N*EY*EX(I)
   43 RYX(I)=SYX(I)/SQRT(ABS(S(I,I)*SYY))
      PRINT 100,N
      PRINT 101,((R(I,J),I=1,5),J=1,5
C
C     INVERSION OF CORRELATION MATRIX
      DO 44I=1,5
      DO 44 J=1-5
   44 RINV(I,J)=R(I,J)
      CALL INVERT(NV,RINV,DET,INDIC)
      PRINT 104
      PRINT 101,((RINV(I,J),I=1,5),J=1,5
      PRINT 106,DET,INDIC
      DO 45 I=1,5
      DO 45 J=1,5
      DO 45 K=1,5
   45 CHK(I,J)=CHK(I,J)+RINV(I,K)*R(K,J)
      PRINT 117
      PRINT 101,((CHK(I,J),I=1,5),J=1,5
C
C     COMPUTATION OF PDT VALUES
      DO 50 I=1,5
      DO 50 J=1,5
   50 A(I)=A(I)+RINV(I,J)*RYX(J)
      PRINT 107,(I,A(I),I=1,5
      DO 52 I=1,5
   52 B(I)=A(I)*SQRT(ABS(SYY/S(I,I)))
      B(0)=EY-B(1)*EX(1)-B(2)*EX(2)-B(3)*EX(3)-B(4)*EX(4)-B(5)*EX(5)
      PRINT 109,(I,B(I),I=0,5
      PRINT 110,(I,RYX(I),I=1,5
      DO 51 I=0,119
   51  KP(I)=-1
      KP(112)=A(1)*1000
      KP(113)=A(2)*1000
      KP(115)=A(3)*1000
      KP(116)=A(4)*1000
      KP(118)=A(5)*1000
      CALL SETPDT(KP,119)
C
C     COMPUTATION OF ANALYSIS OF VARIANCE TABLE
      SST=SUMYY-((SUMY*SUMY)/N)
      SSR=0.
      DO 60 I=1,5
   60 SSR=SSR+B(I)*(SUMYX(I)-(SUMX(I)*SUMY)/N)
      NDF=N-NV-1
```

```
      NT=N-1
      SSRE=SST-SSR
      RMS=SSR/NV
      REMS=SSRE/NDF
      CORR=SSR/SST
      F=RMS/REMS
      PRINT 111,CORR
      PRINT 112
      PRINT 113
      PRINT 114,SSR,NV,RMS
      PRINT 115,SSRE,NDF,REMS,F
      PRINT 116,SST,NT
      TYPE 105
C
C   FORMATION OF ESTIMATED VARIABLE AND RESIDUALS
C
      PAUSE
      TYPE 102
      ACCEPT 103,K1
      TYPE 118
      ACCEPT 103,K2
   70 IF(SENSE SWITCH 2)  72,71
   71 CONTINUE
S     EOM 033421
S     P0T=0100000
      CALL ADCS(IV,0,1,2,3,4,5)
      SUM=B(0)+B(1)*IV(1)+B(2)*IV(2)+B(3)*IV(3)+B(4)*IV(4)+B(5)*IV(5)
      IR(0)=SUM/K1
      IR(1)=IV(0)-IR(0)
      CALL DACS(IR,0,1)
      CALL TIMER(K2)
      GO TO 70
   72 TYPE 119
      GO TO 198
  100  FORMAT(1H1,10X,'*** CORRELATION MATRIX ***',I7,'  SAMPLES')
  101 FORMAT(/,5(5X,E15.7))
  102  FORMAT(' TYPE DESIRED DELAY IN MILLISECONDS')
  103  FORMAT(I7)
  104  FORMAT(///,10X,'*** INVERSE CORRELATION MATRIX ***')
  105  FORMAT('REWIND ANALOG TAPE')
  106 FORMAT (' DETERMINANT =',E15.7,'INDICE =',I7)
  107 FORMAT (1HO,5(3X,'A(',I1,')=',F10.6))
  108 FORMAT(F9.4,5F10.4)
  109 FORMAT (1HO,5(3X,'B(',I1,')=',F10.6))
  110 FORMAT (1HO,5(3X,'RYX(',I1,')=',F10.6))
  111 FORMAT(1HO,3X,'MULTIPLE CORRELATION=',F10.7)
  112 FORMAT(//,18X,'ANALYSIS OF VARIANCE FOR THE REGRESSION')
  113 FORMAT(1HO,4X,'SOURCE',5X,'SUM OF SQUARES',3X,'DEGREE OF FREEDOM',
     13X,'MEAN SQUARE',5X,'F RATIO'/)
  114 FORMAT(3X,'REGRESSION',3X,F14.7,12X,I1, 8X,F14.7)
  115 FORMAT(4X,'RESIDUAL',4X,F14.7,8X,I6,11X,F10.7,4X,F10.7)
  116 FORMAT(5X,'TOTAL',6X,F14.7,8X,I6)
  117 FORMAT(///,10X,'*** CHECK OF MATRIX INVERSION *** RINV*R ***')
  118 FORMAT('  ENTER DESIRED SCALING FACTOR  ')
  119 FORMAT('  *****   END OF RUN   *****')
      END
```

```
      SUBROUTINE INVERT(N,A,DET,INDIC)
      DIMENSION A(15,15),B(15),C(15),IP(15),IQ(15)
      DET=1.
      DO 16 K=1,N
C  DETERMINATION OF PIVOTAL ELEMENT
      PIVOT=C
      DO 4 I=K,N
      DO 4 J=K,N
      IF (ABS(A(I,J))-ABS(PIVOT)) 4,4,3
    3 PIVOT=A(I,J)
      IP(K)=I
      IQ(K)=J
    4 CONTINUE
      IF (ABS(PIVOT)-1.0E-10) 27,27,5
C  EXCHANGE PIVOTAL ROW WITH KTH ROW
    5 IF (IP(K)-K) 6,8,6
    6 DET=-DET
      DO 7 J=1,N
      Z=A(IP(K),J)
      A(IP(K),J)=A(K,J)
    7 A(K,J)=Z
C  EXCHANGE PIVOTAL COLUMN WITH KTH COLUMN
    8 IF(IQ(K)-K) 9,11,9
    9 DET=-DET
      DO 10 I=1,N
      Z=A(I,IQ(K))
      A(I,IQ(K))=A(I,K)
   10 A(I,K)=Z
C  JORDAN STEP
   11 DET=DET*PIVOT
      DO 15 J=1,N
      IF(J-K) 13,12,13
   12 B(J)=1./PIVOT
      C(J)=1.
      GO TO 14
   13 B(J)=-A(K,J)/PIVOT
      C(J)=A(J,K)
   14 A(K,J)=0
   15 A(J,K)=0
      DO 16 I=1,N
      DO 16 J=1,N
   16 A(I,J)=A(I,J)+C(I)*B(J)
C  REORDERING OF THE MATRIX
      DO 25 K=N,1,-1
      IF (IP(K)-K) 18,20,18
   18 DO 19 I=1,N
      Z=A(I,IP(K))
      A(I,IP(K))=A(I,K)
   19 A(I,K)=Z
   20 IF (IQ(K)-K) 21,25,21
   21 DO 22 J=1,N
      Z=A(IQ(K),J)
      A(IQ(K),J)=A(K,J)
   22 A(K,J)=Z
   25 CONTINUE
      INDIC=0
      RETURN
C  PIVOT NEARLY ZERO
   27 TYPE 28
      INDIC=1
      RETURN
   28 FORMAT(//,5PIVOT LESS THAN 10.**-10,//)
```

APPENDIX C

Sample Matrix Inversion

Correlation Matrix

0.100E 01	0.458E 00	0.382E 00	-0.361E 00	0.175E 00
0.458E 00	0.100E 01	0.143E 00	0.562E-01	0.154E 00
0.382E 00	0.143E 00	0.100E 01	0.323E 00	0.605E 00
-0.361E 00	0.562E-01	0.323E 00	0.100E 01	0.547E 00
0.175E 00	0.154E 00	0.605E 00	0.547E 00	0.100E 01

Inverse Correlation Matrix

0.252E 01	-0.102E 01	-0.100E 01	0.159E 01	-0.554E 00
-0.102E 01	0.144E 01	0.324E 00	-0.605E 00	0.912E-01
-0.100E 01	0.324E 00	0.198E 01	-0.620E 00	-0.734E 00
0.159E 01	-0.605E 00	-0.620E 00	0.244E 01	-0.114E 01
-0.554E 00	0.912E-01	-0.734E 00	-0.114E 01	0.215E 01

Determinant = 0.170E 00

Check of Matrix Inversion --- RINV*R

0.100E 01	-0.682E-12	-0.118E-10	-0.818E-11	-0.436E-10
-0.827E-10	0.100E 01	-0.318E-11	-0.454E-11	-0.381E-10
-0.618E-10	-0.250E-11	0.100E 01	0.000E 00	-0.727E-10
-0.218E-10	-0.147E-10	-0.218E-10	0.100E 01	-0.654E-10
-0.436E-10	-0.545E-11	-0.145E-10	-0.727E-11	0.100E 01

Correlation Matrix

0.100E 01	-0.584E 00	-0.201E 00	-0.469E-01	-0.855E-01
-0.584E 00	0.100E 01	0.271E 00	-0.101E 00	0.516E-02
-0.201E 00	0.271E 00	0.100E 01	-0.531E-02	-0.381E-01
-0.469E-01	-0.101E 00	-0.531E-02	0.100E 01	0.620E 00
-0.855E-01	0.516E-02	-0.381E-01	0.620E 00	0.100E 01

Inverse Correlation Matrix

0.155E 01	0.901E 00	0.706E-01	0.135E 00	0.466E-01
0.901E 00	0.162E 01	-0.262E 00	0.275E 00	-0.112E 00
0.706E-01	-0.262E 00	0.108E 01	-0.778E-01	0.972E-01
0.135E 00	0.275E 00	-0.778E-01	0.167E 01	-0.103E 01
0.466E-01	-0.112E 00	0.972E-01	-0.103E 01	0.164E 01

Determinant = 0.358E 00

Check of Matrix Inversion --- RINV*R

0.100E 01	-0.155E-10	-0.229E-10	0.500E-11	-0.400E-10
-0.379E-10	0.100E 01	-0.110E-10	0.104E-10	-0.432E-10
-0.480E-10	-0.721E-10	0.100E 01	0.704E-11	-0.668E-10
-0.557E-11	-0.636E-11	-0.225E-10	0.100E 01	-0.654E-10
-0.313E-10	-0.395E-10	-0.181E-10	-0.218E-10	0.100E 01

VITA

Stephen M. Sloan was born on [redacted], in [redacted] to Don H. and Mildred Sloan. After graduating from Spring Branch High School in Houston, Texas, in 1961, he entered the University of Houston. In 1966 he received the B.S. in Mathematics and in 1967 received the B.S.E.E., both from the University of Houston.

While at the University of Houston, Mr. Sloan was employed by the Department of Industrial Engineering as a teaching assistant and the Department of Electrical Engineering as a member of the Communications Research Group. During the 1966-1967 term he received a teaching fellowship from the Department of Mathematics. In June 1967 he entered The University of Texas Graduate School of Biomedical Sciences at Houston and was employed by the Department of Biomedical Engineering. He is presently employed by the Department of Biomathematics of The University of Texas M. D. Anderson Hospital and Tumor Institute. Mr. Sloan is a member of Tau Beta Pi, Eta Kappa Nu, IEEE, and SCi.

Permanent address: 2640 Cason, Houston, Texas 77005

This thesis was typed by Dorothy Sloan.

MASTER OF SCIENCE DATA SHEET

FULL NAME: Stephen M. Sloan

SPECIAL FIELD OF THE THESIS: Biomedical Engineering

PREVIOUS DEGREES: B.S., University of Houston, 1966
B.S.E.E., University of Houston, 1967

PERMANENT HOME ADDRESS: 2640 Cason, Houston, Texas, 77005

DEGREE SOUGHT: Master of Science

DATE OF GRADUATION: August, 1968

EXACT TITLE OF THESIS: Automated Estimation of the Depth Of Sleep

TOTAL NUMBER OF PAGES: 84

NUMBER OF ILLUSTRATIONS: 27

SUPERVISING PROFESSOR: Dr. Fred B. Vogt

BRIEF SUMMARY OF THESIS

This report describes a system designed to aid in the investigation of relationships that may exist between physiological variables and the depth of sleep. A hybrid computer routine was developed to derive several variables from the ECG and respiration signals and to compute their relationships to the depth of sleep as derived from the EEG. This relationship is formed by utilizing linear regression techniques.